

Founded 1925

Incorporated  
by Royal Charter 1951

*"To promote the advancement  
of radio, electronics and kindred  
subjects by the exchange of  
information in these branches  
of engineering."*

VOLUME 42 No. 10

OCTOBER 1972

# THE RADIO AND ELECTRONIC ENGINEER

The Journal of the Institution of Electronic and Radio Engineers

## Assessing Profit

ANY member of a company, be he a shareholder or employee, is closely identified with the Annual Report and its revelation of success or failure. This 'accounting' of a year's work is just as essential a function for all Societies and Institutions. Much effort is devoted to preparing these Reports but the many contributors are seldom able to assess what impact their work has on the majority of shareholders or members.

Strange as it may seem, it is a fact that the more successful an industrial enterprise, the smaller is the percentage of shareholders attending the Annual General Meeting and, one may guess, even reading the Annual Report! Equally true, however, is the fact that a report of a successful year encourages more investors!

So it seems to be with professional institutions: for, like absent shareholders, it must be assumed that professional engineers are passively recording 'satisfaction' with the reports of achievement that their elected Council has given.

In every IERE Annual Report some sort of assessment of profit can be made for each of the various activities discussed. Obviously in the Accounts the balance of income from all sources against expenditure on membership services and administration shows the financial health of the Institution and is hence fairly easily comprehended. Assessment of profit in other areas is not quite so straightforward, though the statement of gains and losses of membership presents a factual statement from which the Institution's growth may be gauged. A direct numerical assessment of the success or otherwise of the efforts of the Council on, for instance, the educational front or in learned society activities, is seldom possible and here the reader will need to follow the explanations of the background to these parts of the Report if he is to 'assess the profit' of the year. Sometimes, where prolonged negotiations are being reported on, extending over two or even more 'Institution years', an interim progress report may be all that is possible, and time alone will show how effective the Council's policies and arguments have been. In this respect members are better served than the average shareholder in that *The Radio and Electronic Engineer* gives interim reports in editorials and other news items on the progress of matters of interest and value to the member.

This editorial article is thus a preamble to the Annual Report of the Council for 1971-72, to be published in the November issue and an invitation to each member to 'assess the profit' of the Institution itself—and in its relation to him personally. The record of achievement of the past year will surely present favourable answers in both respects. Affirmation of members' general satisfaction with the Institution's operations is always sought at the Annual General Meetings and for this reason alone the Council is heartened to note attendance. This year's meeting on 7th December in London will be no exception.

## Contributors to this issue



**Mr. R. D. Lock** (Member 1970, Graduate 1961) obtained his professional qualifications through part-time study whilst at the Post Office Research Station, Dollis Hill. During that time (1952-1966) he was associated with the development of electronic telephone switching systems. On joining Bell-Northern Research in 1966 his experience in logic design and digital circuit techniques was applied to

development of the S.P.1 computer-controlled telephone exchange. Since 1969 he has been involved in the design of magnetic bubble devices and their applications.



**Dr. John Lucas** graduated from Bristol University in 1964 with an honours degree in physics. He then entered Sussex University where, after completing an M.Sc. in physics, he obtained a D.Phil. degree in materials science through research into amorphous ferrimagnetic oxides. In 1970 he went to Canada to develop magnetic bubble materials for Bell-Northern Research. He has recently joined the Domtar

Research Centre where he is involved in problems of the pulp and paper industry.



**Dr. A. P. Clark** (Member 1964) is a Senior Lecturer in the Department of Electronics and Electrical engineering at Loughborough University of Technology. Before joining the University two years ago, Dr. Clark was in industry for some 15 years, working mainly on data transmission problems with British Telecommunications Research Ltd. (subsequently Plessey Telecommunications

Research). He has contributed several papers in the past to the Institution's *Journal* and was a member of the Organizing Committee for the Conference on Digital Processing of Signals in Communications. (A fuller note on his early career was published in the *Journal* in September 1970.)



**Mr. M. J. Tucker** (Member 1965) obtained his London external degree in physics in 1944 following full-time study at the S. W. Essex Technical College (now part of the N.E. London Polytechnic). After serving briefly at the Admiralty Fuel Experimental Station, Harlow, he joined the newly-formed Oceanographic Group at the Admiralty Research Laboratory at Teddington in December 1944. He was

seconded to the National Institute of Oceanography when this was established in 1950 and has worked there ever since. He is now Head of the Applied Physics Group whose main concern is the development of oceanographic instrumentation. Author or co-author of numerous papers published by the Institution, Mr. Tucker has served on Conference Organizing Committees and he is Alternate Representative of the IERE on the British National Committee for Ocean Engineering. He is Chairman of the Programme Committee of the Society of Underwater Technology.



**Mr. I. S. Bogie** joined the Decca Navigator Company in 1966 and worked initially on ILS echo monitoring experiments. He transferred to the Systems Study and Management Division in 1968 as a systems engineer and has subsequently been involved in a range of projects concerned with air, marine and underwater navigation systems. Before joining Decca, he was with Nuclear Enterprises Ltd. and Steensen,

Varming Mulcahy and Partners. Mr. Bogie has an HNC in electrical and electronic engineering with an endorsement in applied electronics, and a Diploma in Science and Technology of Navigation. He has studied at the then Heriot-Watt College and Bradford Institute of Technology and the City of London Polytechnic.



**Mr. R. M. Dunbar** obtained his B.Sc. degree in electrical engineering at the University of Edinburgh in 1959 and he subsequently received the Diploma in Electronics and Radio. From 1960 to 1963 he worked as research engineer with Ferranti Ltd. on radar systems and transmission line fault location equipment design; during this period he carried out research into predictive control of a.c. circuit

breakers and was awarded the M.Sc. degree of Edinburgh University in 1963. Since 1964, he has been a Lecturer in the Department of Electrical and Electronic Engineering at Heriot-Watt University and has been involved with underwater technology research since 1969, in particular the ANGUS unmanned cable-controlled navigable underwater survey vehicle. He is Honorary Secretary of the Underwater Technology Group at the University and of the East Scotland Branch of the Society for Underwater Technology.

# Magnetic Bubbles and their Applications

R. D. LOCK, C.Eng., M.I.E.R.E. \*

and

J. M. LUCAS, D.Phil.†

## SUMMARY

Magnetic bubble domains may be formed in platelets of certain magnetic materials. They are the basis for an unusual new breed of devices in which bubbles are selectively created, propagated, interacted, detected and annihilated, so that both memory and logic functions may be performed in a single piece of material. Bubble devices are very compact and dissipate little energy. This paper describes the nature of magnetic bubbles, and the materials which support them. Various aspects of device technology are introduced, with discussion of all the functions required, including bubble interaction logic. Applications for bubble devices are indicated.

---

\* Bell Canada Northern Electric Research Ltd., Central Laboratory, P.O. Box 3511, Station C, Ottawa.

† Formerly Bell-Northern Research; now with Domtar Research, Senneville, P.Q.

## 1. Introduction

The last few years have seen the growth of an exciting new development in applied magnetism known as 'Magnetic Bubble Technology'. Research has progressed rapidly from the handful of first publications in 1968, to the present level which alone accounted for over 30 papers at each of the recent annual magnetism conferences.<sup>1, 2</sup> Whether the considerable effort this represents will succeed in establishing a commercial technology has yet to be proved. But the prospects look increasingly favourable.

This paper is therefore designed to give the engineer what we hope is a preview of a technology that will become available towards the middle of the decade.

What promises does bubble technology hold out to the engineer? At first he may be tempted to substitute bubble memories for disk files in his latest system. Though this may not at first save him money, bubble memories will offer greater reliability and far longer continuous service than ever possible with disk files. Bubble devices have no moving parts. Memories are expected to weigh less than disk files, and will require less space. Access time may also be improved by an order of magnitude. The value of these characteristics will, of course, depend on the application. In the telephone industry, for example, high reliability over many years of continuous service will be a considerable asset.

Beyond these memories we envisage entire computers based on bubble technology; both memory and logic functions being performed on the same piece of material. Such possibilities have already been demonstrated but will take time to develop.

Accounts of bubble technology fall naturally into two parts; first we explain what is meant by the somewhat strange term 'magnetic bubble', and discuss the materials which are used to support them; and secondly we review some of the techniques developed for the exploitation of bubbles in devices.

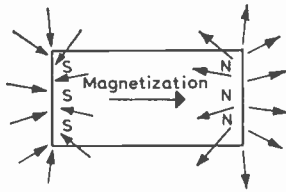
## 2. Magnetic Domains

'Magnetic bubble' is the abbreviated name given to what in the more technical language of magnetism is referred to as a cylindrical magnetic domain. Thus to explain what is meant by a magnetic bubble we begin by offering a brief account of the theory of magnetic domains.<sup>3</sup> To do this we consider the behaviour of a piece of magnetic material in terms of the interplay of a number of forces or energies.

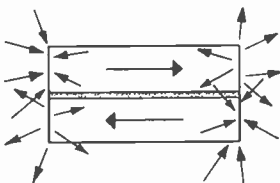
Of these, the first we discuss arises from discontinuities in magnetization which are normally associated with magnetic materials. Discontinuities will occur both where the direction of magnetization intersects surfaces, and at structural imperfections and variations. The poles of a bar magnet are a simple example of magnetization discontinuity.

We are all familiar with the fields surrounding such poles, shown schematically in Fig. 1(a), by virtue of the forces they exert on magnetic objects. Within the material itself the fields due to the poles are known as 'demagnetizing fields' since they oppose the magnetization direction

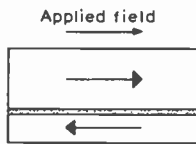
and thereby increase the energy required to maintain magnetization of the material. Energy bound up in this way, and in the fields outside the material, is referred to as 'magnetostatic energy', and is of crucial importance in determining the behaviour of magnetic materials.



(a) The fields surrounding the poles of a bar magnet oppose the magnetization within the material and create a large demagnetizing energy.



(b) The formation of a domain wall reduces the demagnetizing energy through partial cancellation of the pole fields.



(c) Application of a magnetic field can cause one domain to grow with respect to the other.

Fig. 1

One of the most fascinating properties of magnetic materials is their ability to form domains which serve to reduce magnetostatic energy. Here we find the material divided into two or more volumes, or domains, which are distinguished from their neighbours by virtue of differences in magnetization direction. A diffuse transition region known as the 'domain wall' separates domains. Figure 1(b) illustrates how the introduction of one such wall produces two domains within the simple bar-shaped magnet discussed above. Each end of the magnet now consists of a pair of opposite poles, which, since they are opposite, tend to cancel one another. Thus the magnetostatic energy is reduced since both the demagnetizing field within the material and external field are weakened. The more walls we introduce the more effective this reduction becomes. However, since additional energy is associated with the presence of domain walls, a compromise is reached by which the total magnetostatic and wall energies are minimized.

What happens if we now apply a magnetic field along the magnet axis? The resulting greater potential energy of the domain magnetized against the field direction manifests itself as a force on the domain wall acting to reduce the volume of the higher energy domain. Figure 1(c) shows how wall displacement leads to a new mini-

imum energy domain configuration which represents a compromise between lower magnetization but greater magnetostatic energy.

In the foregoing we have assumed that the wall is quite free to respond to the applied field by propagating through the material. Very often, however, we find that domain wall motion is significantly hindered by an opposing force which may be likened to frictional drag arising, in most cases, from the wall's sensitivity to various material imperfections. Thus a threshold field referred to as 'domain wall coercivity', or just 'coercivity', must be applied to initiate wall motion in all but the most perfect materials.

Coercivity is a vital parameter in many magnetic material applications which, it should be emphasized, do not always call for the low coercivities associated with the structurally more perfect materials. For instance, high coercivity in permanent magnet materials is essential for them to support domain structures which do not minimize the magnetostatic and domain wall energies, and thereby retain overall permanent magnetic moments. In bubble materials, as we shall see, the opposite quality of very low coercivity is sought, so that domain walls respond quite freely to changes in magnetic field. This requirement dictates the need for highly perfect single crystal materials, since grain boundaries between crystallites, surface irregularities and the slightest imperfections introduce too high coercivities.

In bubble technology we are not only concerned with being able to initiate wall motion with very low forces, but we are also interested in moving walls very fast. Walls in various materials respond differently to attempts at rapid propagation because they are subject to a retarding force, analogous to viscous drag, which is highly dependent on the chemical composition and structure of the material involved. The mechanisms responsible for this drag are not fully understood. Its magnitude is expressed as 'domain wall mobility', which is inversely related to the drag. High mobility materials are therefore sought for bubble devices.

### 3. Bubble Domains

Domain structures in most materials are complicated both by the variety of directions which may be assumed by the magnetization, and by the presence of relatively large coercivity. Bubble materials present a radical departure from this situation in only supporting domains magnetized parallel to a single axis, and by possessing uniformly low coercivity.

Let us examine Fig. 2(a) which illustrates a typical domain structure for a thin slice of bubble material in a demagnetized condition; that is, in the absence of an applied magnetic field. Since the coercivity is low, the pattern represents the type of compromise already discussed which minimizes the total of wall and magnetostatic energy. Smoothly rounded walls are obviously the best means for reducing wall energy, while the entwined snake-like shapes serve to minimize the magnetostatic fields. Though simply conceived in the above terms, such a domain arrangement is not so readily achieved. Reduction of magnetostatic energy in most

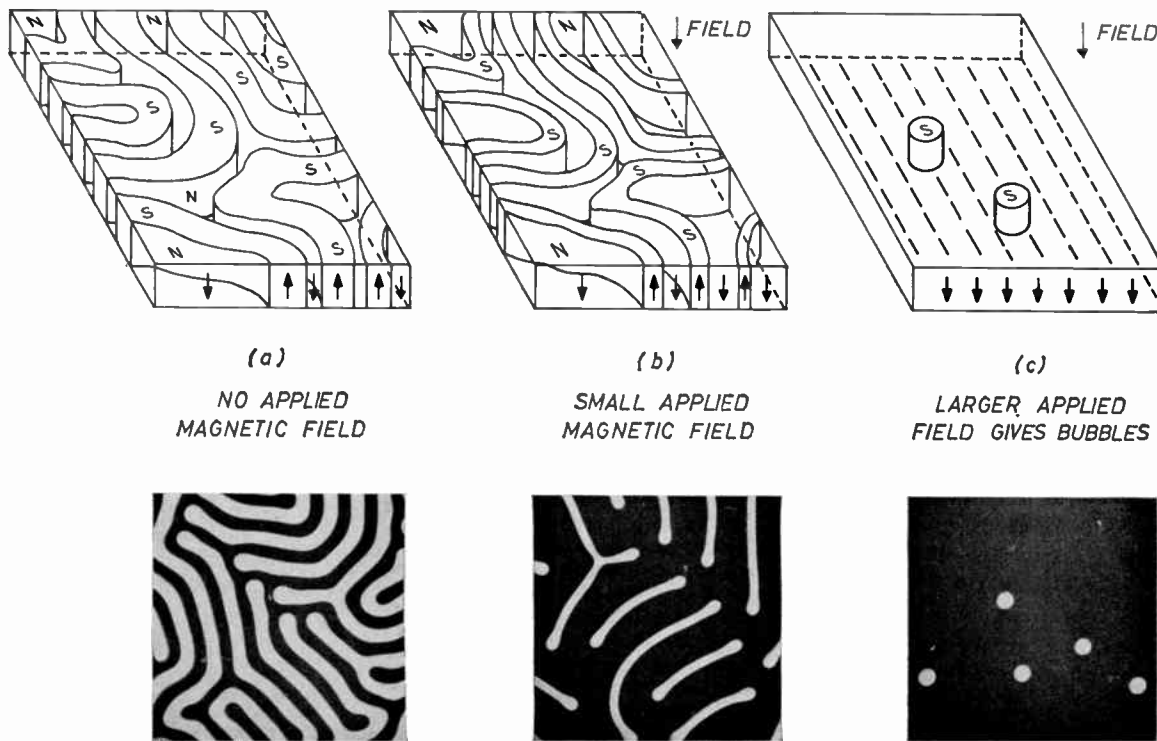


Fig. 2. Bubble domains are formed when material is immersed in a suitable applied bias field. Photographs of domains in actual material are shown.

materials forces domain magnetization directions to lie in, and not perpendicular to, the plane of a slice. To overcome this tendency bubble materials must be endowed with what is known as 'uniaxial anisotropy'. That is to say, the energy of magnetization must vary with direction, and be sufficiently low along a specific direction to resist the magnetostatic force towards in-plane magnetization when the material is prepared with this 'easy axis' normal to the plane of a slice. Hence we should recognize the vital role of uniaxial anisotropy in restricting the magnetization to up and down domains. But once this has been established we may proceed to discuss the behaviour of up and down domains without any particular regard for the presence of uniaxial anisotropy.

We also note that since the easy axis corresponds to a unique crystallographic direction in these materials, single crystals are essential for uniform domain structures over a slice. One might argue that a suitably oriented polycrystalline mosaic can satisfy the need for the easy axis normal to the slice. However, the coercivity associated with crystal grain boundaries rules out this possibility for practical bubble materials.

If we now apply a small magnetic field normal to the slice, domains parallel to the field grow at the expense of those oppositely magnetized, and the pattern is modified to something like that shown in Fig. 2(b). Just as for the bar magnet example, the total energy  $E_t$  which is minimized is given by,

$$E_t = E_w + E_d + E_m \quad \dots\dots(1)$$

where  $E_w$  = wall energy,  
 $E_d$  = magnetostatic energy,  
 and  $E_m$  = magnetization energy.

When the applied field reaches a critical value the 'island' domains shown in Fig. 2(b) snap into stable cylindrical 'bubble' domains as shown in Fig. 2(c). The field may be further increased until, after a threefold reduction in diameter, bubbles collapse leaving the slice completely magnetized in the direction of the applied field. For slices of the optimum thickness (about half the average bubble diameter), the field may be varied as much as  $\pm 20\%$  between the run-out and collapse limits. Additional island domains may be produced by cutting existing domains in demagnetized slices with a high local magnetic field, such as may be produced at the tip of a fine magnetic wire. Figure 10 illustrates this process. We shall, however, see that this operation is more elegantly performed in bubble devices. The graphs in Fig. 3 show how the terms in eqn. (1) sum to give a minimum energy corresponding to a stable bubble diameter at a fixed applied field. Under these conditions bubbles are stable for an indefinite period.

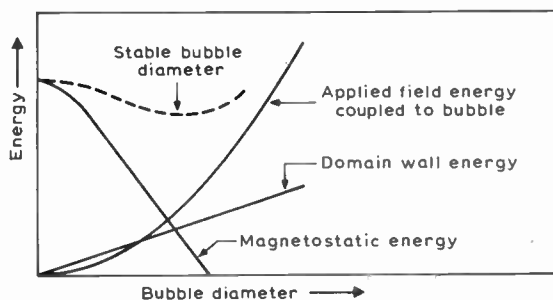


Fig. 3. The stable bubble diameter for a fixed applied field is determined by minimum total energy. (The dotted line represents the total energy.)

One particularly useful attribute of bubble materials under experimental investigation is their transparency to light, which permits domains to be directly observed under a microscope. Figure 4 illustrates how observation depends on the use of polarized illumination. Oppositely magnetized domains rotate the plane of polarization of the transmitted light by small amounts in opposite directions (Faraday rotation) and thus viewing through an analyser reveals domains as clearly defined light and dark regions. Thence the photographs in Fig. 2 illustrate the formation of bubbles under a magnetic field in an actual slice of bubble material.

Magnetic bubbles may be visualized as short cylindrical dipole magnets afloat in a near frictionless plane of reverse magnetization. They are attracted and repelled by field gradients in much the same manner as ordinary magnets, and since they are scarcely constrained by coercivity forces, respond to such gradients with almost frictionless motion. This requires nothing more than the propagation of a cylindrical domain wall; no transport of material is involved, and thus no mechanical inertia limits acceleration of bubbles. Bubbles, just as magnets with like poles placed closest, repel one another, and therefore display a strong tendency to spring apart when moved together. These properties are fundamental to the controlled manipulation of bubbles in devices, but before they are described we briefly review actual bubble materials.

**4. Bubble Materials**

To begin we list the most important properties required of bubble materials:

**Uniaxial anisotropy:** This must be sufficiently large to restrict magnetization to only up and down directions normal to the slice.

**Low saturation magnetization:** This limits the anisotropy required to lower values, sets the magnetic bias field needed for bubble formation at conveniently low strength, and, for the materials available, results in bubbles of the desired diameter. Typically  $4\pi M_s = 200$  gauss.

**Very low domain wall coercivity—less than 24 AT/m.**

**High domain wall mobility— $125 \text{ cm s}^{-1} \text{ A}^{-1}$  is desirable.**

**Bubble diameters of about  $8 \mu\text{m}$ .**

**Good temperature stability.**

The existence of an acceptable method for the preparation of defect-free  $5\text{--}10 \mu\text{m}$  thick single crystal films of material oriented with the easy axis normal to the surface.

To what extent have these goals been reached?

The first materials which provided an experimental vehicle for bubble research were rare-earth orthoferrites—crystals possessing orthorhombic structure, described by the chemical formula  $\text{RFeO}_3$ , where the element R is yttrium, or one of a group known as the rare-earth elements. The most fundamental barrier to the use of the orthoferrites was that none could be found to support small enough bubbles to give economic packing densities (about  $1 \text{ M bit/in.}^2 - 1.5 \times 10^5 \text{ bit/cm}^2$ ). Bubbles  $50 \mu\text{m}$  in diameter—less than human hair—were still too large. In addition it was found extremely difficult to reproducibly-prepare defect free crystals. These problems have been resolved by the discovery at the Bell Telephone Laboratories, Murray Hill,<sup>4</sup> that certain synthetic rare-earth garnet crystals supported ‘right’ sized bubbles. Methods were found for obtaining epitaxial growth of these garnet materials in the form of thin uniform films on the surface of non-magnetic substrates—a far more satisfactory technique than the bulk growth, and subsequent slicing and polishing of single crystal orthoferrites.

In these epitaxial techniques the grown material adopts the crystalline structure and orientation of the substrate on which it is deposited. Rare-earth bubble garnets are thus deposited on suitable single crystal substrates which also provide the mechanical support essential for  $5\text{--}10 \mu\text{m}$  thick bubble films without adversely contributing to their magnetic behaviour.

The rare-earth garnet system offers considerable flexibility for moulding properties to satisfy the above requirements. This can be appreciated from the variability of their chemical composition  $\text{R}_3\text{Fe}_5\text{O}_{12}$ , where R represents yttrium, or/and a combination of rare-earth elements, of which ten are widely used. Additional

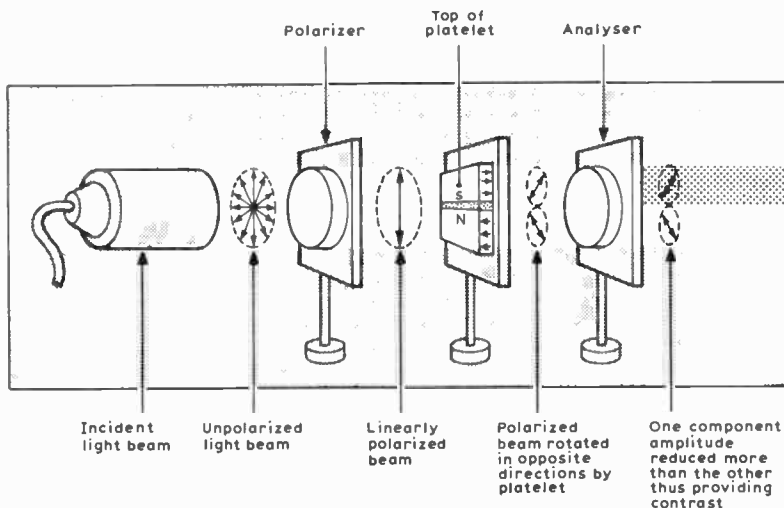


Fig. 4. Faraday rotation of polarized light transmitted by reverse domains is used for optical domain observation.

control over properties is effected by partial substitution of non-magnetic gallium or/and aluminium atoms for the iron, usually to lower the saturation magnetization.

The body of scientific data and understanding which have been assembled over recent years, particularly as a result of interest in the microwave applications of garnets, is a considerable aid in the search for good materials. But actual materials development involves a subtle mixture of scientific reasoning and pure trial and error in a juggling process which, in addition to seeking the best compromise between what often appear to be incompatible properties, must also offer bubble materials well matched to available substrates. The most commonly used substrate is gadolinium gallium garnet which, unlike bubble materials, is commercially available. Compositions such as  $Y_{1.3}Gd_1Yb_{0.7}Ga_{0.9}Fe_{4.1}O_{12}$  and  $Er_1Gd_2Ga_{0.8}Fe_{4.2}O_{12}$  are typical of those grown on this substrate material.

No 'ideal' material has yet been claimed and the best composition may have to be selected for each particular application. Excellent materials have however been prepared to high standards of perfection and successfully operated in devices. Mobility and temperature stability are the principal areas requiring improvement.

## 5. Growth of Bubble Materials

Two techniques for the epitaxial growth of bubble materials are widely used. Both have their merits.

Liquid phase epitaxy (l.p.e.) involves the dipping of specially polished substrate crystals into a melt of the constituent oxides of the garnet composition to be grown, mixed with suitable fluxing compounds, at about 950°C. Once mastered, this technique is relatively simple, and also has the advantage of being fairly inexpensive to install and operate. Excellent films have been grown with a degree of reproducibility. Figure 5 shows a substrate coated with a l.p.e. garnet film, alongside a polished substrate and the transparent garnet boule from which it was sliced.

Chemical vapour deposition (c.v.d.), as the name suggests, is based on the epitaxial deposition of bubble garnet films from gaseous mixtures of the appropriate metal halides, oxygen and other gases, at temperatures around 1200°C. Though considerably more complex than l.p.e., and also more costly to set up, the proponents of c.v.d. see it as the better process for the production of bubble materials on an industrial scale.

## 6. Bubble Devices

We have described the physical properties of magnetic bubbles and their host materials in some detail. We will now discuss how these properties may be utilized to implement magnetic bubble devices such as memories and data processing systems.

A basic requirement of any bubble device is the provision of a steady magnetic bias field and the use of permanent magnet structure, for this ensures the integrity of the stored information in the event of power failure. This field, applied normal to the magnetic material slice, may

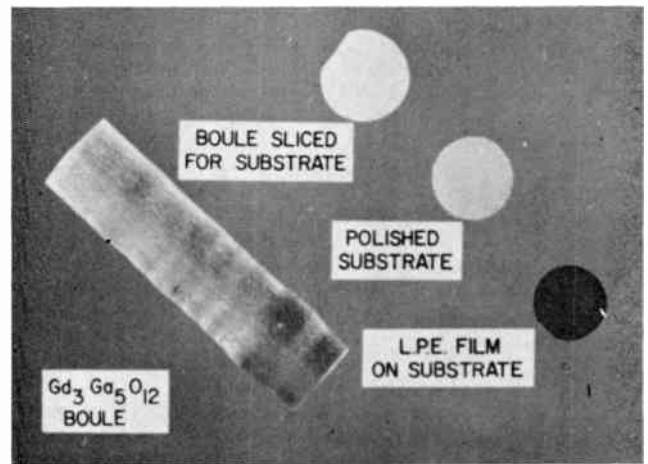


Fig. 5. Preparation sequence of substrates coated with bubble material by liquid phase epitaxy.

be varied within a  $\pm 20\%$  range without exceeding the stability limits of the bubbles, the only effect being a threefold reduction in bubble size on increasing the bias field between the run-out and collapse stability limits.

In the bubble devices, which we now describe, the presence or absence of bubbles at specific locations constitutes a binary pattern, which is used to represent binary information. If we now provide for the controlled creation, transfer, interaction and detection of bubbles, we have the basis of a very compact information storage and processing system; a bubble device. Such a system need have no moving parts, can be designed with a small number of electrical connexions, consumes little power, and promises to be cheap and reliable. Single crystal garnet materials which support bubble sizes in the order of 8  $\mu\text{m}$  are available. Packing densities up to about  $10^6$  bubbles/in<sup>2</sup> ( $1.5 \times 10^5/\text{cm}^2$ ) may be achieved for this size before the repulsive forces between bubbles interfere with device operation.

Bubble generation and annihilation are means by which information may be written into and removed from devices. Used in this manner it is clear these functions must be controlled. Information may also be introduced without these functions by rearranging the locations of a fixed number of bubbles, rather like beads on an abacus. However, such a system loses the freedom of allowing every bubble location to be used to store a bit. Propagation allows function facilities such as bubble generation and detection to be restricted to a few locations on the material, between which information is transferred by propagation.

Also in the processing of bubble patterns the repulsive interaction between bubbles in close proximity may be utilized. This effect can be used to divert a bubble in two alternate directions depending on the presence or absence of another bubble in some adjacent position. Such magnetic bubble systems will also be provided with read-out facilities, that is, detection devices for bubbles or bubble patterns.

Thus to convey what is involved in the design of a complete magnetic bubble system we describe how the

following essential operational functions may be realized and organized to yield various device properties:

PROPAGATION GENERATION ANNIHILATION  
DETECTION INTERACTION

### 7. Bubble Propagation

The ease with which bubbles can be moved about their host material is fundamental to all devices. Various propagation techniques which are employed for the controlled movement of bubbles along selected routes will be described. The propagation tracks themselves normally consist of linear arrays of bubble locations, which also function as the memory of the device. Propagation normally involves translation of all the bubbles in a track by the same number of locations in a shift register fashion.

The velocity of propagation<sup>2</sup>  $v$  of a bubble is described by the equation of motion,

$$|v| = \left(\frac{\mu_w}{2}\right) \left[ \left(\frac{\partial H_z}{\partial x}\right) d - H_c \frac{8}{\pi} \right], \quad \dots\dots(2)$$

where

- $\mu_w$  = wall mobility,
- $H_c$  = domain wall coercivity,
- $H_z$  = applied field normal to the slice,
- $x$  = distance in the plane of the slice,  
in the direction along which  $H_z$  changes,
- and  $d$  = bubble diameter.

Also

$$\mu_w = \frac{2M_s}{\beta},$$

where  $\beta$  is the viscous damping factor and  $M_s$  is the saturation magnetization.

Hence the term

$$\left(\frac{\partial H_z}{\partial x}\right),$$

which defines a gradient in the bias field across a bubble, constitutes the motivating force for bubble propagation. Bubbles tend to move away from regions of high field by a process of repulsion similar to that occurring when a bar magnet is held in the non-uniform field of another similar magnet. Conversely they are attracted by regions of lower field. The wall coercivity  $H_c$  determines the magnitude of the field gradient required to initiate bubble motion, after which the velocity that may be achieved depends on the mobility term. (Velocities of 200–1500 cm/s have been achieved.) The distance a bubble can move along a particular field gradient is limited by the need to maintain the bias field within the bubble run-out and collapse field limits. Thus low coercivities, generally below 24 AT/m, are important in ensuring adequate bubble propagation distances within the stability limits.

If, however, a moving field gradient is applied to the bubble, there need be no limit to the propagation distance. The bubble will effectively ‘slide’ on the gradient, on which it finds a position such that the motivating force associated with the magnitude of the gradient at that point just balances the retarding forces arising from coercivity and viscous damping.

As the bubble moves in response to the field gradient the volume of material between its starting and finishing positions is switched from magnetization in one direction normal to the platelet surface to the opposite direction, and back again. The minute energy required to switch this volume of material must be supplied by the applied field, and represents the basic mechanism of power dissipation in moving a bubble.

If a travelling periodic series of suitable field gradients, with a spatial period of a few bubble diameters, can be generated near the surface of a platelet a stream of bubbles can be propagated in the plane of the platelet. Several means of generating such travelling field gradients have been experimented with successfully, notably the 3-phase conductor and T-bar magnetic propagation circuits.

#### 7.1. Three-phase Conductor Propagation Circuit

Figure 6 shows a linear array of gold conductors photoengraved on a glass plate. This pattern is a square spiral of three conductors, which are connected together at the centre of the spiral. When driven with a 3-phase sinusoidal oscillator, the pattern generates a travelling magnetic wave which has been used to propagate magnetic bubbles in a variety of orthoferrites and garnet platelets.

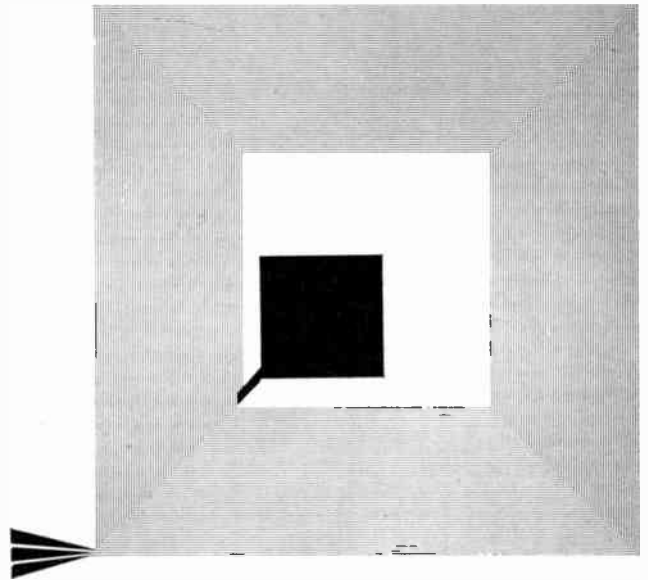


Fig. 6. 3-phase conductor spiral for bubble propagation.

A platelet was simply placed close to the pattern, and provided the magnetic bubble diameter was comparable to the conductor pattern period, propagation occurred at the rate of three conductor periods per complete cycle of the three phase drive currents. Typical drive currents of 10 mA r.m.s. per phase were required.

Defects in the material, such as crystal and surface polishing imperfections, can cause deviations in the propagation path of a bubble, or cause the bubble to stop entirely. Bubbles propagated by such a pattern may be confined to specific paths by the introduction of permalloy guide rails perpendicular to the conductors. Guide rails photoetched from a 5000 Å (0.5 µm) thick

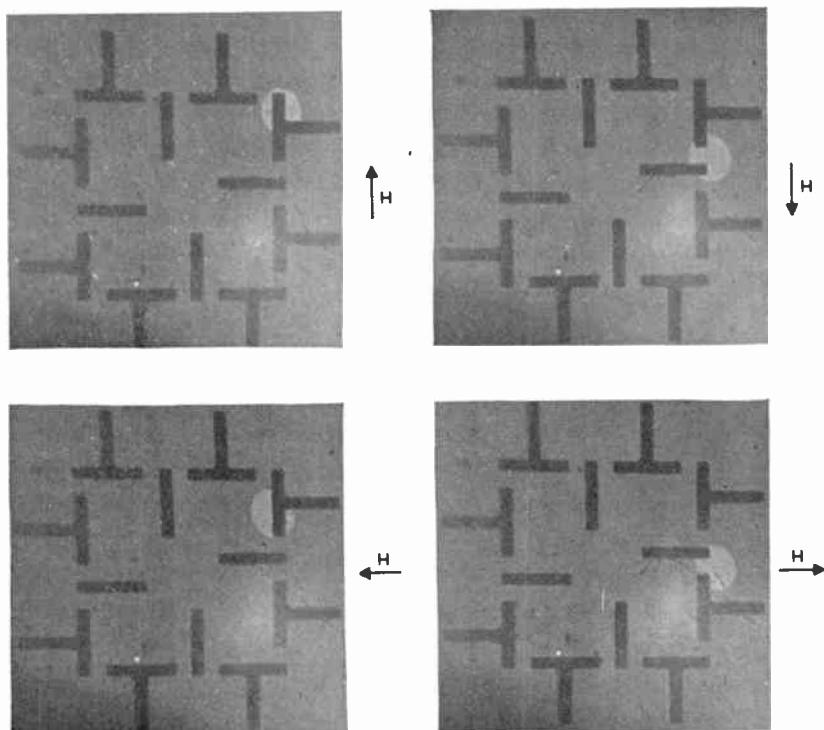


Fig. 7. T-bar array showing the propagation of a 0.002 in diameter bubble for a single field rotation.

evaporated permalloy film and of approximately the same width as the conductor lines were introduced on the other side of the magnetic platelet. Propagation rates of 1-10 M bit/s are feasible using conductor patterns.

7.2. T-bar Magnetic Propagation Circuit

Figure 7 shows a pattern of T and I shaped bars<sup>5</sup> fabricated on a glass substrate from a 5000 Å thick 81% Ni 19% Fe evaporated permalloy film using standard photo-lithographic techniques. This pattern provides another method of producing a periodic series of travelling magnetic field gradients at the platelet surface, when it is immersed in a magnetic field which rotates in the plane of the platelet. Figure 8 indicates how the rotating field induces attractive and repulsive poles in the permalloy elements. A bubble will be propagated one period of the pattern per 360° rotation of the drive field. During fabrication, evaporation of the permalloy is carefully controlled to produce films with isotropic magnetic properties, and low coercivity ( $H_c$ ). Films with  $H_c$  less than 120 AT/m are acceptable, and a rotating field amplitude of about 1600 AT/m is sufficient to saturate the permalloy elements along their longest dimensions. The bar elements in Fig. 9 are approximately  $25 \times 5 \mu\text{m}$ , and are suitable for propagating  $10 \mu\text{m}$  diameter bubbles. The 5:1 aspect ratio of these elements provides them with what is known as shape anisotropy. While easy saturation of the elements is possible along their length, the larger demagnetizing field across the elements tends to prevent saturation in this direction. Without such shape anisotropy the magnetic bubbles would tend to rotate around the permalloy elements in a spurious propagation mode.

These permalloy elements can be arranged in large arrays to form long serial shift registers that can be used for storage applications. Such patterns have the

advantage that magnetic bubbles may be stored and moved without any physical connexions, access being achieved through rotations of the in-plane rotating magnetic field. The energy required to switch the permalloy elements and move bubbles through the platelet drivers, is, of course, supplied by the rotating field drivers.

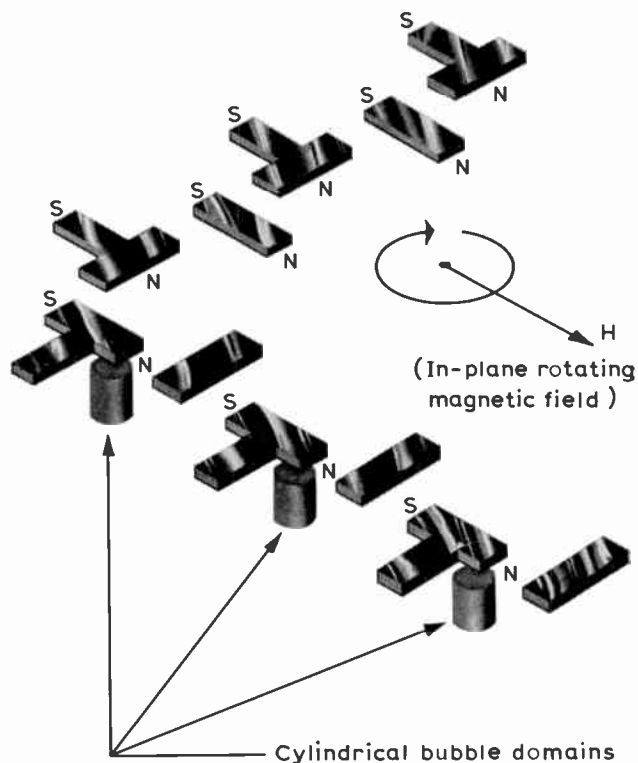


Fig. 8. The bubble is attracted to poles induced in T-bar elements by a rotating in-plane magnetic field.

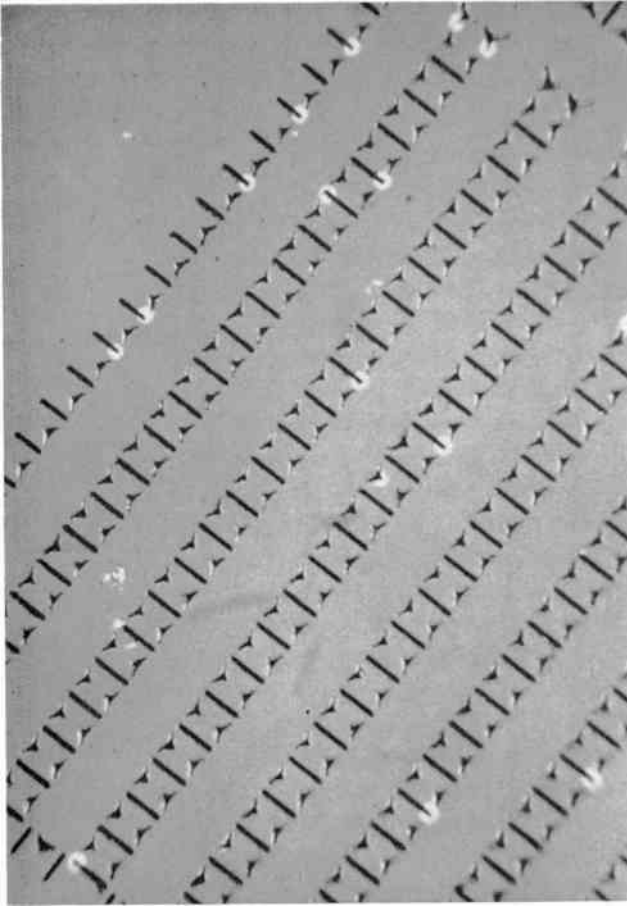


Fig. 9. A section of a large bubble shift register array.

Propagation rates of 1–2 M bit/s have been reported for this type of circuit. The in-plane rotating magnetic field may be generated by two sets of mutually perpendicular Helmholtz coils. These are driven by sinusoidal currents with 90° phase difference between each coil set, thereby producing a uniform rotating magnetic field. Helmholtz coils provide a large volume of uniform field. They are driven by integrated circuit drivers which are controlled by means of a Johnstone ring counter controlled by a master clock. Ring counters provide a convenient method of controlling the phase shift between the two drive currents. Such a digital control arrangement allows easy decode of the field rotation increments for timing purposes. The arrangement is also a convenient source of trigger pulses for stroboscopic observation of the dynamic magnetic domain behaviour.

### 8. Bubble Generation

Figure 10 shows the path left by a magnetic wire probe after cutting across and subdividing the light strip domains. A magnetic cutting field can also be generated by means of current pulses in conductor loops. Larger currents than used to propagate bubbles are necessary.

Figure 11 shows the configuration of a conductor-controlled generator that utilizes a permalloy pattern to stretch the magnetic domain which may then be cut by means of a current pulse through the conductor loop.

The generator is loaded with a seed domain which will

rotate around the perimeter of the square pattern under the influence of magnetic poles induced in the permalloy by the rotating magnetic field. The sequence (b) to (g) in Fig. 11 shows the seed domain rotating. When the seed domain is influenced by poles induced on the other permalloy elements, as in the sequence at (e) and (f), the domain is stretched. A current pulse in the conductor loop at the time shown in (f) will cause the generation of a bubble as shown in (g). This bubble will then be propagated away along the permalloy track. If the conductor loop is not pulsed with current the stretched domain will be pulled back under the square shaped permalloy by a strong pole induced as shown in (b). Thus no bubble generation occurs. The conductor is pulsed with current according to the input information. This process of generating bubbles may be continued indefinitely without depleting the seed domain because the energy required to maintain the size of the seed is supplied continuously from the rotating field through the interaction of the seed domain and permalloy generating element. Free-running permalloy generators which generate one bubble for every complete rotation of the field without the aid of a conductor have also been fabricated.

### 9. Annihilation

In a magnetic bubble device such as a memory, facilities for erasing information are required. This means we must be able to annihilate unwanted magnetic bubbles. The simplest means of achieving this is locally to increase the bias field above the critical value for bubble collapse. This can easily be accomplished with a conductor loop,



Fig. 10. The path left by a magnetic wire probe demonstrates the cutting of domains.

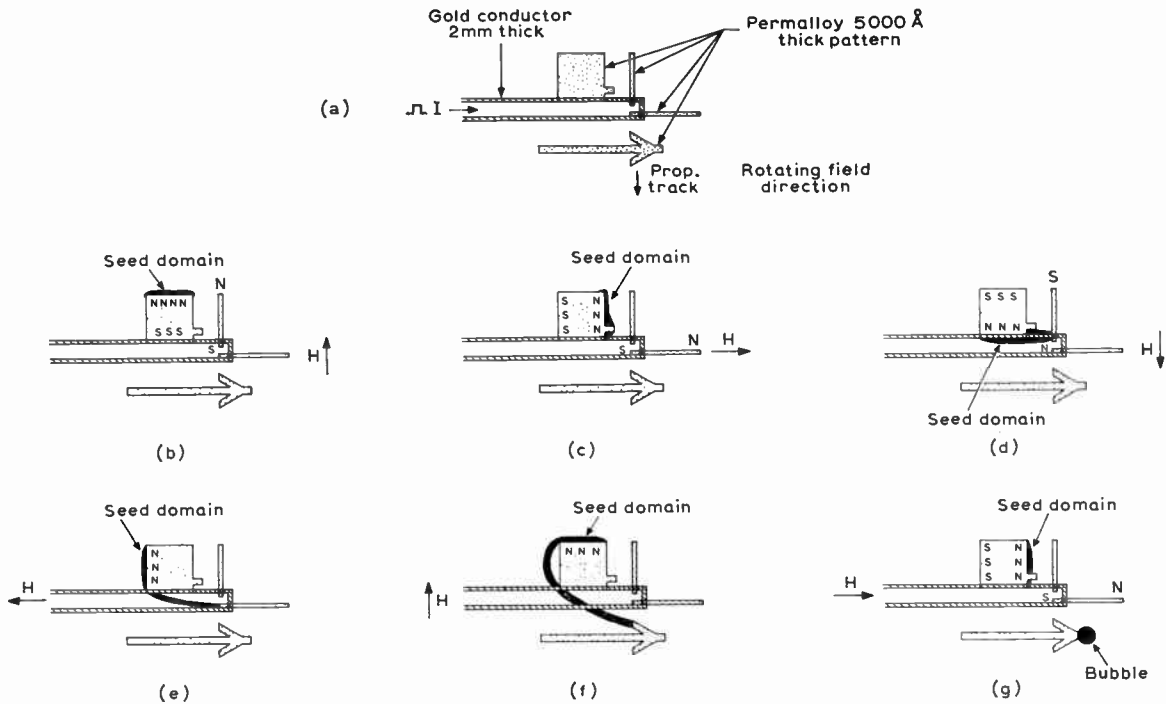


Fig. 11. Bubble generation circuit.

which requires connexions and a current source. However, permalloy patterns have been devised that can cause a bubble to collapse under the influence of the rotating magnetic field used for propagating and generating bubbles.

10. Detection

A bubble detector forms an essential part of the devices. Three basic methods of detection are shown in Fig. 12. In Fig. 12(a) is shown a simple method of electromagnetic induction where a conductor loop is arranged so that the magnetic field of a passing bubble will couple with it, thus inducing a small electromotive force. In orthoferrites, at typical bubble propagation velocities, no more than 100  $\mu$ V output can be obtained for a single loop. The output voltage could be increased by expanding a bubble at a read-out location, but this would require excessive platelet area. Also the detector loop could be made into a multi-turn coil, but this is difficult on such a small scale.

The magneto-optic detection method shown in Fig. 12(c) is almost identical to the system used for domain observation as shown in Fig. 4, with an appropriately small light source and a photo-diode replacing the human eye. The source, detector and other optical components as shown in Fig. 12(c) are carefully aligned either side of the platelet at the desired read-out location. This read-out method has the advantage that it can operate with stationary bubbles but is severely limited in sensitivity for small bubble diameters. The multiple layers of optical components would be difficult to assemble and the losses in the various layers demand a high intensity source and the accompanying power dissipation.

Conventional Hall effect devices which respond to

magnetic fields are too large for the detection of magnetic bubbles. A much smaller silicon Hall effect device with an active area matching that of the bubble has been developed.<sup>6</sup> A usable signal of 1 mV is obtained by means of the interactions of the flux emanating from a 0.05 mm (2 mils) diameter bubble with an externally supplied current of 10 mA flowing in the Hall device (Fig. 12(b)).

Experiments with magnetoresistors<sup>7, 8</sup> indicate that these devices are very suitable for magnetic bubble detection. The magnetoresistor consists of a 200 Å (20 nm) thin film rectangle of permalloy with two connecting leads of 5000 Å (0.5  $\mu$ m) thick gold. When activated with a current flow its resistance will be reduced by a magnetic flux density at right angles to the current flow and in the plane of the device. This device is also sensitive to an in-plane rotating field as well as the tangential component of a bubble's magnetic field.

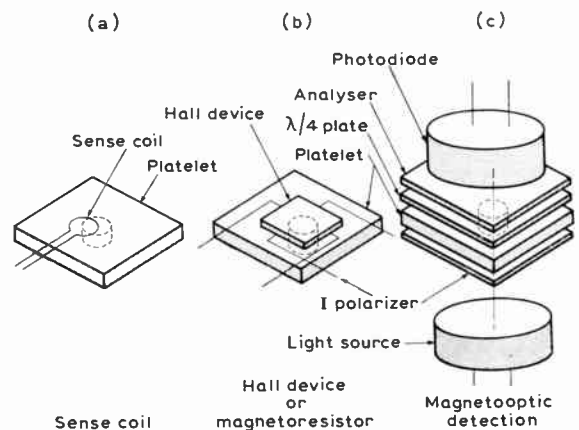


Fig. 12. Detection methods.

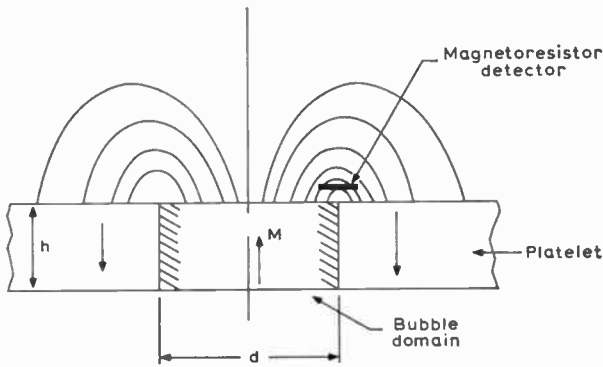


Fig. 13. Side view of the contours of constant in-plane field from a typical bubble domain.

Changes in resistance of approximately 3% can be obtained. Figure 13 shows the magnetic field of the bubble. Optimum output from this detector is obtained when the centre of the magneto-resistor is directly over the edge of the magnetic bubble and as close as possible to the surface of the platelet.

Figure 14 shows typical outputs from a magneto-resistor arranged in a bridge circuit as a bubble crosses over the detector. Curves A3 and A5 are the responses of a 0.03 mm wide detector to 0.076 mm and 0.127 mm diameter bubbles respectively, and B3 and B5 are the corresponding responses of a 0.005 mm wide detector to the same bubbles. C5 is the response with the detector further away.

Figure 15 shows how the output of the device is limited by heating effects at higher current densities.

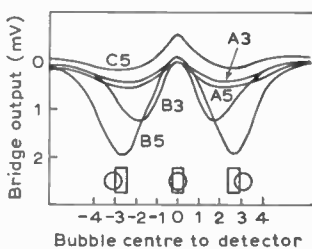


Fig. 14. Magneto-resistive bridge detector output with bubble to detector spacing.

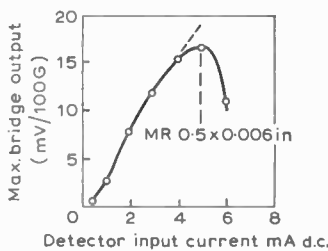


Fig. 15. Magneto-resistive bridge detector output against detector input current.

have a flat frequency response up to at least 30 MHz and operate at power levels of a few milliwatts, they are very suitable for bubble detection. The bridge configuration permits cancellation of voltages derived from magneto-resistance variations due to the in-plane rotating field. The magneto-resistor bridge can be fabricated to have resistance and output signal characteristics suitable for amplification by integrated circuits. Figure 17 shows an arrangement used.

### 11. Bubble Interaction Logic

The effect of a magnetic field gradient on a bubble has been discussed. In bubble circuits performing logic functions magnetic bubbles are moved into the influence of magnetic fields, which can emanate from other magnetic bubbles, current-carrying conductors or magnetic circuit elements, the resulting interaction causing alternative routing of magnetic bubbles.

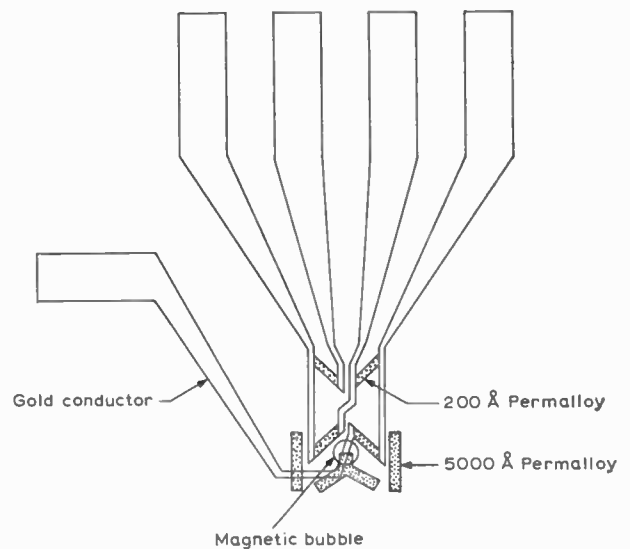


Fig. 16. Magneto-resistive bridge configuration for magnetic bubble detection.

In the bubble devices described so far the manipulation and reconfiguration of bubble patterns by externally controlled means only have been discussed. This control is exercised by the in-plane rotating drive field in interaction with the permalloy patterns and/or electrical signals supplied to conductor loops on the surface of the bubble carrier.

The repulsive interaction between bubbles can be utilized to execute internal control over propagation, generation and annihilation, by employing device elements similar to T-bar structures to cause two bubble streams in different propagation tracks to be incident at an interaction area.

The simplest interaction device, called a conditional transfer gate, is shown schematically in Fig. 18(a). It features two input channels S and X, three output channels S', V, W, and an interaction area between the channels X and S. A bubble entering channel S is propagated straight to the output S'. If, at the same time, another bubble enters the input X, then this bubble will

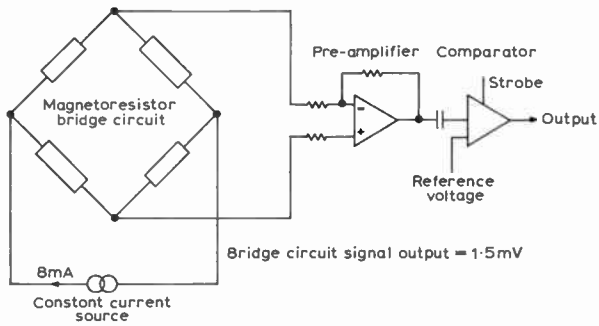


Fig. 17. Bubble detecting circuit.

be deflected into channel W by the repulsive force from the bubble in channel S. If channel S is empty, then the bubble in channel X propagates to the output V instead. This gate resembles a transfer relay and performs the logic functions,

$$S' = S; \quad V = \bar{S} \cdot X; \quad W = S \cdot X.$$

When the input channel X is connected to a free running bubble generator which, in fact, provides the signal  $X = 1$ , then the outputs yield,

$$S' = S; \quad V = \bar{S}; \quad W = S.$$

Thus, the gate can be operated in a logically complete way, since inversion, replication and the AND function can be realized.

A particularly useful feature of this gate is the conservation of one input variable. This allows the design of logic networks, which in combination with a free-running bubble generator can compute any desired logic function and its complement.<sup>11</sup> The conservation of the input pattern is an important feature for associative processing where several successive computations have to be executed on the same logic variables.

Another useful basic logic element is a device merging two propagation tracks. This gate, shown schematically in Fig. 18(b), can be used to perform the OR function between two mutually exclusive signals.

As an example, a tree-structured network employing a bubble generator, conditional transfer gates and merging gates is shown in Fig. 18(d). It computes all minterms of three input variables and merges the appropriate terms to yield the complementary functions,

$$Z = V_1 V_2 V_3 + V_1 V_2 \bar{V}_3 + V_1 \bar{V}_2 V_3 + \bar{V}_1 V_2 V_3$$

$$\bar{Z} = \bar{V}_1 \bar{V}_2 V_3 + \bar{V}_1 V_2 \bar{V}_3 + V_1 \bar{V}_2 \bar{V}_3 + V_1 V_2 \bar{V}_3.$$

As can be seen in the diagram the input pattern is preserved.

Other logic gates utilizing bubble interactions and track merging have been described in the literature, the common feature of all these gates being bubble conservation between inputs and outputs. For instance, devices which perform the AND and OR functions simultaneously, and another one which yields two AND and an exclusive OR function have been reported.<sup>9</sup> These gates combine either one interaction area and a merging area, or two interaction areas and a merging area respectively. In all

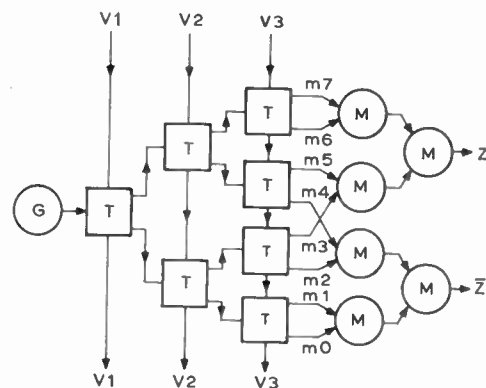
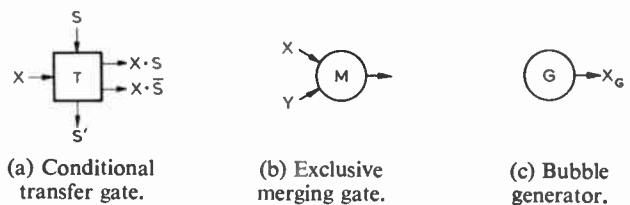
the gates logic functions are performed on every corresponding bubble in two serial bubble streams.

### 12. Potential Applications

The methods of generating, moving, detecting, annihilating, and interacting bubbles form the basis for constructing bubble devices with many applications in the telephone and computer industry. The high packing density, very low power requirement, small size and simplicity of interconnexions promise the development of a mass memory with a capacity of more than  $10^7$  bits contained within less than half of one cubic foot. By utilizing the unique properties of bubbles such a memory would be inherently low in cost, would have no moving mechanical parts, and would retain all stored information in the event of an electrical power failure. Very high reliability and lifetimes may therefore be expected. It seems that replacement of disk files is an attractive target for bubble memories. Such memories would probably operate in the serial mode and would not therefore be able to compete with the speed of semiconductor and other fast memories. They should, however, be cheap and fast enough to replace disk files by offering more reliable operation, in less volume and at lower power levels.

The development of a gate that allows bidirectional transfer of magnetic bubbles from one circulatory storage loop of permalloy elements to another under the control of a conductor field, will provide greater flexibility in the organization of a mass memory.

Figure 19 shows a useful mass memory organization<sup>10</sup> which consists of a number of storage loops arranged so that bubbles may be transferred to an empty access loop by means of bidirection transfer gates controlled by conductors. These gates may transfer one or several bubbles according to the memory organization. The



(d) Example of tree-structured logic network that generates all minterms and yields a desired output logic function.

Fig. 18.

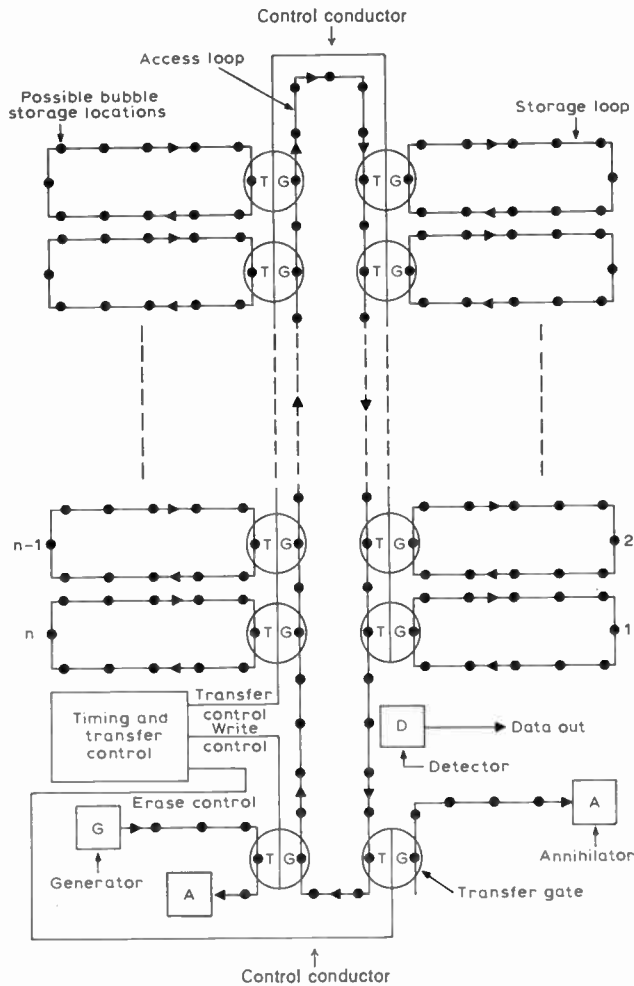


Fig. 19. Mass memory organization. Bubbles are stored in closed loops from which they may be transferred to an access loop for read-out and write operations.

bubbles in all the storage loops, and the access loop, are circulated around their respective loops in the same direction under the influence of a rotating in-plane field. When bubbles are transferred to the access loop they are propagated past the detector for read-out purposes. Whilst data is in the access loop it can be erased and replaced with new data if required. Otherwise, after passing the detector, the bubbles continue around the access loop, until they return to positions adjacent to their original storage loops, from which they can be transferred back into their storage sites. Erasure of data is accomplished by transferring bubbles into a minor loop terminated by an annihilator. New information is written into the memory by transferring bubbles from a bubble reservoir, formed by a minor loop fed by a generator and terminated by an annihilator, to the access loop, by means of a transfer gate controlled by incoming information. These new bubbles are circulated in the access loop for subsequent transfer to their storage loops. This type of organization is flexible, and allows a high ratio of storage capacity to the number of detectors which are relatively expensive. A number of blocks as shown in Fig. 19 can be arranged in an array, so that large blocks of information could be read out for transfer to

a faster memory in a system employing a hierarchy of memories.

An appropriate mix of storage and logic function could result in cheap associative memories and processors. Such memories could overcome access and serial search time limitations by the use of multiple access methods that would enable simultaneous search for, and output of, information.

### 13. Conclusion

We have given a broad account of many aspects of magnetic bubble technology, ranging from a description of the nature of bubbles and their host material, to a survey of the repertoire of techniques which has been devised to exploit their unique properties.

The feasibility of this technology has been well established, and what remains is the not inconsiderable task of development. While there seems little doubt of a place for magnetic bubble technology in future data storage and processing systems, many novel applications may also be expected to emerge.

### 14. Acknowledgments

The authors wish to thank members of their research group for helpful collaboration.

This work was supported in part by the Defence Research Board of Canada through its Defence Industrial Research program.

### 15. References

- 17th Conference on Magnetism and Magnetic Materials, Chicago, 1971.
- I.E.E.E. International Magnetics Conference, Denver, 1971.
- Thiele, A. A., 'The theory of the static stability of cylindrical domains in uniaxial platelets', *J. Appl. Phys.*, **41**, p. 1139, 1970.
- Bobbeck, A. H., *et al.*, 'Uniaxial magnetic garnets for domain wall "bubble" devices', *Appl. Phys. Lett.*, **17**, p. 131, 1st August 1970.
- Perneski, A. J., 'Preparation of cylindrical magnetic domains in orthoferrites', *I.E.E.E. Trans. on Magnetics*, **MAG-5**, p. 554, 1969.
- Strauss, W. and Smith, G. E., 'Hall-effect domain detector', *J. Appl. Phys.*, **41**, p. 1169, 1970.
- Almasi, G. S., *et al.*, 'A magnetoresistive detector for bubble domains', *J. Appl. Phys.*, **42**, No. 4, p. 1268, March 1971.
- Lama, U., 'Optimization of magnetoresistive bubble domain detectors', Unpublished.
- Sandfort, R. M. and Burke, E. R., 'Logic functions for magnetic bubble devices', *I.E.E.E. Trans. on Magnetics*, **MAG-7**, p. 358, 1971.
- Bonyhard, P. I., *et al.*, 'Applications of bubble devices', *I.E.E.E. Trans. on Magnetics*, **MAG-6**, No. 3, p. 447, September 1970.
- Kluge, W., 'Computation of switching functions using input-pattern-conserving magnetic-bubble manipulations', *Electronics Letters*, **8**, No. 12, p. 313, June 1972.

Manuscript received by the Institution on 22nd May 1972. (Paper No. 1475/CC150.)

# Conduction and Magnetic Signalling in the Sea

## A Background Review

I. S. BOGIE\*

*Based on a paper presented at a Joint I.E.R.E.-S.U.T. Colloquium on 'Conduction and Magnetic Signalling in the Sea', held in London on 10th February 1972.*

### SUMMARY

Electromagnetic, conduction and magnetic induction techniques for communicating or navigating underwater are discussed in the light of some 75 published references.

\* The Decca Systems Study and Management Division, Jubilee Way, Chessington, Surrey.

### 1. Introduction

The author's interest in the application of electric and magnetic fields underwater originated from a study into underwater navigation sponsored jointly by the Decca Navigator Company Limited and the National Research Development Corporation. The study considered all possible techniques which might be used to provide a medium for communication, position fixing and navigation including obstacle detection, for use by divers, submersible vehicles and surface support units.

At the time of the study, detailed information on the subject of electric and magnetic fields underwater appeared to be lacking. Some recent reports, however, have shown a renewed interest and describe new devices which use these techniques and are currently available.

This paper is intended to provide an introduction to the subject and to the associated papers, and refers to some of the 'new devices' which have recently been developed. A comprehensive, but by no means exhaustive, bibliography is given for those wishing to pursue the subject.

### 2. Applications

The last few years have seen a tremendous increase in the number of organizations with interests in the peaceful exploration and exploitation of the sea and the seabed. Reasons vary from purely economic and political considerations to the need to seek alternative and additional sources of food, minerals and energy to meet the world's increasing demand.

The nature of the environment and its vast size have necessitated the development of sophisticated equipment and techniques to facilitate exploration. Submersible vehicles have been designed to transport men and instruments on extended midwater and seabed excursions. Very recently the use of manned submersibles for pipeline survey in the North Sea has been suggested by a major oil company.

Whatever the application, however, whether it concerns an instrument package, a diver or manned or unmanned vehicle, whether operating in the comparatively shallow continental shelf regions or in the deep oceans, information links of some kind or another are prerequisite. The link may be used for a variety of purposes such as:

- |                      |                             |
|----------------------|-----------------------------|
| position fixing      | obstacle detection          |
| guidance             | communication of data/voice |
| measurement of speed | remote control              |

### 3. Methods

Information can be transmitted underwater in a variety of ways. Direct methods necessitate the use of a mechanical link or electrical cable. Other methods involve the transmission of information in the form of light, sound or electric and magnetic fields. Invariably, however, there are limitations. Optical systems are generally limited to extremely short ranges because of backscatter and absorption. In the North Sea, for example, visibility is often zero or at best limited to 1-2 feet due to suspended matter in the water. Acoustic

systems are the most versatile and widely used means of underwater signalling and communication generally available. Both optical and acoustic systems however are unable to penetrate behind an object and suffer from shadow zones. In shallow water, the use of acoustic techniques can be severely affected by multi-path propagation due to reflection and refraction. The comparatively slow speed of propagation in water of the order of 1500 m/s is a limiting factor in terms of data rate. Where optical systems fail because of suspended matter in the water, and acoustic systems because of the existence of high ambient noise levels, methods using electric and magnetic fields may offer an effective alternative for use over short distances. Such methods would not be so liable to shadowing and could be used where security is required.

For the purposes of this paper only, the application of electric and magnetic field techniques to underwater signalling have been defined as follows:

**Electromagnetic propagation**—radio signals which are transmitted through air and water (e.g. the *Omega* navigation system).

**Conduction**—techniques in which an electric field is created by current flow through the water between spaced electrodes.

**Magnetic induction**—methods in which a magnetic field is created due to current in an insulated conductor.

The above classification is primarily one of convenience based on the method of transmission and reception, although clearly the above effects cannot be so isolated for theoretical treatment.

#### 4. Theoretical Considerations

Before reviewing some of the more recent 'new devices' it is perhaps appropriate to note some of the properties of seawater affecting the generation and propagation of electric and magnetic fields.

**Conductivity:** Typically 4 siemens per metre for seawater and 0.001 siemens per metre in the case of fresh water. Conductivity depends on a number of factors including salinity, temperature, pressure and excitation frequency.

**Permeability:** Usually taken to be that of free space, i.e.  $4\pi \times 10^{-7}$  henrys per metre. Both fresh and salt water are non-ferromagnetic and hence have negligible magnetic polarization.

**Permittivity:** Depends on frequency because water is a polar liquid but considered constant at frequencies below  $10^9$  Hz. The permittivity relative to free space varies between 78–81.

**Polarization:** Sea water is an electrolyte and subject to polarization effects unless current flow through the water is alternating.

The theory of electromagnetic radiation underwater will not be considered here but for convenience the various parameters such as wavelength, attenuation, skin depth and velocity are shown plotted with respect to frequency on Fig. 1 based on a value of conductivity

equal to 4 siemens per metre. The graph is correct for frequencies in the e.l.f., l.f. and m.f. bands where conduction currents dominate and displacement currents are negligible.

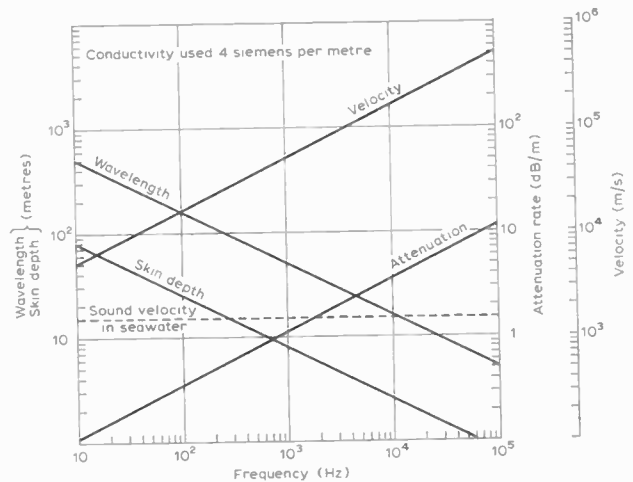


Fig. 1. Wavelength, attenuation and velocity of electromagnetic waves in sea water.

The graph illustrates the vast difference in wavelength between air and water.

At 100 kHz, for example,

$\lambda_{\text{air}} = 3000$  m whereas  $\lambda_{\text{sea}} = 5$  m (a reduction of 600:1)

At 10 kHz,

$\lambda_{\text{air}} = 30\,000$  m  $\lambda_{\text{sea}} = 15.9$  m (a reduction of 190:1)

At frequencies at which conductivity effects predominate sea water is considered to be a good conductor and the attenuation rate increases rapidly with increase in frequency. At 100 kHz it is approximately 11 dB/m whereas at 10 kHz it is approximately 3.5 dB/m.

Velocity of propagation is very much reduced in water and at a frequency of 1 Hz approaches the velocity of sound in sea water, i.e. 1500 m/s.

Electromagnetic radiation incident at the air–water interface is nearly all reflected, only a very small fraction, dependent on frequency, polarization, sea-state, etc., being refracted. There is thus a considerable interface loss.

#### 5. Electromagnetic Propagation

Underwater reception of electromagnetic signals propagated through the atmosphere is limited to the low and very low frequency bands because of the severe loss at the air/water interface and subsequent attenuation within the medium.

The first practical development in this area took place in 1918 when a loop antenna was adopted for use on submarines of the U.S. Navy.<sup>1</sup> The antenna was intended to be used for communication and direction finding. Apart from this early work very little is reported until the theory of electromagnetic radiation underwater was described in a thesis by Moore in 1951.<sup>2</sup> This paper, dealing with the theory of communication between submerged submarines, considered both electric and magnetic field components of vertical and horizontal dipoles

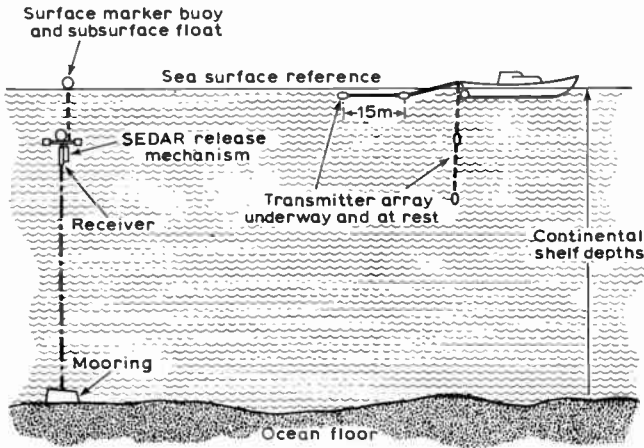


Fig. 2. Typical SEDAR application with the transmitter/receiver unit inset.

immersed in a conducting half space. The bibliography lists various other significant contributions in this area.

At the present time efforts are continuing into the use of *Omega* by submarines for near surface position fixing. *Omega* is a very low frequency (10–14 kHz) c.w. hyperbolic navigation system designed to provide coverage on a world-wide basis using a network of eight ground stations. Very little has been published into the use of *Omega* underwater. Difficulties are known to exist due to uncertainty as to the magnitude of the phase shift which occurs at the air–sea interface. Because of the difference in wavelength between air and water, depth must also be known so that the depth component can be eliminated.

In fresh water the picture is improved because the conductivity is much less than in sea water although the interface loss remains. During operations with the Vickers submersible *Pisces* in Loch Ness communication between surface and submersible were established in water depths greater than 30 m (100 ft) using portable receivers with a simple whip antenna mounted on the submersible. The reason for this extreme range is due to the purity of the water of Loch Ness. The frequency used is believed to be 150 MHz.

The successful transmission of electromagnetic waves underwater at frequencies up to 7 MHz have been reported in the literature.<sup>3</sup> In experiments with a 6 m dipole lowered to a depth of 76 m in sea water, a range of 460 m was claimed using a 250 W transmitter.

## 6. Conduction Fields

A discussion of theories of conduction signalling is given in the companion paper by M. J. Tucker.<sup>4, 5</sup> The three systems described below illustrate the way in which conduction field techniques have been reported as being used with some success. The applications described include:

- Remote command signalling
- Obstacle detection
- Voice communication

### 6.1. Remote Command Signalling

The system described by the Braincon Corporation<sup>6</sup> is designed to actuate a remote release mechanism to facilitate the recovery of deployed gear or instrument packages at or near the seabed. The system is usually referred to under the trade name SEDAR which stands for Submerged Electrode Detection And Ranging. The equipment consists of a surface towed transmitter array and a combined receiver and release mechanism moored at depths down to 200 m. A typical application is illustrated in Fig. 2. It is claimed that the system will operate at slant ranges up to 1000 m. Power output is quoted as 1000 W at 115 V ac.

### 6.2. Obstacle Detection

Another practical application using underwater electric fields is that of obstacle detection which has recently been reported.<sup>7</sup> The application is described as an effective aid to blind navigation in restricted waters. It is claimed that the system can be used by both surface and underwater vessels for negotiating narrow channels and operating in close proximity to the seabed.

The principle of operation is analogous to that of the electrolytic tank in which the distribution of potential is obtained by field plotting techniques. In the present application, by applying an alternating potential across two electrodes mounted in the water at bow and stern respectively, an electric field is produced in the water surrounding the hull, with the current flowing in the sea between the electrodes. A functional diagram is given in Fig. 3.

For the purposes of this explanation, it is assumed that the water surrounding the hull extends to infinity in all directions and that the hull is symmetrical in shape about the longitudinal vertical centre line, and has a continuous surface constructed of similar material.

Under these idealized conditions, therefore, current between bow and stern electrodes, will be symmetrically distributed in some manner either side of the hull. Thus no potential difference will exist between two electrodes symmetrically disposed about the hull since they would be located on a line of equipotential across which current cannot flow. If now a material, which is either a conductor, with conductivity different to that of the media, or

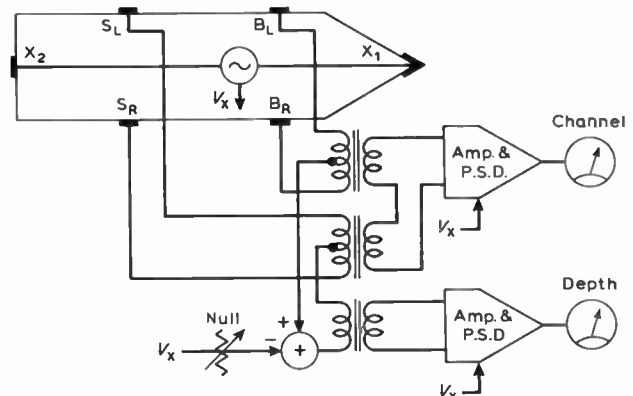


Fig. 3. Functional diagram of obstacle detection system.

an insulator is placed in the vicinity of the hull but on one side only, then the lines of current flow around the hull on that side will be distorted depending upon whether current has to flow around or through the material. When this occurs however, because the current distribution is affected, so also are the lines of equipotential about the hull. Thus by comparing port and starboard potentials with respect to the bow electrode, a port or starboard obstacle can be detected as shown in Fig. 4. This device can thus be used to detect the presence of obstacles which produce anomalies in the known electric field surrounding the ship's hull.

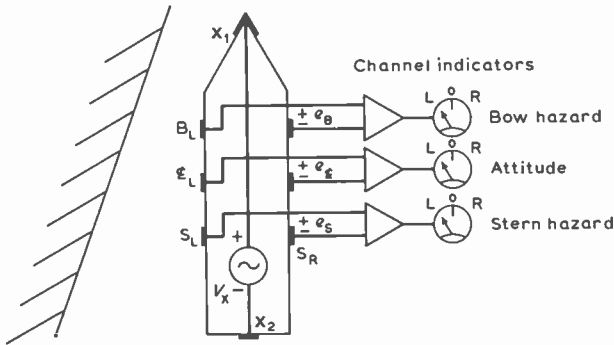


Fig. 4. Typical configuration of obstacle detecting system.

In practice it has been found that wave action and the boat's pitch and roll determine the useful detection range. This was quoted as of the order of  $1\frac{1}{2}$  boat lengths for the smaller vessels but was expected to be of the order of 2-3 boat lengths on larger ships and submarines.

Certain fish are capable of generating an electric field around themselves and using this as a means for detecting the presence of obstacles and prey. In some electrically strong fish the power generated is considerable and is used for stunning their prey and foe.<sup>8</sup>

### 6.3. Voice Communication

A system described as operating on the principle of power-modulated 'conduction current signalling' appeared in a press announcement in the latter part of 1968.<sup>9</sup> The system, which had been demonstrated to the U.S. Navy, was claimed to provide a means of communication, close-in area surveillance, navigation and guidance, and could be used by divers or in diver warfare. Attenuation rate using this method of propagation, according to the announcement, was 0.077 dB per metre (0.026 dB/ft) compared with 2.3 dB/m (0.75 dB/ft) for electromagnetic energy. No frequency was given, although 2.3 dB/m indicates a frequency of about 4 kHz (see Fig. 1).

A communication system using the same principle was developed by the same company to enable SCUBA divers to communicate with one another and with their surface support units.<sup>10</sup> Each diver wears a combined transmitter-receiver unit strapped to his chest and has two electrodes, one forming part of the chest pack, the other attached to the ankle. The diver uses a throat microphone and has headphones in his helmet. Ranges

of up to 100 m in 30 m water depths are claimed using 10 W of power. A shore-to-diver system providing coverage over 5 km<sup>2</sup> is possible with electrode separation of 355 m and 160 W of power, for the base station.

## 7. Magnetic Field Systems

Two applications of magnetic field systems have been described, the first of which is used to provide a means of guidance, the second is a voice communication system.

### 7.1. Guidance System

The use of leader cable to provide a means of guidance has been employed in both aircraft and marine applications. The system is based on the detection of the magnetic field surrounding a conductor carrying a low-frequency alternating current. A loop antenna is used to detect the field and this information is processed to provide a left/right steering indication. In the aircraft application, which is no longer in use, two cables were installed, one either side of the runway and its approaches, to provide a means of defining the runway centre line.

The use of leader cables for marine applications was first investigated by the Admiralty Research Laboratories in 1918 and a system was in use about this time in the approaches to Portsmouth Docks from the Nab Tower. Similar systems are believed to have been installed subsequently at Harwich and at New York. A report published in 1924<sup>11</sup> contains a good account of both theoretical and practical investigations into the use of submarine cables with sea-return and submarine loops.

A more recent review into the use of leader cables for marine navigation has been prepared by Sothcott.<sup>12</sup>

### 7.2. Voice Communication

A communication system designed for surface air to diver voice transmission, and named SEA-TEL, has been developed which, according to the literature,<sup>13</sup> radiates a strong alternating magnetic field as a carrier which is modulated at audio frequency. The method, it is claimed, is not affected by the air-water interface and has a range of 30 m at a frequency of 12 kHz.

The third paper of this colloquium, by R. M. Dunbar, outlines some recent experimental work which has been carried out in this field.<sup>14</sup>

## 8. Conclusions

It would appear that electric and magnetic field methods might be employed over short ranges in circumstances where acoustic noise levels are very high or where multi-path interference is severe or where security is a requirement. Without comprehensive experimental data no proper conclusions can be drawn and it is clear that further research is required.

## 9. References

- Willoughby, J. A. and Lowell, P. D., 'Development of loop aerial for submarine radio communication', *J. Amer. Phys. Soc.*, 14, No. 2, p. 193, 1919.
- Moore, R. K., 'Theory of radio communication between submerged submarines', Ph.D. Thesis, Cornell University, 1951.

3. 'Underwater radio communication', *Wireless World*, 73, p. 80, February 1966.
4. Tucker, M. J., 'Conduction signalling in the sea', *The Radio and Electronic Engineer*, 42, No. 10, pp. 453-6, October 1972.
5. Tucker, M. J., 'Conduction signalling in the sea'. National Institute of Oceanography, Int. Report No. 53, September 1971.
6. 'SEDAR—Submerged Electrode Detection and Ranging system using electric conduction fields' (Braincon Corp., Marion, Mass.). 'Signals by electric fields', *Oceanology International*, p. 22, May/June 1969.
7. Swain, W. H., 'An electric field aid to underwater navigation', I.E.E.E. Int. Conf. on Engineering in Ocean Environment, Panama, Florida, 1970.
8. Bennett, M. V. L., 'Sensory systems and electric organs', in 'Fish Physiology', Vol. V., Ed. W. S. Hoar and D. J. Randall, Chapter 10, pp. 347-491.
9. 'Sub-surface Communications', AGARD Conference Proceedings No. 20, April 1966.
10. Schultz, C. W., 'Underwater communication using return current density', *Proc. Inst. Elect. Electronics Engrs*, 59, p. 1025, June 1971.
11. Butterworth, S. and Drysdale, C. V., 'The distribution of the magnetic field and return current round a submarine cable carrying alternating current', *Phil. Trans. Roy. Soc.*, 124, pp. 95-184, 14th April, 1924.
12. Sothcott, P., 'A Preliminary Review of Marine Navigational Methods using Leader Cables', Standard Telecommunication Laboratories, Technical Paper R21/PS/FD2/SS, January 1969.
13. 'SEATEL—Underwater Communication System using Magnetic Field as Carrier'. Barton Industries Ltd., Vancouver, February 1969.
14. Dunbar, R. M., 'The performance of a magnetic-loop transmitter-receiver system submerged in the sea', *The Radio and Electronic Engineer*, 42, No. 10, pp. 457-63, 1972.
- H. A. Wheeler, 'Fundamental limitations of a small v.l.f. antenna for submarines', Symposium on VLF Radio Waves, Paper No. 14, 1957, Boulder, Colo.
- J. R. Wait, 'Insulated loop antenna immersed in a conducting medium', *J. Res. Nat. Bur. Stand.*, 59, No. 2, August 1957.
- P. I. Richards, 'Transients in conducting media', *I.R.E. Trans. on Antennas and Propagation*, AP-6, p. 178, April 1958.
- J. R. Wait, 'A transient magnetic dipole source in a dissipative medium', *J. Appl. Phys.*, 24, p. 341, March 1953.
- J. Kielson and R. V. Row, 'Transfer of transient electro-magnetic surface waves into a lossy medium', *J. Appl. Phys.* 30, p. 1595, October 1959.
- W. L. Anderson and R. K. Moore, 'Frequency spectra of transient electromagnetic pulses in a conducting medium', *I.R.E. Trans. on Antenna and Propagation*, AP-8, p. 603, November 1960.
- G. Ziehm, 'Receiving and taking bearings in sea water on electromagnetic waves', *Telefunken-Z.*, 28, pp. 141-150, June 1960.
- W. L. Anderson, 'The Fields of Electric Dipoles in Sea Water—The Water-Air-Ionosphere Problem', D.Sc. Thesis, University of New Mexico, 1961.
- M. B. Kraichman, 'Basic experimental studies of the magnetic field from electromagnetic sources immersed in a semi-infinite conducting medium', *J. Res. Nat. Bur. Stand.*, 64D, No. 1, pp. 21-25, January 1960.
- R. H. Lien and J. R. Wait, 'Radiation from horizontal dipole in a semi-infinite dissipative medium', *J. Appl. Phys.*, 24, pp. 1-5, January 1953; pp. 958-9, July 1953.
- J. R. Wait, 'Radiation from a small loop immersed in a semi-infinite conducting medium', *Can. J. Phys.*, 37, p. 672, May 1959.
- J. R. Wait, 'The electromagnetic fields of a horizontal dipole in the presence of a conducting half-space', *Can. J. Phys.*, 39, p. 1017-28, July 1961.
- R. K. Moore and W. E. Blair, 'Dipole radiation in a conducting half space', *J. Res. Nat. Bur. Stand.*, 65D, No. 6, November/December 1961.
- R. K. Moore, 'Effects of a surrounding conducting medium on antenna analysis', *I.E.E.E. Trans. on Antennas and Propagation*, AP-11, p. 216, May 1963.
- H. A. Wheeler, 'The spherical coil as an inductor, shield, or antenna', *Proc. Inst. Radio Engrs*, 46, pp. 1595-1602, September 1958.
- R. W. Turner, 'Submarine communication antenna systems', *Proc. Inst. Radio Engrs*, 47, pp. 735-9, May 1959.
- G. J. Monser, 'Pickup devices for vlf reception', *Electronics*, 34, pp. 68-9, April 1961.
- M. B. Kraichman, 'Impedance of a circular loop in an infinite conducting medium', *J. Res. Nat. Bur. Stand. (Radio Science)*, 66D, pp. 499-503, July/August 1962.
- R. W. P. King and C. W. Harrison, 'Half wave cylindrical antenna in a dissipative medium: current and impedance', *J. Res. Nat. Bur. Stand. (Radio Sciences)*, 64D, pp. 365-80, July/August 1960.
- R. W. P. King, 'Dipoles in Dissipative Media', Cruft Lab., Harvard University Report 336, 1961.
- W. E. Blair, 'A modelling technique for experimental verification of dipole radiation in a conducting half space', University of New Mexico, Tech. Report EE-59, July 1962.
- T. T. Wu, 'Theory of the dipole antenna and the two wire transmission line', *J. Math. Phys.*, 2, pp. 550-75, July/August 1961.
- D. W. Gooch, C. W. Harrison, R. W. P. King and T. T. Wu, 'Impedance of long antenna in air and in dissipative media', *J. Res. Nat. Bur. Stand. (Radio Science)*, 67D, pp. 355-60, May/June 1963.
- R. W. P. King and K. Iizuka, 'The complete electromagnetic field of dipoles in dissipative media', *I.R.E. Trans. on Antennas and Propagation*, AP-11, pp. 275-85, May 1963.
- K. Iizuka and R. W. P. King, 'The dipole antenna immersed in a homogeneous conducting medium', *I.R.E. Trans. on Antennas and Propagation*, AP-10, pp. 384-92, July 1962.

- R. N. Ghose, 'The radiator-to-medium coupling in an underground communication system', *Proc. Nat. Elec. Conf.*, 16, 1960.
- K. Iizuka, 'An experimental study of the insulated dipole antenna immersed in a conducting medium', *I.E.E.E. Trans. on Antennas and Propagation*, AP-11, pp. 518-32, September 1963.
- R. W. P. King, 'Theory of the terminated insulated antenna in a conducting medium', *I.E.E.E. Trans. on Antennas and Propagation*, AP-12, pp. 305-18, May 1964.
- J. R. Wait and K. P. Spies, 'A note on the insulated loop antenna immersed in a conducting medium', *J. Res. Nat. Bur. Stand. (Radio Science)*, 68D, No. 11, November 1964.
- T. S. Jorgensen, 'On the radio noise level at low and very low frequencies in polar regions', *J. Res. Nat. Bur. Stand. (Radio Science)*, 69D, No. 9, September 1965.
- R. H. Williams, 'Insulated and loaded loop antenna immersed in a conducting medium', *J. Res. Nat. Bur. Stand. (Radio Science)*, 69D, No. 2, February 1965.
- J. R. Wait, 'Receiving properties of a wire loop with a spheroidal core', *Can. J. Tech.*, 31, No. 1, pp. 9-14, 1953.
- R. H. Williams, R. D. Kelly and W. T. Cowan, 'Small prolate spheroidal antenna in a dissipative medium', *J. Nat. Bur. Stand. (Radio Science)*, 69D, No. 7, July 1965.
- W. L. Anderson, 'Submerged Antennas', University of New Mexico, Tech. Memo, TM-2, 1961.
- W. L. Anderson, 'Submerged Magnetic Antennas with Cores and Radomes', University of New Mexico, Tech. Memo. TM-4, 1961.
- R. C. Hansen, 'Radiation and reception with buried and submerged antennas', *I.E.E.E. Trans. on Antennas and Propagation*, AP-11, No. 3, pp. 207-16, 1963.
- G. R. Swain, 'The small magnetic toroid antenna imbedded in a highly conducting half space', *J. Res. Nat. Bur. Stand. (Radio Science)*, 69D, No. 4, pp. 659-65, 1965.
- T. Padhi, 'Theory of coil antennas', *J. Res. Nat. Bur. Stand. (Radio Sciences)*, 69D, No. 7, July 1965.
- R. W. P. King, C. W. Harrison and D. G. Tingley, 'The Admittance of Bare Circular Loop Antennas in a Dissipative Medium'. Sandia Corporation Monograph SCR-674, 1963.
- K. Sivaprasad and R. W. King, 'A study of arrays of dipoles in a semi-infinite dissipative medium', *I.E.E.E. Trans. on Antennas and Propagation*, AP-11, pp. 240-56, May 1963.
- K. Sivaprasad, 'An Asymptotic Solution of Dipoles in a Conducting Medium', Cruft Lab. TR 354, Harvard University, 1962.
- S. Stein, 'Electromagnetic Radiation over and into an Imperfect Dielectric', Cruft Lab. TR 226, Harvard University, 1955.
- R. K. Moore and W. E. Blair, 'Vertical and horizontal electric and magnetic dipole radiation in a conducting half space', *J. Res. Nat. Bur. Stand. (Radio Science)*, 65D, November/December 1961.
- R. K. Moore, 'Radio communication in the sea', *I.E.E.E. Spectrum*, 4, pp. 42-51, November 1967.
- A. Banos, Jr., 'Dipole Radiation in the Presence of a Conducting Half Space', (Pergamon, New York, 1966).
- 'Underwater Wireless', 'Underwater communications', Report refers to development by Underwater Electronics Corporation, West Hartford, Conn., Ordnance November/December 1968.
- V. Horvat, 'Underwater radio-wave transmission', pp. 3-36 to 3-40, in 'Handbook of Ocean and Underwater Engineering', J. J. Myers, C. H. Holm and R. F. McAllister (Eds), (McGraw-Hill, New York, 1969).
- M. Siegel and R. W. P. King, 'The submerged insulated travelling wave antenna', I.E.E.E. Int. Conf. on Engineering in the Ocean Environment, Panama, Florida 1970.
- M. Siegel, 'Dipole Arrays and Horizontal Linear Antennas in a Dissipative Half Space', Cruft Lab. T.R. 608, Harvard University.
- K. Iizuka, 'Experimental study on the circular loop antenna immersed shallowly in a conducting medium', *J. Res. Nat. Bur. Stand. (Radio Science)*, 69D, No. 9, September 1965.
- T. T. Wu, 'Theory of the thin circular loop antenna', *J. Math. Phys.*, 3, pp. 1301-4, 1962.

*Manuscript first received by the Institution on 6th July 1972 and in final form on 14th August 1972. (Paper No. 1476/AMMS 51.)*

© The Institution of Electronic and Radio Engineers, 1972

# Conduction Signalling in the Sea

M. J. TUCKER,  
B.Sc., F.Inst.P., C.Eng., M.I.E.R.E.\*

*Based on a paper presented at a Joint I.E.R.E.-S.U.T. Colloquium on 'Conduction and Magnetic Signalling in the Sea', held in London on 10th February 1972.*

## SUMMARY

The concept of conduction signalling is that electric currents are injected into the sea by means of electrodes, producing resistive potential differences which are detected using another pair of electrodes at a distance. It is shown that even at low audio frequencies electromagnetic effects must be taken into account, and doing so leads to the conclusion, surprising at first sight, that the electrodes are largely incidental and that it is the wires connecting them which control the launching and detection of the signals.

---

\* National Institute of Oceanography, Wormley, Godalming, Surrey.

## 1. Introduction

The conduction signalling discussed in this paper and the magnetic signalling discussed in an associated paper by R. M. Dunbar<sup>1</sup> are different aspects of signalling by electromagnetic waves in the sea. The difference lies both in the conceptual approach and in the means used for launching the waves, so that different theory is also required.

The theory of a conducting cable in the sea carrying alternating current and with an earth return was worked out by Carson and Gilbert<sup>2</sup> in 1921. This is an excellent piece of work and has been and is likely to remain the definitive paper. However, it has the vices of its virtues. Its mathematics is too complex for the average busy engineer to follow in detail, and thus the underlying physics of the problem tends to get obscured. Because it is obviously correct and the conclusions have been tested against measurement (in carefully-controlled circumstances), it tends to be taken for granted. Taken together, these mean that when someone tests a cable in real conditions and finds that the results are not as expected, he is surprised and at a bit of a loss as to what to do. (Such a case, reported by Jones *et al.*,<sup>3</sup> has been discussed elsewhere.<sup>4</sup>) Also, the work is concerned with the transmission characteristics of the cable and it is difficult to extract the results relevant to conduction signalling. Thus, the present author does not apologize for presenting a simplified analysis.

The detailed theory is given in an Appendix: only the relevant results are quoted in the main body of the paper.

As pointed out in the associated paper by Bogie,<sup>5</sup> there is remarkably little literature on the subject of conduction signalling and what there is, is remarkable for its incorrect theory and inadequate descriptions of experiments. The trouble with the latter seems to be that the authors have not appreciated the basic physics of the problem and therefore have not presented the facts which would enable one to assess the results. For a more general discussion of electromagnetic propagation in the sea, the reader is referred to the paper by Moore.<sup>7</sup> Some of his results relate to what is in effect a form of conduction signalling.

## 2. Theory

Electromagnetic waves in the air depend on the interaction of electromagnetic e.m.f.s and displacement currents: or one can think in terms of a balance of electromagnetic and electrostatic voltages. In the sea, however, at the sort of frequencies we are concerned with, the effect of the displacement currents is negligible: they are completely swamped by the conduction currents. Thus, the basic equation in the absence of boundaries is that the electromagnetic e.m.f. equals the resistive back e.m.f.

In these circumstances the problem of a long, straight, single, insulated conductor surrounded by an infinite sea, carrying an alternating current and with a return through the sea, becomes very similar to the conventional skin effect problem but turned inside out. The effect of the concentrated current in the conductor is to hold the return current flow close to it. The density of the return

current falls off with increasing distance from the wire according to a Bessel's function with a scale parameter  $r_0 = (\mu\sigma\omega)^{-\frac{1}{2}}$  (for the definitions of symbols see the Appendix). However, when the equation is converted to its far-field form it is more convenient to use the 'skin depth',

$$\delta = r_0\sqrt{2} = \sqrt{2/\mu\sigma\omega}. \quad \dots(1)$$

This is plotted as a function of frequency in Fig. 1.

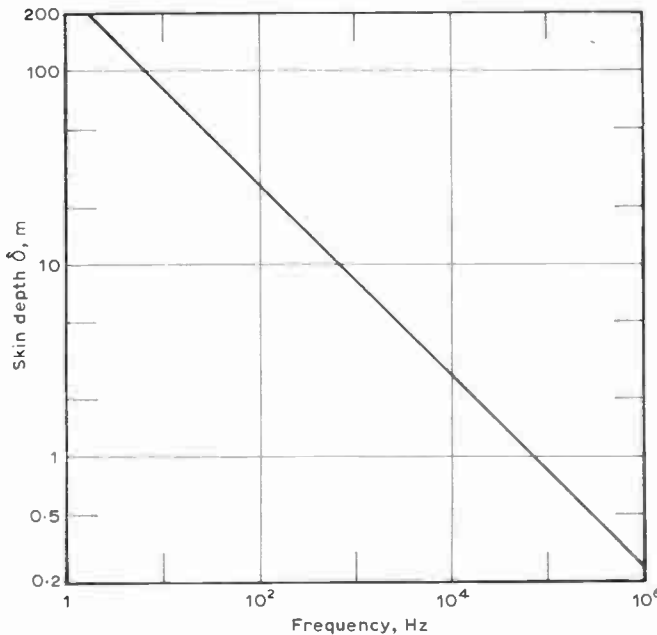


Fig. 1. Skin depth as a function of frequency (assuming  $\sigma = 4$  siemens per metre).

Equation (12) in the appendix gives the return current density as a function of the radial distance  $r$  from the wire exactly, and for practical cases this reduces to equation (14). When  $r$  is much greater than  $r_0$  this equation further simplifies to show a wave propagating radially with heavy attenuation:

$$\frac{i}{I_w} = \frac{1}{2^{\frac{1}{2}} \delta^{\frac{1}{2}} (\pi r)^{\frac{1}{2}}} \exp\left(\frac{r}{\delta}\right) \exp j\left(\frac{r}{\delta} + \frac{5\pi}{8}\right). \quad \dots(2)$$

This equation is derived by using the assumption that the wire diameter is much smaller than  $r_0$ , which will normally be the case. It may be noted that the diameter of the wire then has no effect on the result.

The first term on the right-hand side represents the cylindrical spreading, the second term the exponential attenuation, and the third term the propagating wave.

One other important fact may also be noted. As has already been pointed out, the basic equation used balances the electromagnetic e.m.f. against the resistive back e.m.f. Thus, *there are no potential differences produced in the water*. One can see that this must be so using another argument. There is no current flow at a great distance from the wire and therefore no potential differences. There is no mechanism for producing radial e.m.f.s, therefore there are no potential differences near the wire. The energy dissipated by the current flowing in the resistive medium is supplied by an increase in the

real part of the wire impedance. (The alternating currents flowing in the water induce a back e.m.f. in the wire.) When one connects two electrodes in the water by a wire parallel to the main conductor one picks up an e.m.f. equal to the back e.m.f. of the current in the resistive medium, but it is in fact *induced in the wire* by the changing magnetic field, and the electrodes are only acting as sliprings. It thus depends on the routing of the wire and not on the position of the electrodes. It is lack of appreciation of this fact which has led to most of the confusion in the reports of experiments, and may indeed partially account for some of the unexpected results.

The final factor which we must take account of is dispersion. From equation (1) it can be seen that the skin depth  $\delta$  varies inversely as the square-root of the angular frequency ( $\delta \propto \omega^{-\frac{1}{2}}$ ). Thus, at a given distance  $r$ ,  $i$  is heavily dependent on frequency. Putting

$$\left| \frac{i}{I_w} \right| = A,$$

some manipulation of equation (2) gives

$$\left( \frac{\delta A}{\delta \omega} \right)_{r \text{ const}} \cdot \frac{\omega}{A} = \frac{3}{4} - \frac{r}{2\delta}. \quad \dots(3)$$

### 3. Calculations on Some Typical Cases

It is useful to put in some figures in order to get a feel for the problem. Assuming that the conductivity  $\sigma = 4$  siemens/metre, which is a typical value for sea water,

at 300 Hz,  $\delta = 14.6$  m

Voltage gradient =  $|i|/\sigma \approx i/4$  volts/metre

$$= |I_w| \frac{2.24 \times 10^{-3}}{\sqrt{r}} e^{-r/14.6} \text{ V/m}$$

At a range of 100 m, the voltage gradient is therefore

$$|I_w| \times 2.2 \times 10^{-7} \text{ V/m.}$$

Beyond this the gradient falls off by slightly more than  $1/e$  for every 14.6 m.

One must remember that the impedance and bandwidths are very low, so that an  $I_w$  value of 100 A is probably attainable, and  $10^{-8}$  V can probably be detected. Even so, this formula would lead to the conclusion that the maximum range at 300 Hz is unlikely to exceed 200 m.

Even at 30 Hz, the voltage gradients at 500 m range are approximately  $2.5 \times 10^{-10} I_w$  V/m, which must be near the limit of detectability.

Thus one is working at values of  $x (=r/r_0)$  of up to about 20. Putting typical values into equation (3) to calculate the dispersion effect:

when  $x = 10$ ,  $\left( \frac{\delta A}{\delta \omega} \right)_{r \text{ const}} \cdot \frac{\omega}{A} \approx -2.8$

when  $x = 20$ ,  $\left( \frac{\delta A}{\delta \omega} \right)_{r \text{ const}} \cdot \frac{\omega}{A} \approx -6.3.$

Thus, in the first case the received voltage changes nearly 3 times as fast in proportion as frequency changes, and in the second case over 6 times as fast. It is therefore

rather surprising that Schultz<sup>6</sup> is able to say about experiments to transmit speech over such a link that 'tests show that there is no serious loss of intelligibility due to dispersion'.

3.1. *The Effects of Short Source Wires*

We have assumed so far that the primary wire is infinitely long. Equation (2) shows that we are dealing with propagating electromagnetic waves with a wavelength of  $2\pi\delta = 8.88 r_0$ . This is, as one would expect, the wavelength calculated for plane electromagnetic waves.<sup>7</sup> However, the attenuation length is only  $\lambda/2\pi$  and so the beam-forming process will not work in the normal way. It might be possible to calculate the patterns, but for the present discussion we need only make two elementary points concerning the effect of shorter wires:

(i) The field strengths will never be significantly above those calculated for an infinite source wire and will usually be less.

(ii) They will generally be greatest in a plane perpendicular to the wire and passing through its centre.

3.2. *Anomalous Results of Experiments*

As pointed out in the associated paper by Bogie<sup>5</sup>, various authors quote measured ranges far in excess of those calculated by the above methods. It seems likely that these are due to the sea not in fact being infinite. All the effects of a nearby surface which is comparatively an insulator will tend to increase the range, but the process usually considered to be most likely to predominate is an 'escape' of the transmitted wave into the air where it travels as an air wave along the sea surface, leaking energy back into the sea which is picked up by the receiver.

4. **References**

*Note:* Only papers specifically referred to in the text are given here. For a fuller bibliography, see ref. 5.

1. Dunbar, R. M., 'The performance of a magnetic-loop transmitter-receiver system submerged in the sea', *The Radio and Electronic Engineer*, 42, No. 10, pp. 457-63, 1972.
2. Carson, J. R. and Gilbert, J. J., 'Transmission characteristics of the submarine cable', *J. Franklin Inst.*, 192, pp. 705-35, 1921.
3. Jones, F. and others, 'The Voice Frequency Transmission Characteristics of Certain Types of Submarine Telephone Cables', G.P.O. Engng. Dept. Research Report No. 20202, 1961.
4. Tucker, M. J., 'Conduction Signalling in the Sea', N.I.O. Internal Report No. A.53, 1971.
5. Bogie, I. S., 'Conduction signalling: a background review', *The Radio and Electronic Engineer*, 42, No. 10, pp. 447-52, 1972.
6. Schultz, C. W., 'Underwater communication using return current density', *Proc. I.E.E.E.*, 59, pp. 1025-26, June 1971. (Letters.)
7. Moore, R. K., 'Radio communication in the sea', *I.E.E.E. Spectrum*, 4, pp. 42-51, November 1967.
8. Olver, F. W. J., 'Bessel functions of integer order', Chapter 9 in 'Handbook of Mathematical Functions', Abramowitz, M. and Stegun, I. A. (Eds.) (National Bureau of Standards, U.S.A., 1964).

5. **Appendix**

**The Theory of the Return Current Distribution**

**List of Symbols**

$\sigma$  conductivity of sea water, S/m  
(SI unit for conductance is the siemen— $S = \Omega^{-1}$ )

$i$	electric current density, A/m <sup>2</sup>
$I$	total electric current within a radius $r$ , A
$I_w$	electric current in the conductor, A
$B$	magnetic flux density, Wb/m <sup>2</sup>
$r$	radial distance from the centre of the conductor
$R$	radius of the cable
$\mu$	permeability of sea water taken as $\mu_0 = 4\pi \times 10^{-7}$ , Wb A <sup>-1</sup> m <sup>-1</sup>
$\omega$	angular frequency of $I_w$
$k = (\mu\sigma\omega)^{\frac{1}{2}}$	parameter with dimensions of L <sup>-1</sup>
$r_0 = 1/k$	characteristic length defining the scale of the phenomenon
$\delta = r_0\sqrt{2}$	'skin depth'
$x = r/r_0 = kr$	non-dimensional normalized radius
$X = R/r_0 = kR$	

Consider an insulated long straight conductor of overall radius  $R$  surrounded by an infinite volume of sea water. The following assumptions will be made:

- (i) Axial symmetry.
- (ii) The displacement current term in the electromagnetic equations may be neglected. In plane wave propagation in the sea<sup>7</sup> this is valid for frequencies below about 10<sup>7</sup> Hz. It is equivalent to saying that the scale of the phenomenon with which we are dealing is small compared to the wavelength in a medium with the same permeability and dielectric constant but no conductivity. The results show this to be the case.

Note that  $i$  and  $I_w$  have been taken as positive in opposite directions. Though not perhaps formally correct, this avoids the currents in the water appearing with a negative sign.

Referring to Fig. 2, consider e.m.f.s round the loop marked with arrows. The e.m.f. due to the change in current density with radius is given by

$$(1/\sigma)[i + \delta r(\partial i/\partial r)] - i/\sigma = (i/\sigma)\delta r \partial i/\partial r.$$

That due to the changing magnetic field is

$$\partial(B\delta r)/\partial t = \delta r(\partial B/\partial t).$$

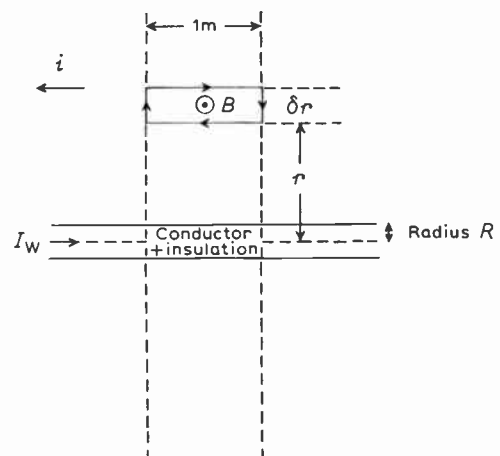


Fig. 2. Geometry for the calculations.

These must balance, so that

$$\frac{1}{\sigma} \frac{\partial i}{\partial r} - \frac{\partial B}{\partial t} = 0. \quad \dots\dots(4)$$

If the total electric current within the radius  $r$  (including the current in the conductor) is  $I$ , then  $B = \mu I / 2\pi r$ . Inserting this in equation (4) gives

$$r \frac{\partial i}{\partial r} - \frac{\mu\sigma}{2\pi} \frac{\partial I}{\partial t} = 0. \quad \dots\dots(5)$$

Since  $\partial I / \partial r = 2\pi r i$ , one can differentiate equation (5) with respect to  $r$ , substitute this equality, and with some reduction obtain

$$\frac{\partial^2 i}{\partial r^2} + \frac{1}{r} \frac{\partial i}{\partial r} - \mu\sigma \frac{\partial i}{\partial t} = 0 \quad \dots\dots(6)$$

which is the basic differential equation of the phenomenon.

The temporal term is eliminated in the usual way by considering a sinusoidal current with angular frequency  $\omega$ , so that

$$i = F \exp(j\omega t) \quad \dots\dots(7)$$

where  $F$  is a function of radius  $r$ .

Substituting in equation (6) gives

$$\frac{d^2 F}{dr^2} + \frac{1}{r} \frac{dF}{dr} - \mu\sigma \cdot j\omega F = 0.$$

Putting  $\mu\sigma\omega = k^2$  and  $x = kr$  gives

$$x^2 \frac{d^2 F}{dx^2} + x \frac{dF}{dx} - jx^2 F = 0. \quad \dots\dots(8)$$

The solution of this is a Bessel function expressed in Kelvin functions (see, for example, Olver<sup>8</sup>, equations (9.9.3)) and is

$$F = C(\text{ber}_0 x + j \text{bei}_0 x) + D(\text{ker}_0 x + j \text{kei}_0 x).$$

Now  $\text{ber}_0 x$  and  $\text{bei}_0 x$  are functions increasing rapidly with  $x$ , whereas from physical reasoning we know that  $F$  decreases as  $x \rightarrow \infty$ . Therefore  $C = 0$  and (following the usual convention and omitting the subscript 0)

$$F = D(\text{ker } x + j \text{kei } x) \quad \dots\dots(9)$$

$\text{ker } x$  and  $\text{kei } x$  are tabulated (for example, by Olver<sup>8</sup>) and are plotted in Fig. 3.

The value of the constant  $D$  must now be determined,

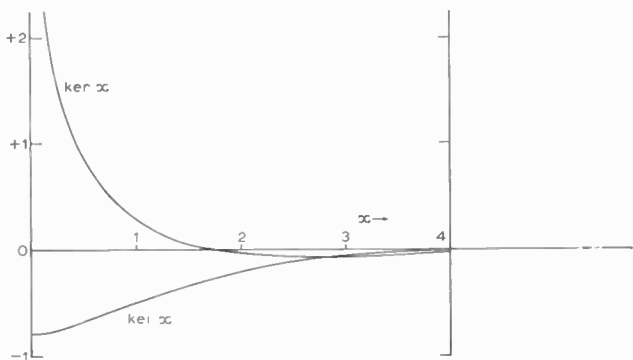


Fig. 3. The Kelvin functions  $\text{ker } x$  and  $\text{kei } x$ .

the criterion being that

$$\int_R^\infty 2\pi r i \, dr = I_w$$

$$\text{or} \quad k^2 I_w / 2\pi = \int_0^\infty x i \, dx \quad \text{where} \quad X = kr$$

$$= \int_0^\infty x i \, dx - \int_0^X x i \, dx. \quad \dots\dots(10)$$

Using equations (7) and (9)

$$\int_0^X x i \, dx = \exp(j\omega t) D \int_0^X (x \text{ker } x + j x \text{kei } x) \, dx$$

$$= \exp(j\omega t) D (x \text{kei}' x - j x \text{ker}' x) \quad \dots\dots(11)$$

(Olver,<sup>8</sup> equation (9.9.21))

The second bracket in (11)  $\rightarrow 0$  as  $x \rightarrow \infty$ , so equation (10) becomes:

$$k^2 I_w / 2\pi = - \exp(j\omega t) D X (\text{kei}' X - j \text{ker}' X)$$

$$\text{or} \quad D = -k^2 I_w / 2\pi X (\text{kei}' X - j \text{ker}' X) \exp j\omega t.$$

Using equations (7) and (9)

$$\frac{i}{I_w} = \frac{k^2}{2\pi X} \frac{1}{\text{kei}' X - j \text{ker}' X} \cdot (\text{ker } x + j \text{kei } x). \quad \dots\dots(12)$$

In practice one is concerned with values of  $X$  less than 0.1, which, for example, represents the value for a cable 5 cm in diameter carrying 500 kHz in water with a salinity of 35% at 15°C. By considering the polynomial expansions of  $\text{kei}' x$  and  $\text{ker}' x$ , and neglecting terms less than  $10^{-3}$  of the modulus, one finds that

$$\frac{1}{\text{ker}' X - j \text{kei}' X} = \frac{\text{kei}' X + j \text{ker}' X}{(\text{kei}' X)^2 + (\text{ker}' X)^2}$$

$$\simeq -0.5X^3 \ln(X/2) - \frac{jX}{1 - 0.393X^2} \dots\dots(13)$$

When  $X = 0.1$  the real term here is less than 2% of the imaginary term and  $0.393 X^2$  is less than  $4 \times 10^{-3}$ , so for approximation purposes this expression reduces to  $-jX$ . This is valid to better than 1 part in  $10^3$  when  $X < 0.02$ . Using this approximation

$$\frac{i}{I_w} = \frac{k^2}{2\pi} (\text{kei } x - j \text{ker } x). \quad \dots\dots(14)$$

It is interesting to note that one can partially check this result very easily as follows. The total in-phase return current as a fraction of  $I_w$

$$= \int_R^\infty \text{real part of } (i/I_w) \cdot 2\pi r \, dr$$

$$= -k^2 \int_R^\infty r \text{kei } x \, dr = - \int_X^\infty x \text{kei } x \, dx$$

$$\simeq - \int_0^\infty x \text{kei } x \, dx = 1$$

which is correct.

$$\text{Similarly, } \int_R^\infty \text{imaginary part of } (i/I_w) \cdot 2\pi r \, dr$$

$$\simeq \int_0^\infty x \text{ker } x \, dx = 0.$$

Manuscript received by the Institution on 29th March 1972 (Paper No. 477/AMMS52)

© The Institution of Electronic and Radio Engineers, 1972

# The Performance of a Magnetic Loop Transmitter-Receiver System Submerged in the Sea

**R. M. DUNBAR,**  
M.Sc., C.Eng., M.I.E.E.\*

*Based on a paper presented at a Joint I.E.R.E.-S.U.T. Colloquium on 'Conduction and Magnetic Signalling in the Sea' held in London on 10th February 1972.*

## SUMMARY

The theoretical predictions for an electromagnetic wave in both free-space and an infinite conducting medium are considered and an experimental technique is described which was used to measure the variation of signal strength with distance for a magnetic-loop transmitter-receiver system submerged in sea-water, at a mid-water depth (100 m) where boundary effects could be ignored safely.

Underwater communication of audio-frequency signals in real time is normally carried out using acoustic techniques, but occasionally there are reports in the press of 'magnetic carrier' or 'conduction field' systems having ranges in the sea which apparently exceed those expected for a conventional electromagnetic wave.

\* Underwater Technology Group, Department of Electrical and Electronic Engineering, Heriot-Watt University, 31-35 Grassmarket, Edinburgh EH1 2HT.

## 1. Introduction

Long-range electromagnetic wave communication through a water mass of high conductivity is to all practical purposes impossible due to high attenuation,<sup>1</sup> except at extremely low frequencies where low information rates permit only slow-speed telegraphy. However, for work underwater by SCUBA divers a maximum range of 50 m is very often more than adequate, particularly in areas of poor visibility where the diving team maintains close contact, and while this requirement is usually met by standard acoustic communications equipment there are certain circumstances where an alternative would be desirable; for example, in regions of high acoustic noise, or when working on opposite sides of an acoustically reflective mass.

For this reason and the fact that a commercial instrument with intriguing claims of performance was advertised in the U.S. press,<sup>2</sup> together with the author's belief that submarine electromagnetic wave propagation was a subject which would lead to long-term interesting university project work, not necessarily directly concerned with communications, theoretical and experimental studies in this area were commenced.

## 2. Scope of Study

On occasions, terms such as 'conduction current signalling'<sup>3, 4</sup> and 'magnetic carrier system'<sup>2</sup> have appeared in the press and while it is not doubted that communication over a distance underwater was achieved in these cases it is believed that the fields described were but aspects of the complete electromagnetic wave generated by the relevant sending device and were not in themselves new types of information carriers.

Essentially this brings one to the study of electromagnetic waves generated, propagated and received within an infinite or bounded dissipative medium, and to practical considerations such as suitable antenna designs, radiation resistance concepts and electrical noise.

Much work has been carried out concerning these problems,<sup>1, 5-10</sup> together with relevant studies in the field of subterranean electromagnetic wave propagation,<sup>11-13</sup> but the practical aspect of a compact diver-to-diver electromagnetic wave communication system did not appear to have been covered explicitly.

The requirement of a compact communication equipment immediately ruled out ideas of large diameter magnetic loop antennas, trailing wires<sup>3</sup> for conduction field signalling, certain forms of electric dipoles used for submarine-submarine communications, while for further reasons of electrical performance electric dipoles, in general, seemed less suitable<sup>13</sup> than equivalent magnetic dipoles.

For these reasons it was decided to study the application of a small magnetic loop antenna to the problem, both theoretically and experimentally, in order to derive design criteria and the predicted performance of such a communication system.

The specific aims of the study were as follows:

- (i) Theoretical: The prediction of the electromagnetic field components generated by a magnetic loop

antenna immersed in a dissipative medium, and the estimation of the e.m.f. induced in a similar loop immersed in the same medium at various distances, and at various frequencies. (An infinite dissipative medium is assumed.)

- (ii) Experimental: The development of equipment to generate a variable frequency time-varying magnetic field, produced by a magnetic loop antenna, immersed at sufficient depth in sea water to enable sea-surface and sea-bed boundary effects to be safely ignored; the receiving loop being adjustable in position relative to the transmitting loop, while remaining in mid-water, with readings of induced e.m.f. being taken remotely on board a support vessel.

While it is possible to use increased salinity and frequency physically to scale down experimental equipment,<sup>14, 15</sup> it was decided to carry out tests using full-scale equipment under actual operating conditions, in order that real problems would be encountered and that effects of atmospheric noise would be introduced realistically.

### 3. Theoretical Background

#### 3.1. The Magnetic Loop in Free Space

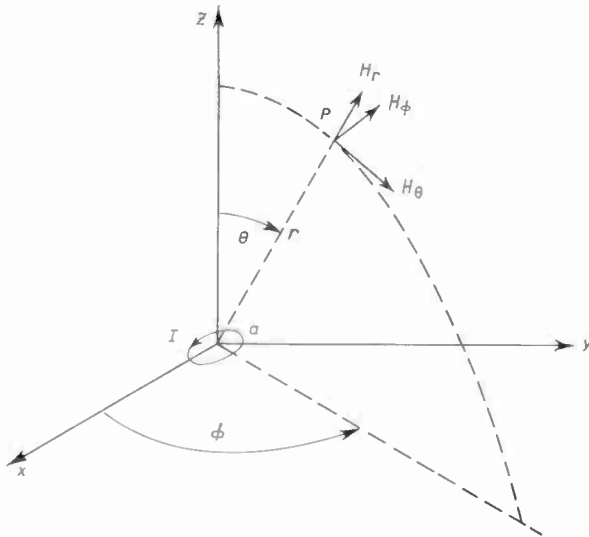


Fig. 1. Components of magnetic field at a distance  $r$  associated with a loop carrying a current  $I$ .

At a radial distance  $r$  from a small circular loop carrying a current  $I = I_0 e^{j\omega t}$  two components of magnetic field,  $H_\theta$  and  $H_r$ , exist. Because of circular symmetry there is no variation with respect to  $\phi$ .  $H_\theta$  and  $H_r$  are given as follows:

$$H_\theta = \frac{m_0 \sin \theta e^{j(\omega t - \beta r)}}{4\pi} \left\{ -\frac{\beta_0^2}{r} + j\frac{\beta_0}{r^2} + \frac{1}{r^3} \right\} \dots\dots(1)$$

$$H_r = \frac{m_0 \cos \theta e^{j(\omega t - \beta r)}}{2\pi} \left\{ j\frac{\beta_0}{r^2} + \frac{1}{r^3} \right\} \dots\dots(2)$$

- where  $m_0 =$  loop current  $\times$  loop area
- $=$  'magnetic moment'
- $= I_0 S$
- $= I_0 \pi a^2$
- $\beta_0 =$  phase constant of free-space
- $= \omega/c$
- $= 2\pi/\lambda_0$ .

At any point in space the total time-varying field will be the vector sum of  $H_\theta$  and  $H_r$ . If we take  $\theta = 90^\circ$ , i.e. the point of measurement in the plane of the loop,  $H_\theta \rightarrow H_{\theta \max}$  and  $H_r \rightarrow 0$ .

Conventionally, the three terms of the  $M_0$  expression are described as follows:

- $1/r$  variation: radiation component;
- $1/r^2$  variation: induction component;
- $1/r^3$  variation: magnetostatic component.

At small distances (compared to wavelength) from the loop the  $1/r^2$  and  $1/r^3$  terms predominate, and it is only in the far-field where  $r > 1/\beta_0$ , i.e.  $r > \lambda_0/2\pi$ , that the radiation term ( $1/r$ ) becomes the predominant component. Further, the concept of radiation resistance is defined in terms of the radiation component, and can be shown<sup>16</sup> to have the value  $R_R = 20\pi^2(\beta_0 a)^4$  ohms.

When this is evaluated for loops of normal dimensions, and in any case it is only valid for  $2\pi a \ll \lambda_0$ ,  $R_R$  has a very small value, usually much smaller than the a.c. resistance of the loop.

Consequently a loop antenna is very inefficient for transmission purposes and is usually employed only for reception in conjunction with a high- $Q$  tuned circuit. However, if a loop is used as a transmitting antenna with an m.m.f. of the order of 50 AT (ampere-turn) useful levels of magnetic field exist within the near field of the loop and it is within this region that measurements were obtained during this study.

Returning to the expression for  $H_\theta$  (as given in eqn. (1)) it can be seen that, for a given applied current and range,  $H_\theta$  is proportional to the area of the loop. For portable equipment the loop must have small dimensions and consequently one is forced to increase the effective area artificially through the use of a permeable core<sup>17</sup> and a multi-turn coil. This is quite successful provided the flux density is kept well below the saturation level.

Thus the effective area becomes  $N_1 S_1 \mu_{r(\text{eff})1}$  where  $N_1$  is the number of turns, and  $\mu_{r(\text{eff})1}$  is the effective relative permeability of the core of the transmitting loop. Many shapes of core are possible<sup>17, 18</sup> but the present experimental work was carried out using conventional ferrite rods with a measured  $\mu_{r(\text{eff})}$  of approximately 50.

The magnetic flux density at a distance  $r$  from the loop, in its plane, is  $B_\theta = \mu_0 H_\theta$ , and if a similar loop is used as a receiving antenna at this point, the magnetic flux linkages through this second coil will be

$$\Phi_2 = B_\theta (N_2 \mu_{r(\text{eff})2} S_2),$$

assuming the loops to be aligned for maximum induced signal by the  $H_\theta$  component.

Thus the e.m.f. induced across the receiving loop will be

$$e = - \frac{d\Phi_2}{dt} = -j\omega\Phi_2,$$

assuming sinusoidal variation.

Hence the final expression for the induced e.m.f. in the receiving loop is

$$e_{\max} = \frac{-j\omega\mu_0 I_0 (N_1 \mu_{r(\text{eff})1} S_1) \times (N_2 \mu_{r(\text{eff})2} S_2) \exp j(\omega t - \beta r) \times}{4\pi} \times \left\{ -\frac{\beta_0^2}{r} + j\frac{\beta_0}{r^2} + \frac{1}{r^3} \right\}.$$

This equation has been evaluated using the parameters of the practical system and the predicted and measured results for free space are compared in Section 4.

### 3.2. The Magnetic Loop in a Conducting Medium

In Section 3.1, it was assumed for a wave propagating in free-space, that the propagation constant consisted solely of the phase constant  $\beta_0$ . In certain special cases, of for example, a wave travelling through an ionized gas,<sup>19</sup> through rock deep underground,<sup>11</sup> or through a conducting liquid as under consideration here, the propagation constant is complex, being a function of both the conductivity and the permittivity of the region. The following conditions apply:

(i) free space

$$\gamma = \sqrt{j\omega\mu \cdot j\omega\varepsilon} = j\omega\sqrt{\mu\varepsilon} = j\beta_0$$

(ii) conducting medium

$$\gamma = \sqrt{j\omega\mu(\sigma + j\omega\varepsilon)}.$$

For sea water with  $\sigma \simeq 4 \text{ S/m}$ ,  $\sigma \gg \omega\varepsilon$  at frequencies of interest, therefore

$$\begin{aligned} \gamma &\simeq \sqrt{j\omega\mu\sigma} \\ &= \sqrt{\frac{\omega\mu\sigma}{2}} \cdot (1+j). \end{aligned}$$

Thus the exponent of the field components for the free-space expression is modified from  $j(\omega t - \beta_0 r)$  to  $(j\omega t - \gamma r)$ , where  $\gamma$  itself is complex.

For simplification of analysis<sup>16</sup> the term expressing the time variation,  $e^{j\omega t}$ , is usually omitted from equations, and this procedure will be adopted for the rest of this paper.

Referring to the same coordinate diagram as used for Section 3.1, the  $H_\theta$  component of magnetic field from an identical loop antenna, this time immersed in an infinite, uniform, homogeneous conducting medium, is given by

$$H_\theta = \frac{M \exp(-j\gamma r)}{4\pi r} \left\{ j\omega\varepsilon + \frac{1}{\eta r} + \frac{1}{j\omega\mu r^2} \right\} \sin \theta \text{ A/m} \dots\dots(4)$$

where

$$\begin{aligned} M &= j\omega\mu_0 \mu_{r1} I S_1 N_1 \text{ (Ref. 27)} \\ &= \text{'magnetic moment'} \end{aligned}$$

$$\gamma = \sqrt{\frac{\omega\mu\sigma}{2}} (1+j)$$

= propagation constant

$j\omega\varepsilon = \sigma + j\omega\varepsilon \simeq \sigma$  for sea-water

= complex permittivity

$$\eta = \sqrt{\frac{\omega\mu}{2\sigma}} (1+j)$$

= intrinsic impedance.

Continuing from the expression for  $H_\theta$  as in Section 3.1, an expression may be obtained for the e.m.f. induced in a similar ferrite-cored receiving loop at a distance  $r$  from the transmitting loop, the loops being in the same plane to maximize the  $H_\theta$  component. Thus

$$e_{\max} = \omega^2 \mu_0^2 \mu_{r1} \mu_{r2} N_1 N_2 S_1 S_2 I \exp(-j\gamma r) \times \left\{ \frac{j\omega\varepsilon}{r} + \frac{1}{\eta r^2} + \frac{1}{j\omega\mu r^3} \right\} \dots\dots(5)$$

where all constants are as previously defined.

Equation (5) has been evaluated for a range of values of  $r$ , for various operating frequencies and for the various parameter values encountered during field trials. The results are presented in Section 5 together with experimental results, for comparison.

### 3.3. Radiation Resistance of Loop

The calculation of radiation resistance for an antenna in free-space involves obtaining an expression for the power flow through a spherical surface and dividing this by the square of the current which creates that power flow.<sup>16</sup> In a conducting medium, however, the expression for the total power crossing a sphere of radius  $R$  is found to be a function of  $R$  unlike the free-space case which is independent of  $R$ .<sup>11, 20</sup> Therefore the evaluation of radiation resistance, so useful in antenna design, becomes impractical for a conducting medium.

This dependence of power flow on  $R$  is intuitively reasonable since the electromagnetic wave is continuously attenuated as it progresses through the dissipative region. Furthermore, the 'inductive'  $1/r^2$  component, normally associated with a 'reactive power flow' to and fro in the near field of the antenna, is now associated with a real power loss<sup>1</sup> in the dissipative medium, since the amount of power returning to the antenna each cycle is obviously less than that leaving it, due to dissipation in the near field.

### 3.4. Enclosure of Loop in a Radome

Following on from Section 3.3 it is reasonable to assume that the highest attention of field components will take place close to the antenna, but this effect has been shown to be considerably more serious with electric dipoles than with magnetic dipoles.<sup>6</sup> Also it has been shown<sup>9</sup> that for the case of the magnetic dipole the field components are not significantly affected by the presence of the enclosure, provided its dimensions are small compared to the skin-depth of the surrounding medium. This

is fortunate since the size of a portable instrument must be minimized, and simple laboratory tests with the experimental loops referred to in this paper confirmed this detail.

3.5. Conductivity and Permittivity

In sea-water for the frequencies used in these experiments

$$\sigma \gg \omega\epsilon, \text{ by a factor of } 10^4$$

If however  $\sigma \simeq \omega\epsilon$  the analysis is considerably more complicated, as can be the case for subterranean communication.<sup>11</sup>

4. Experimental Techniques

4.1. Aims of the Experimentation

The aims may be grouped under three headings:

- (i) verification of predicted values of induced e.m.f. for various ranges and frequencies, including the effects of ambient electrical noise;
- (ii) development of relevant electronic circuits, bearing in mind the limitations in power of equipment capable of being carried by SCUBA divers;
- (iii) packaging of the circuitry for operation with high ambient water pressure and operation of the equipment under real conditions at sea.

4.2. Free-space Measurements

It was possible to use available laboratory equipment without modification for field measurements in air. The block diagram of Fig. 2 is self-explanatory.

Measurements were taken along a 50 m calibrated range, the transmitting and receiving loops being kept in the same plane as they were moved apart.

The audio frequency modulation facility was found to be useful for signal identification during initial experiments when working at maximum range.

4.3. Deep Sea-water Measurements

In order that the assumption of an infinite conducting region be justified it was necessary to carry out the

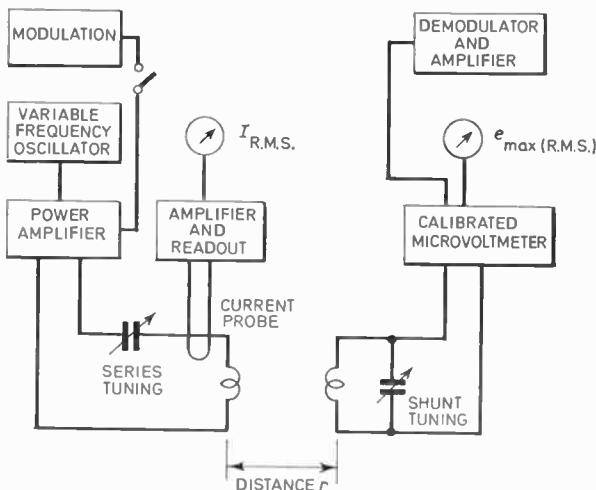


Fig. 2. Block diagram of the experimental set-up for the free-space measurements.

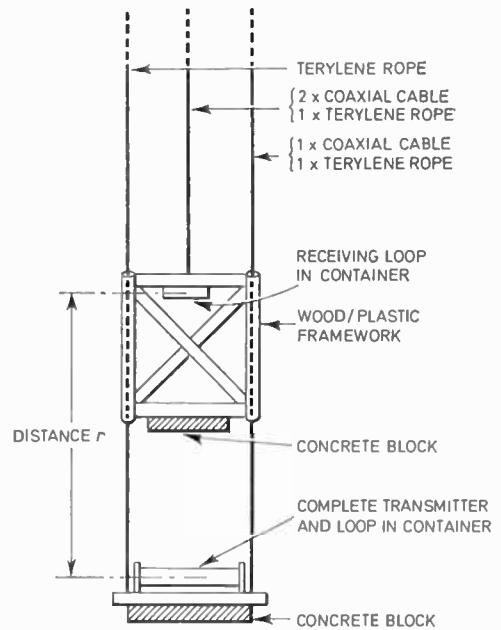


Fig. 3. Arrangement used for loop-positioning.

measurements with both the transmitter and receiver loops immersed in deep water, at such a depth that boundary effects could be neglected. With a loop m.m.f. of 50 AT a maximum range of approximately 20 m was anticipated before the signal would fall below 0.1 μV across the receiver loop. A location was found where tests could be carried out with 90 m of water both above and below the measurement loops and this was considered to be entirely satisfactory.

The location for sea-trials held on 16th December 1971 was off the West Coast of Scotland, and experiments were carried out near Oban, at two miles from Rudha an Ridire, bearing 280° Magnetic, where the depth was 200 m.

4.3.1. Loop positioning equipment

The problem of moving the loops apart precise distances under water while maintaining the same orientation was solved eventually by constructing a framework carrying the receiving loop which would slide up and down a pair of plastic ropes supporting a heavily weighted platform on which was mounted the transmitting loop: this is illustrated in Fig. 3. It must be stated that there was no remote reading facility for checking the relative orientation of the loops, to avoid any twist in the rope-framework arrangement being interpreted as a genuine fall in readings of induced e.m.f. However, the following precautions were taken:

- (i) the spacing between the ropes was made reasonably wide (1.5 m);
- (ii) the 'fixed' transmitter unit was attached to a heavy concrete block (50 kg), keeping the ropes taut;
- (iii) all measurements were made with the support vessel stationary and during the period when slack water conditions existed.

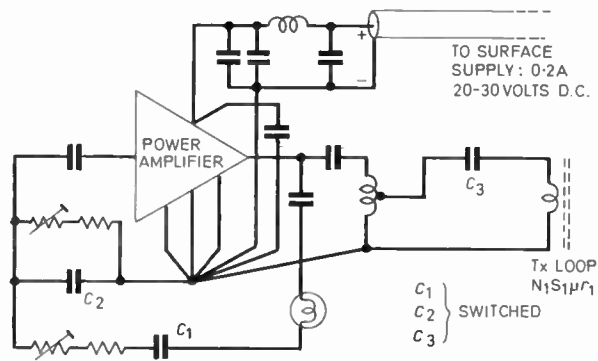


Fig. 4. Transmitter circuit.

While it cannot be stated with certainty that there was no twist of one loop relative to the other, there were no indications of periodic variations in signal strength and all measurements followed similar patterns when repeated. Also, any small relative angular motion would be of little effect since a 25° rotation causes the signal to fall by only 10%, due to the  $\sin \theta$  variation.

#### 4.3.2. Transmitter

It was desirable to have a completely self-contained transmitter and loop, partly to simulate conditions that might have to be met with a diver communication system, and partly to avoid problems of spurious conduction pick-up due to any inadvertent electrical leakage. Furthermore the problems of series tuning the transmitting loop through a 100 m length of coaxial cable were avoided. However, it was felt necessary to have a d.c. power feed from the surface to give some flexibility in control.

The transmitter circuit (Fig. 4) was found to perform quite satisfactorily. It is based on a Wien-bridge power oscillator followed by a matched series tuned circuit incorporating the transmitting loop.

The loop current is controlled by varying the d.c. feed current (one reason for the d.c. power feed from the surface) and a linear relationship exists between these two currents, as can be seen from Fig. 5. Less than a 1% frequency variation occurs when the d.c. current is varied over a 2:1 range.

Since the transmitter would be operating in a cold environment of varying temperatures, its temperature stability was checked in an environmental chamber. The stability was found to be more than adequate (see Fig. 6).

To cater for immersion in 100 m of water the transmitter circuit and loop were mounted in a 12.5 cm

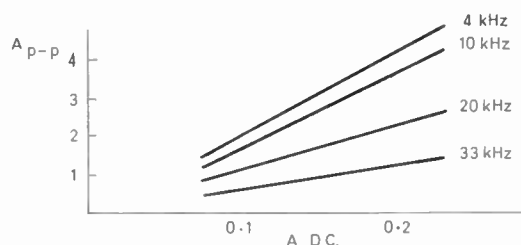


Fig. 5. Graph of loop current against d.c. feed current.

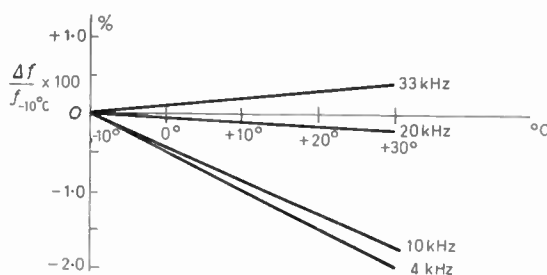


Fig. 6. Transmitter frequency stability against temperature variations

diameter PVC cylinder with removable end flanges, the cylinder being filled with transformer oil to pressure-balance the equipment. Compression of the oil with increasing depth was compensated for by a flexible end-plate, and all electronic components used were selected for suitability under this mode of operation.<sup>21</sup>

#### 4.3.3. Receiver

The receiving loop antenna was coupled through a balanced 100 m feeder cable to a tuned preamplifier with a gain of 10, and the output taken to a calibrated wide-band transistor microvoltmeter. The block diagram of the complete receiver is shown in Fig. 7.

### 5. Predicted and Experimental Results

#### 5.1. Magnetic Loop in Air

The variation of the e.m.f. induced in a loop antenna at various distances and frequencies for a transmitter current of 1.0 A r.m.s. is shown in Figs. 8(a) and (b). It will be noticed that the theoretical and measured values are in close agreement.

The minimum signal that could be received was a loop e.m.f. of 0.8 μV. At this level electrical noise was of a comparable magnitude.

#### 5.2. Magnetic Loop in a Conducting Medium

The variations of predicted and measured values of loop e.m.f. for a transmitter loop current of 1.0 A r.m.s. and various frequencies and distance are shown in Figs. 9(a) and (b).

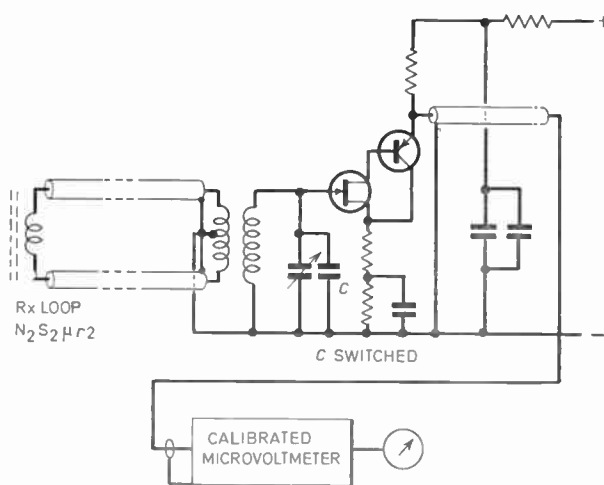
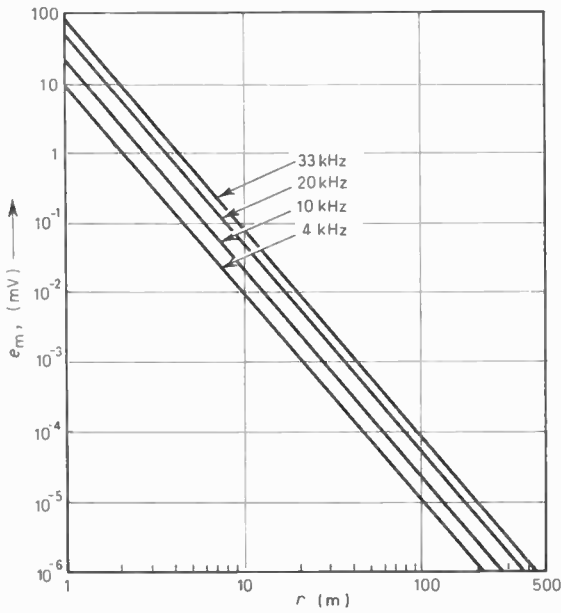
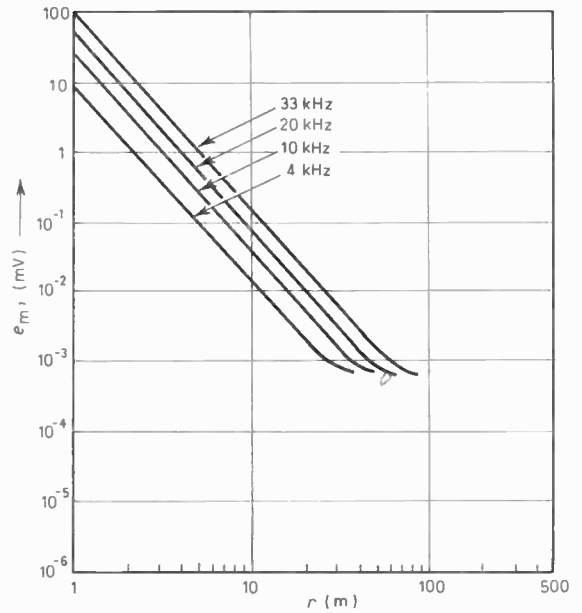


Fig. 7. Block diagram of the receiver.



(a) Computed values.



(b) Measured values.

Fig. 8. Variation of e.m.f. induced in a loop antenna in free-space with distance,  $r$ , at different frequencies.

In this case the forms of the two sets of curves are very similar. The minimum detectable signal was approximately  $0.2 \mu\text{V}$ , being limited by atmospheric and receiver noise.

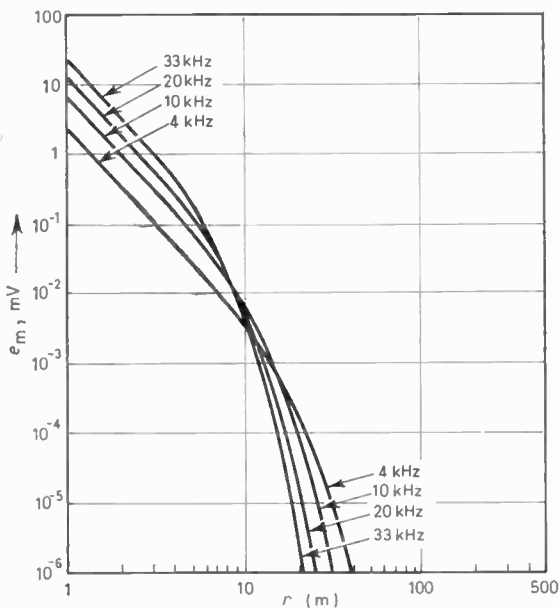
5.3. General Observations from Results

The variation in induced e.m.f. in air follows a  $1/r^3$  variation approximately showing the predominance of the near-field terms for ranges considered here. Furthermore, there is an expected increase in e.m.f. as the frequency is increased, and the curves remain parallel.

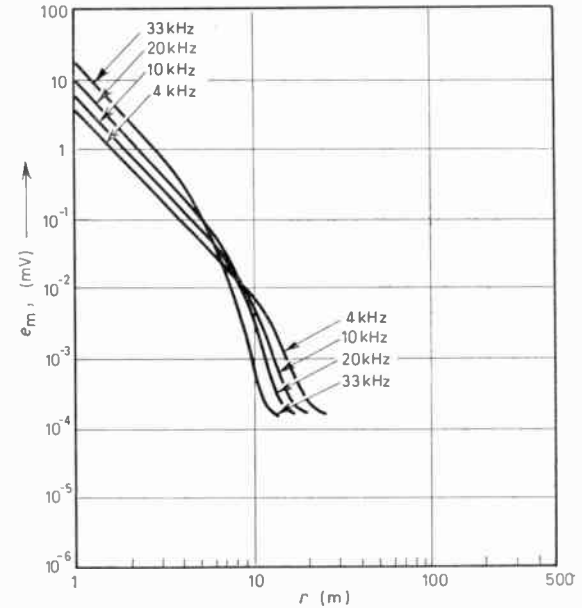
In contrast, the variation in e.m.f. for a conducting

medium displays a more complex variation with the slope continuously changing, with a crossover point where the relative amplitudes of signals of different frequencies are reversed. This illustrates the dispersive nature of a conducting medium.

Electrical noise noted during field trials was largely atmospheric in origin,<sup>22</sup> man-made low frequency signals being heavily attenuated before reaching the receiving antenna at a depth of 100 m. One interesting feature noted was that there was a relative absence of noise at the lowest frequency used (4 kHz), this corresponding to a noise attenuation frequency band.<sup>23</sup>



(a) Computed values.



(b) Measured values.

Fig. 9. Variation of e.m.f. induced in a loop antenna in conducting medium with distance  $r$ , at different frequencies.

## 6. Final Comments

The experimental results for electromagnetic waves in the sea illustrate clearly the rapid fall in loop e.m.f. as the distance between transmitter and receiver is increased, and suggest that the maximum range of a low frequency communication equipment using small loop antennas with permeable cores is likely to be approximately 50 m for a transmitting m.m.f. of 50 AT. However, the range is dependent on several factors, particularly the salinity of the water, and hence greater ranges would be expected<sup>11</sup> in regions with a large fresh water inflow.

For a typical salinity (conductivity about 4 S/m) the results indicate that greatest ranges are achieved using the lowest frequencies, particularly in the noise attenuation band,<sup>2,3</sup> and further suggest that the 'magnetic moment'  $M$  of eqn. (4) should be as large as possible. Since the physical size of the loop is limited by considerations of portability this means that  $\mu_r(IN)$  should be maximized.

During the experiments the transmitter current was produced by a power oscillator, but tests have shown that if the loop is made the inductor of a parallel-tuned amplitude-modulated class-C oscillator, then the loop current becomes  $Q(\text{effective}) \times \text{feed current}$ , with obvious advantages as regards battery-operated equipment.

Receiver sensitivity and signal/noise ratio have a large bearing on the maximum attainable range, and conventional techniques such as superheterodyne receivers and single-sideband transmission would be expected to give a considerable improvement over the simple single-tuned receiver and c.w. transmission used for the tests.

Operation in very shallow water can give higher received signal levels than in deep water, but this is due to a large proportion of the transmitted energy being propagated above the water mass. Such a mode of propagation is difficult to predict quantitatively but at best the received level can only approach the free-space results shown in Fig. 8(a).

## 7. Acknowledgments

The author is grateful to the Director of the Scottish Marine Biological Association, Dunstaffnage Marine Laboratory, for making available the Research Vessel *Calunas* for the deep-water trials, and to the Heriot-Watt University for the facilities which enabled this study to be carried out.

## 8. References

- Moore, R. K., 'The Theory of Radio Communication between Submerged Submarines', Ph.D. Thesis, Cornell University, Ithaca, U.S.A., June 1951.
- 'SEA-TEL' Magnetic Carrier Underwater Communication System: Berton Industries Limited, 1177 West Hastings Street, Vancouver 1, British Columbia, Canada.
- 'SEDAR' Modulated Electric Field System; Braincon Corporation, Marion, Massachusetts, 02738, U.S.A.
- 'UNDERCOM' system; reported in *Ordnance*, 53, p. 224, November/December 1968.
- Willoughby, J. A. and Lowell, P. D., 'Development of loop aerials for submarine radio communication', *Phys. Rev.*, 14, pp. 193-4, August 1919.
- Wait, J. R., 'The magnetic dipole antenna immersed in a conducting medium', *Proc. Inst. Radio Engrs*, 40, pp. 1244-5, October 1952.
- Wait, J. R. and Campbell, L. L., 'Fields of an oscillating magnetic dipole immersed in a semi-infinite conducting medium', *J. Geophys. Res.*, 58, p. 167, June 1953.
- Wheeler, H. A., 'Fundamental limitations of a small v.l.f. antenna for submarines', Paper No. 14, Symposium on V.L.F. Radio Waves, January 23-25, 1957, Boulder, Colorado, U.S.A.
- Wait, J. R., 'Insulated loop antenna immersed in a high conductivity medium', *J. Res. Nat. Bur. Stand.*, 59, No. 2, pp. 133-7, August 1957.
- Fenwick, R. C. and Weeks, W. L., 'Submerged antenna characteristics', *I.E.E.E. Trans. Antennas and Propagation*, AP-11, No. 3, pp. 296-305, May 1963.
- Bitterlich, W., 'Final Scientific Report on the Propagation of V.L.F. Waves in Solids', 31st December 1965, U.S. Government Contract No. 61, (052)-490. (W. Bitterlich, Kaiser Franz Josefstrasse 5, Innsbruck, Austria.)
- Hansen, R. C., 'Radiation and reception with buried and submerged antennas', *I.E.E.E. Trans. Antennas and Propagation*, AP-11, No. 3, pp. 207-16, May 1963.
- Bitterlich, W., 'Fourth Scientific Report on Antennas for the V.L.F. and L.F. Region', 1st September 1970, (For address see Ref. 11.)
- Kraichman, M. B., 'Basic experimental studies of the magnetic field from electromagnetic sources immersed in a semi-infinite conducting medium', *J. Res. Nat. Bur. Stand.*, 64D, No. 1, pp. 21-5, January/February 1960.
- Iizuka, K., 'Experimental study on the circular loop antenna immersed shallowly in a conducting medium', *J. Res. Nat. Bur. Stand.*, 69D, No. 9, pp. 1243-8, September 1965.
- Ramo, S., Whinnery, J. R. and Van Duzer, T., 'Fields and Waves in Communication Electronics', pp. 656-7, (Wiley, New York, 1965.)
- Williams, R. H., 'Insulated and loaded loop antenna immersed in a conducting medium', *J. Res. Nat. Bur. Stand.*, 69D, No. 2, pp. 287-9, February 1965.
- Williams, R. H., Kelly, R. D. and Cowan, W. T., 'Small prolate spheroidal antenna in a dissipative medium', *J. Res. Nat. Bur. Stand.*, 69D, No. 7, pp. 1003-9, July 1965.
- Kraus, J. D., 'Radio Astronomy', Chapter 5. (McGraw-Hill, New York, 1966.)
- Moore, R. K., 'Effects of surrounding conducting medium on antenna analysis', *Trans. I.E.E.E. Antennas and Propagation*, AP-11, No. 2, pp. 216-25, May 1963.
- Anderson, V. C., Gibson, D. K. and Ramey, R. E., 'Electronic components at 10,000 psi', Marine Physical Laboratory, Scripps Institute of Oceanography, California 92152, 1st May 1965, S.I.O. Reference 65-6.
- 'World Distribution and Characteristics of Atmospheric Radio Noise', C.C.I.R. Report No. 322, International Telecommunication Union, Geneva, 1964.
- Maxwell, E. L. and Stone, D. L., 'Natural noise fields from 1 c.p.s. to 100 kc/s', *I.E.E.E. Trans. Antennas and Propagation*, AP-11, No. 3, pp. 339-43, May 1963.
- Kraichman, M. B., 'Impedance of a circular loop in an infinite conducting medium', *J. Res. Nat. Bur. Stand.*, 66D, No. 4, pp. 499-503, July-August 1965.
- Zieh, G., 'Receiving and taking bearings in sea-water on electromagnetic waves', *Telefunken-Zeitung*, 33, No. 128, pp. 141-50, June 1960.
- Myers, J. J., Holm, C. H. and McAllister, R. F., 'Handbook of Underwater Engineering', pp. 3-36 to 3-40. (McGraw-Hill, New York, 1969.)
- Schellkunoff, S. A., 'Electromagnetic Waves', pp. 163. (Van Nostrand, New York, 1943.)

Manuscript received by the Institution on 15th March 1972. (Paper No. 1478/AMMS 53.)

## MEETING REPORT

# Implantable Cardiac Pacemakers\*

R. E. TROTMAN,

M.Sc., Ph.D., F.Inst.P., C.Eng., M.I.E.E.†

A COLLOQUIUM organized jointly by the Medical and Biological Electronics Group Committees of the IERE and the Institution of Electrical Engineers entitled 'Implantable Cardiac Pacemakers', was held at the London School of Hygiene and Tropical Medicine on 11th May 1972.

Dr. E. Sowton (Guy's Hospital, London) introduced the subject with a brief history. Research into artificial electric cardiac pacemaking began in 1954, and the first pacing of a patient—by means of electrical stimuli, applied across the closed chest, produced by an external pulse generator—took place in 1957. The first attempt to implant part of the pacemaker was carried out in Sweden in 1959, the technique being to attach the electrodes directly to the heart and to bring the wires out through the skin to an external pulse generator. The major problems were that the wires were easily broken, and infection set in and reached the heart easily. The endocardial technique, in which electrodes are passed to the heart through a vein, was also used. In this technique infection less easily reaches the heart. The first implant of a complete pulse generator/electrode system took place in the USA in 1962.

There are two commonly used types of totally implantable pacemaker: the fixed-rate pacemaker and the demand pacemaker. In the fixed-rate pacemaker a continuous train of



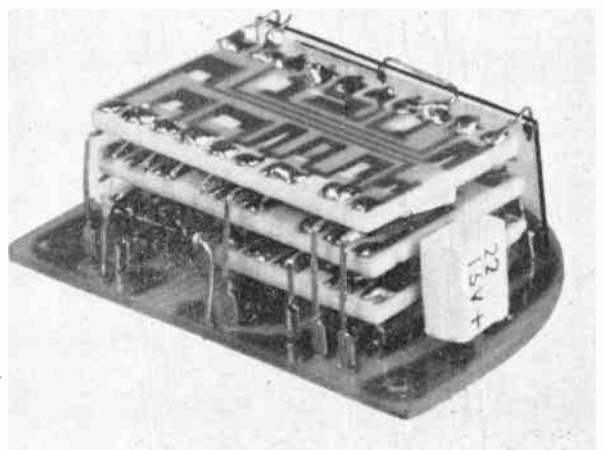
*Devices Implants Ltd., Photograph*

Implantable Demand Pacemaker showing the platinum-iridium indifferent electrode.

pulses is produced regardless of the heart's action. In the demand pacemaker a continuous train of pulses is produced unless a QRS wave from the heart is detected, in which case the wave inhibits the pulse generator for a period equal to the interval between two successive QRS waves of a heart beating at a given rate. There is a short period (of the order of 100 to 200 ms) immediately after a stimulus during which neither a QRS wave, nor any other wave, will inhibit the device.

One particularly dangerous condition may arise with a demand pacemaker. External electrical interference may produce the same effect as a QRS complex and inhibit the pulse generator. Some recent devices are so designed that interference causes the apparatus to operate at a fixed, but high, pulse rate, which is not dangerous but which warns the patient the apparatus is not functioning properly.

Totally implanted pacemakers were said to have a five-year lifetime, but in practice, even today, they seldom operate satisfactorily for more than three years.



*Devices Implants Ltd., Photograph*

The thick film circuit module of the Implantable Demand Pacemaker.

\* Reprinted, by permission of the Editor, from *Bio-Medical Engineering*, 7, pp. 277-9, July 1972.

† Instrument Department, Wright-Fleming Institute, St. Mary's Hospital Medical School, London W2 1PG.

Another device, the induction pacemaker, is also used for artificially stimulating the heart, but its use is limited mainly to hospitals in the Birmingham area of the UK. In this technique an electrode system and a coil are implanted with the coil situated just under the surface of the skin, and the pulse generator is mounted externally. A current is induced into the implanted coil by means of an external coil, which is mounted in the same module as the pulse generator, positioned over the implanted coil. (The technique is discussed later.) It is estimated that in the UK 20% of new pacemakers fitted are the induction type, the remainder being the totally implanted type.

Dr. Sowton also discussed various technical requirements and problems. The amount of energy required to stimulate the heart (the threshold energy) increases over the first eight to ten days of stimulation and then decreases over the next few days, usually up to the tenth to fourteenth day. It then remains constant. The output of the generator has to be adequate to stimulate the heart at its maximum threshold level, and 50  $\mu\text{J}$  has been found to be adequate.

An early problem, that of electrode fracture, appears now to have been solved. Similarly, electrolysis of the electrodes used to be a problem, but recently a system in which a small negative bias potential is applied to the positive-going electrode, so that it does not normally go positive, has been devised and this has reduced the problem with certain types of electrode.

The primary cause of pacemaker failure today is battery deterioration. In one make of pacemaker, it was found that in 80% of devices that failed in under 24 months the cause was deterioration of the battery. In all manufacturers' devices, the current required for demand devices is greater than that for fixed-rate devices, and therefore demand devices usually fail more rapidly than fixed-rate devices. For example, one manufacturer (Cordis) found that 45% of demand pacemakers were still functioning at 21 months, but that 45% of fixed-rate devices were still functioning at 30 months.

One of the most important facets of pacemaking is the detection of impending battery failure and the design of fail-safe systems. In some cases, as the battery deteriorates the pulse rate of the generator increases. This is very dangerous, and a decrease of the rate, instead, is considered preferable. Means for checking battery condition, and for checking parameters such as threshold energy, are being built into some modern devices. (A technique for checking pacemaker performance was discussed later.)

The technique of artificial electric cardiac pacemaking with totally implantable devices has improved very considerably in the decade since 1962. In the period 1962 to 1966, 67% of patients who received an implant survived two years, but in the period 1966 to 1970, 93% of such patients survived two years. At Guy's Hospital 60% survived five years. Clinical results of pacemaking show a greatly improved prognosis compared with drug treatment.

The number of new devices being implanted in the UK is unknown, but in the USA it is 5000 per month. This is equivalent to 1300 per month in the UK, although the actual figure is certainly less than that: Dr. Poole (whose paper was read later) estimates that it is approximately 250 per month. The figure of 1300 per month is equivalent to 10 per million of the population per year which compares with 100 per million of the population per year in Sweden, the highest figure known.

### Ventricularly Inhibited Pacemaker

Dr. J. Fyson (Atomic Weapons Research Establishment, Aldermaston) discussed the requirements and design con-

siderations of demand pacemakers, and gave details of one developed in collaboration with Dr. J. Kenny (Devices Implants Ltd.). The requirements are: low current consumption, a pulse width of 1 to 1.5 ms, current-limited pulses, means of detecting the QRS complex of the e.c.g., warning to the patient of impending battery failure, reliability and compatibility with the environment. Voltage- and current-limited pulses were discussed, the conclusion being that a current-limited system is preferable because it has a lower current consumption than a voltage-limited system, and because voltage-limited pulses may cause ventricular fibrillation should the heart be stimulated during ventricular repolarization (during the T wave).

The problems of battery failure and of inhibition of demand pacemakers by interference were discussed. The authors have devised a demand pacemaker which produces pulses at a rate of 70 per minute with a battery voltage of 5.4 V, the normal operating voltage. As the voltage decreases so the pulse rate decreases to approximately 65 per minute with a battery voltage of 4 V. Should the battery voltage drop below 4 V the pulse rate goes up to 100 per minute.

The pacemaker is not triggered unless the QRS wave of the heart is received at intervals equivalent to a heart rate of less than 60 beats per minute. Electrical interference switches on a continuous train of pulses at a rate of 100 per minute.

The power source is a mercury oxide cell, and one cause of failure of this type of pacemaker is that the battery gives off corrosive fluids which damage other parts of the device.

Encapsulating materials were also discussed. These must prevent the ingress of moisture and not apply a stress to the components: pressures of the order of 200 lb/in<sup>2</sup> (1380 kN/m<sup>2</sup>) have been created in some devices encapsulated in epoxy resins.

### Radioisotope-powered Pacemaker

Dr. M. J. Poole's paper on the radioisotope battery of the Atomic Energy Research Establishment at Harwell† was read by Dr. Penn.

The present patient survival times suggest that a battery with a ten-year life would be adequate, and it would certainly eliminate many of the re-operations due to battery failure that are necessary at present. The battery requirements, although varying slightly, could be satisfied by a cell that gives an output voltage of 6 V and a maximum power of 200  $\mu\text{W}$ . The device at present being developed produces 0.5 V, which is increased to 6 V by means of a d.c. to d.c. converter, and the input power required is 400  $\mu\text{W}$ . It has been calculated that the output power will decrease from 350  $\mu\text{W}$  to 250  $\mu\text{W}$  over 30 years.

The basic element of the battery is 180 mg of Pu-238 and the heat produced in the plutonium is converted to electricity by a bismuth telluride thermoelectric converter. A special grade of bismuth telluride, which is mechanically stronger than normally available grades, was developed for this purpose. Pu-238 is very hazardous and, in consequence, much effort has been devoted to developing and testing the capsule in which it is contained. The capsule has to withstand the heat to which it might be subjected (say, in a fire in the premises in which the pacemaker is situated, or in cremation, during which temperatures up to 1300°C are obtained), pressure due to helium gas which is released during the  $\alpha$  particle reaction of Pu-238 decay (up to 500 atmospheres) and high static and dynamic local and general forces (in collisions, forces up to 200 g are obtained).

† *Bio-Medical Engineering*, 6, p. 192, 1971.

The present capsule is cylindrical, made of Hastalloy steel, weighs less than 50 grams, and is 40 mm long and 17 mm in diameter. It has been tested under a two-ton (2000 kg) compression force applied along its axis and along a radius. Whilst it was deformed it was not broken in either case.

### Inductively Coupled Pacemakers

Mr. R. Lightwood (The Queen Elizabeth Hospital, Birmingham) described the induction pacemaker (mentioned earlier), work on which started in 1960. He saw its advantages as being as follows:

- (1) Since only a coil and leads are implanted there are no sterilization problems.
- (2) The stimulus is a damped sinusoid, so there is no electrode polarization.
- (3) Stimulus parameters, such as pulse amplitude and width, can be readily altered and can be adapted to particular 'dysrhythmias'.
- (4) The pulse generator can be switched off, by means of a switch on the external module, to see if the patient is progressing.
- (5) The pulse generator can easily be changed, if faults develop, without reoperation.
- (6) It is not necessary to hold regular clinics for checking the performance of the pacemaker.
- (7) Any improvements in electronics and other techniques can readily be incorporated in the external module.
- (8) The system is not affected by external electrical interference, because of the poor coupling between the internal and external coils.
- (9) The specification for electronics components is not so stringent as it is for components to be implanted so reliability can be the primary criterion.
- (10) The pacemaker is cheaper than totally implantable types. The complete system, including a spare stimulator which the patient has at all times, costs about £140.

The major disadvantages are that some patients will not accept the external equipment which is attached to them at all times, some do not like being reminded of their condition, and, since information from the heart cannot be fed back to the pacemaker, only simple fixed-rate pacemaking can be attempted. In some cases, irritation of the skin, to which the external module is attached, is a problem.

Mr. P. D. Jones (Joseph Lucas Ltd.), who designed the induction pacemaker, gave a few practical details about the device. The implanted coil, an air core coil, is encapsulated in silicone rubber. The pulse rate drops as the battery voltage drops. A microphone is provided to assist the patient to check the pulse rate, which is normally done every morning: the pulse rate is simply varied by a control on the external module.

In the four centres in the Birmingham area in which the device is used, 500 patients have had pacemakers fitted in the past 11 years. In The Queen Elizabeth Hospital, 360 patients have had pacemakers fitted in that period and at present 274 are still alive; of the 360, 77% had only the initial operation. Some 203 survived at least two years, 13 survived 9 years, 9, 10 years and 2, 11 years.

### Assessment of Implanted Pacemaker

Mr. G. D. Green (Department of Clinical Physics and Bio-Engineering, Western Regional Hospital Board, Glasgow)

briefly described his technique and apparatus for the rapid assessment of any totally implanted fixed-rate or demand pacemaker.† In this technique the potential difference between each pair of three external electrodes, placed in the positions for monitoring the e.c.g. at the standard leads (RA, LA and LL), is measured. Each potential difference is considered to be due to a dipole and the vector of the three dipoles is automatically calculated and presented on an oscilloscope. The vector is measured shortly after implantation and subsequently at regular 'follow up' clinics. Any changes in the vector may indicate a fault in the pacemaker or, of course, in the patient's condition.

The following are examples of problems discovered by this technique:

- (a) Increased current consumption was noted: this would have led to premature battery failure.
- (b) In a case of exit block, it was shown that the pacemaker was functioning satisfactorily.
- (c) Fibrous tissue formed round the end of an electrode lead.
- (d) A catheter, used in the endocardial method, was found to be displaced.
- (e) Although there was no clinical sign, a reduced pulse generator output was discovered.
- (f) Insulation on an electrode lead was found to be broken.

The great advantage of the method is that problems can be detected before there are any clinical symptoms, and thus the probability of emergency readmission and operation being necessary is significantly reduced.

Mr. Green stated that in Glasgow, 250 totally implanted pacemakers have been fitted in the last ten years, which is approximately one per week. Reoperations have also been at the rate of approximately one per week. Most patients were enabled to lead perfectly normal lives. To date, 50 patients have died, but very few deaths were due to failure of the pacemaker. The majority of failures occurred between 22 and 32 months, but a few devices were still functioning satisfactorily at 44 months.

### Metal Encapsulation

Professor M. Schaldack (Biomedical Engineering Department, Erlangen University, West Germany) discussed encapsulation, more particularly the use of a Co/Cr/Mo alloy for this purpose. He finds its advantages are:

- (1) Low tissue interaction.
- (2) Very easy to clean and sterilize.
- (3) Robust and easy to construct.
- (4) Reduced interference due to the electromagnetic screening of the capsule.

Experiments on the last effect were described. It appears that high-frequency interference, due to, say, microwave ovens or radar installations, in all makes of pacemaker, was significantly reduced when the device was placed in aluminium foil. Only metal encapsulating materials will reduce such interference.

Professor Schaldack said that in six years 10 000 pacemakers encapsulated in his alloy have been implanted. Only two had failed due to corrosion, and these failures were due to leaking batteries.

† *Amer. Heart J.*, 81, p. 1, 1971.

# Synchronous Multiplexing of Digital Signals using a Combination of Time- and Code-Division Multiplexing (T.D.M. and C.D.M.)

A. P. CLARK,

M.A., Ph.D., D.I.C., C.Eng., M.I.E.R.E.\*

## SUMMARY

The paper describes some arrangements for multiplexing and demultiplexing digital signals in element synchronism. The multiplexed signals are transmitted over a common channel, from a single transmitter to a single receiver, and the demultiplexing of the signals is achieved in the detection process at the receiver. A combination of time division and code division multiplexing (t.d.m. and c.d.m.) is used, in which the t.d.m. signal-elements are orthogonal, as are the c.d.m. elements, but simultaneously transmitted t.d.m. and c.d.m. signal-elements are not orthogonal. Arrangements using a linear combination of the two sets of orthogonal signals are studied, with various iterative detection processes, and their performances are compared with that of a system using a non-linear combination of the two orthogonal sets. It is shown that the latter system achieves a considerable advantage over the others and is particularly well suited to applications where the number of multiplexed signals is typically a little greater than the maximum number orthogonally multiplexed. Computer simulation has been used to measure the performances of the different systems.

\* Department of Electronic and Electrical Engineering, University of Technology, Loughborough, Leicestershire LE11 3TU

## Mathematical Notation

$|x|$  magnitude of the real scalar  $x$

$\{x_i\}$  the set  $x_1, x_2, \dots, x_k$ , where  $k$  is given in the text

$X^T$  transpose of the matrix or vector  $X$

Vectors and matrices are represented by capital letters and scalar quantities by lower-case letters.

Vectors are treated as matrices having one row or column.

## 1. Introduction

It is well known that in the synchronous multiplexing of digital signals, prior to feeding these over a common transmission path, either time, frequency or code-division multiplexing (t.d.m., f.d.m. or c.d.m.) can be used. The multiplexed signals are normally arranged to be orthogonal, so that at the receiver the individual received elements (digits) from the different multiplexed signals may be detected without interference from each other.

For a given bandwidth of the transmission path and a given signal-element rate per channel (multiplexed signal), there is a limit to the number of channels which may be multiplexed, so long as the individual received elements are required to remain orthogonal. With non-orthogonal multiplexing, many more channels may be multiplexed but at the expense of a reduced tolerance to additive noise and a greater equipment complexity.

The arrangements studied here use a combination of t.d.m. and c.d.m., in which the t.d.m. signal-elements are orthogonal, as are the c.d.m. elements, but simultaneously transmitted t.d.m. and c.d.m. elements are not orthogonal. The transmitted signals are designed to minimize the maximum intersymbol-interference between individual t.d.m. and c.d.m. elements. With these signals, up to twice as many channels may be multiplexed, for a given transmission path and signal-element rate per channel, as is possible with orthogonal multiplexing using either t.d.m. or c.d.m. The arrangements are of particular interest for those applications where the number of multiplexed channels varies with time.

The transmitted signal-elements are arranged in separate groups, which are transmitted sequentially, and there is no intersymbol-interference between elements in different groups. Each group contains one element from each channel. At any particular time, the total number of channels may have any value from 0 to  $2n$ , where  $n$  is the maximum number of orthogonal t.d.m. or c.d.m. channels. If a group of  $m$  elements contains  $u$  elements from different t.d.m. channels and  $v$  elements from different c.d.m. channels, then clearly  $u \leq n$ ,  $v \leq n$ , and

$$u + v = m. \quad \dots(1)$$

In a group of  $m$  signal-elements the two sets of orthogonal elements (t.d.m. and c.d.m.) may be combined linearly or non-linearly. In either case an iterative detection process is used, which detects simultaneously a group of  $m$  received signal-elements. At the end of a detection process, the detector has determined the values of the  $m$  received elements involved in the detection

process, and the demultiplexer identifies each detected element value with the corresponding channel.

Arrangements using a linear combination of the two sets of orthogonal signal-elements (t.d.m. and c.d.m.) are studied, with various iterative detection processes. Such processes have been described elsewhere.<sup>1-3</sup> The performances of these systems are compared with that of a particular arrangement where the two sets are combined non-linearly.

**2. Linear Combination of T.D.M. and C.D.M. Signal-Elements**

**2.1 Basic Assumptions**

The model of the multiplexer, transmission system and demultiplexer is shown in Fig. 1.

At the transmitter, an element timing waveform of period  $nT$  seconds is fed from the coder and multiplexer to the data sources, whose output binary signals have an element duration of  $nT$  seconds and reach the coder and multiplexer in element synchronism. Only the  $m$  sources and destinations of data, which are actually in operation, are shown in Fig. 1. Over any given element period the  $m$  received binary values at the coder and multiplexer are determined and stored in a buffer store. The coder converts each of the  $m$  binary values to a sequence of  $n$  impulses, with a different sequence for each channel. The multiplexer then combines these impulses and transmits the resultant signal over the following element period of  $nT$  seconds.

Consider the  $m$  multiplexed binary elements at the output of the coder and multiplexer and assume these to be present over the time period 0 to  $nT$  seconds. The set of  $n$  impulses corresponding to the binary signal-element of

the  $i$ th channel is given by

$$\sum_{j=1}^n z_i s_{ij} \delta(t-jT) \tag{2}$$

$$\delta(t) \text{ is a unit impulse at time } t=0, \text{ and } n=2^k \tag{3}$$

where  $k$  is a positive integer. Throughout this paper it will for convenience be assumed that  $n=16$ .

The binary value of the signal element in the  $i$ th channel is given by

$$z_i = \pm c_i \tag{4}$$

so that each element given by eqn. (2) is binary antipodal.  $c_i$  is positive and determines the level of the corresponding element; it has a fixed value for each orthogonal set of signal elements, but its value for one set is not necessarily the same as that for the other. It is assumed that the  $\{z_i\}$  are statistically independent and equally likely to have either binary value.

If the signal element in the  $i$ th channel, over the period 0 to  $nT$  seconds, is one of the  $u$  orthogonal t.d.m. elements, then one of the  $n$  components  $\{s_{ij}\}$  in eqn. (2) has the value 1 and the remainder have the value 0. Thus the  $n$ -component row-vector

$$S_i = s_{i1} s_{i2} \dots s_{in} \tag{5}$$

is given by one of the rows of the  $n \times n$  identity (unit) matrix. Each of the  $u$  t.d.m. elements has a different vector  $S_i$ . The complete set of  $n$  t.d.m. elements will be referred to as the orthogonal set A.

If the signal element of the  $i$ th channel is one of the  $v$  orthogonal c.d.m. elements, then, with  $n=16$ , the  $n$ -component row vector  $S_i$  is given by one of the rows of the  $16 \times 16$  Hadamard matrix

$$S = \frac{1}{4} \begin{bmatrix} 1 & 1 & 1 & 1 & 1 & 1 & 1 & 1 & 1 & 1 & 1 & 1 & 1 & 1 & 1 & 1 \\ 1 & -1 & 1 & -1 & 1 & -1 & 1 & -1 & 1 & -1 & 1 & -1 & 1 & -1 & 1 & -1 \\ 1 & 1 & -1 & -1 & 1 & 1 & -1 & -1 & 1 & 1 & -1 & -1 & 1 & 1 & -1 & -1 \\ 1 & -1 & -1 & 1 & 1 & -1 & -1 & 1 & 1 & -1 & -1 & 1 & 1 & -1 & -1 & 1 \\ 1 & 1 & 1 & 1 & -1 & -1 & -1 & -1 & 1 & 1 & 1 & 1 & -1 & -1 & -1 & -1 \\ 1 & -1 & 1 & -1 & -1 & 1 & -1 & 1 & 1 & -1 & 1 & -1 & -1 & 1 & -1 & 1 \\ 1 & 1 & -1 & -1 & -1 & -1 & 1 & 1 & 1 & 1 & -1 & -1 & -1 & -1 & 1 & 1 \\ 1 & -1 & -1 & 1 & -1 & 1 & 1 & -1 & 1 & -1 & -1 & 1 & -1 & 1 & 1 & -1 \\ 1 & 1 & 1 & 1 & 1 & 1 & 1 & 1 & -1 & -1 & -1 & -1 & -1 & -1 & -1 & -1 \\ 1 & -1 & 1 & -1 & 1 & -1 & 1 & -1 & -1 & 1 & -1 & 1 & -1 & 1 & -1 & 1 \\ 1 & 1 & -1 & -1 & 1 & 1 & -1 & -1 & -1 & -1 & 1 & 1 & -1 & -1 & 1 & 1 \\ 1 & -1 & -1 & 1 & 1 & -1 & -1 & 1 & -1 & 1 & 1 & -1 & -1 & 1 & 1 & -1 \\ 1 & 1 & 1 & 1 & -1 & -1 & -1 & -1 & -1 & -1 & -1 & -1 & 1 & 1 & 1 & 1 \\ 1 & -1 & 1 & -1 & -1 & 1 & -1 & 1 & -1 & 1 & -1 & 1 & 1 & -1 & 1 & -1 \\ 1 & 1 & -1 & -1 & -1 & -1 & 1 & 1 & -1 & -1 & 1 & 1 & 1 & 1 & -1 & -1 \\ 1 & -1 & -1 & 1 & -1 & 1 & 1 & -1 & -1 & 1 & 1 & -1 & 1 & -1 & -1 & 1 \end{bmatrix} \tag{6}$$

Again, each of the  $v$  c.d.m. elements has a different vector  $S_i$ . The complete set of  $n$  c.d.m. elements will be referred to as the orthogonal set B.

The resultant signal fed to the transmitter filter over the period 0 to  $nT$  seconds is

$$\sum_{i=1}^m \sum_{j=1}^n z_i s_{ij} \delta(t-jT) \tag{7}$$

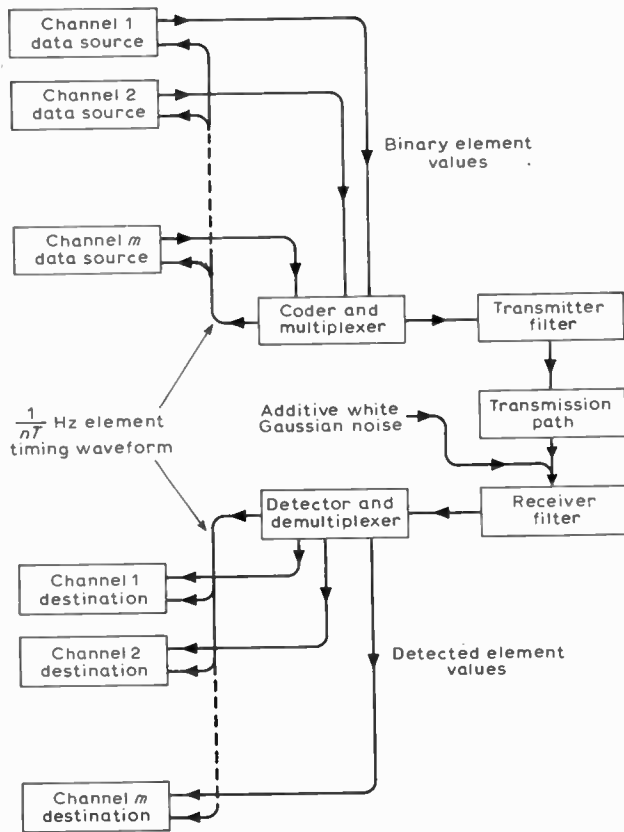


Fig. 1. Model of multiplexer, transmission system and demultiplexer.

In a practical arrangement of the system, a suitably-shaped baseband signal would be used in place of the set of impulses, the transmitter filter characteristics being suitably modified to give the same transmitted signal as that assumed here. It is however simpler to analyse the system in terms of the ideal impulses.

At irregular intervals, new channels will start operation and channels already in operation will cease transmission. During a transmission over a given channel, the vector  $S_i$  used by that channel remains unchanged and is not used by any other channel. It is assumed that when a new channel starts operation, its vector  $S_i$  is selected at random from the  $\{S_i\}$  not already in use. Thus, not only does the number of channels in operation,  $m$ , vary over the range 0 to  $2n$ , but for any given number of channels in operation at two widely separated times, two different sets of vectors  $\{S_i\}$  will in general be in use. The vector  $S_i$  used by any channel will be referred to as the address vector of that channel.  $S_i$  has unit length for all  $\{i\}$ .

The transmission path is assumed to be a linear baseband channel, which could include a modulator, band-pass channel and demodulator, and which introduces no signal attenuation or distortion. The transmitter and receiver filters in Fig. 1 are equivalent to all transmitter and receiver filters respectively, including any involved in modulation or demodulation.

White Gaussian noise with a two-sided power spectral density of  $\sigma^2$  is added to the data signal at the output of the transmission path, giving the Gaussian waveform  $w(t)$  added to the data signal at the output of the receiver filter.

The impulse response  $h(t)$  of the transmitter and receiver filters in cascade is assumed to be such that  $h(0) = 1$  and  $h(jT) = 0$  for all non-zero integer values of  $j$ , the delay introduced by the filters being neglected. This impulse response is achieved here in a conventional manner by using the same transfer function  $H^{1/2}(f)$  for the transmitter and receiver filters, where

$$H(f) = \begin{cases} \frac{1}{2}T(1 + \cos \pi fT) & \text{for } -1/T < f < 1/T \\ 0 & \text{elsewhere} \end{cases} \dots\dots(8)$$

Alternative transfer functions having the same values of  $h(jT)$  for all integers  $j$ , as assumed here, but using bandwidths down to a half that of  $H(f)$ , could of course be used instead.<sup>3</sup>

The detector samples the received signal  $n$  times per element, at regular intervals of  $T$  seconds, the sampling instants being suitably phased with respect to the received data signal. In a practical arrangement of the system, the required phase for the sampling instants may be determined either from the received data signal itself or through the transmission of a separate timing signal.

The signal at the output of the receiver filter, resulting from the transmission of a group of  $m$  signal elements over the period 0 to  $nT$  seconds, and neglecting the delay in transmission, is

$$r(t) = \sum_{i=1}^m \sum_{j=1}^n z_i s_{ij} h(t-jT) + w(t). \dots\dots(9)$$

At the detector input,  $r(t)$  is sampled at the time instants  $t = jT$ , for  $j = 1, \dots, n$ . Since  $h(0) = 1$  and  $h(jT) = 0$  for all non-zero integer values of  $j$ , the  $n$  sample values of  $r(t)$  are given by the  $n$  components of the row vector  $R = (r_j)$ , where

$$\begin{aligned} R &= \sum_{i=1}^m \sum_{j=1}^n z_i s_{ij} + W \\ &= \sum_{i=1}^m z_i S_i + W \\ &= ZS + W. \end{aligned} \dots\dots(10)$$

$Z = (z_i)$  is an  $m$ -component row vector,  $W = (w_j)$  is an  $n$ -component row vector, and  $S$  is an  $m \times n$  matrix whose  $i$ th row is  $S_i$ . It may be shown<sup>3</sup> that the  $\{w_j\}$  are sample values of statistically independent Gaussian random variables with zero mean and variance  $\sigma^2$ .

The detector detects the  $m$  received elements  $\{z_i S_i\}$  simultaneously in a single detection process, using the received vector  $R$ , and the demultiplexer allocates each detected element value to the corresponding channel. The  $n$ -component vectors  $R, ZS$  and  $W$  may be represented by points in an  $n$ -dimensional Euclidean signal-space, and the detection process may be described in terms of operations involving these vectors.<sup>1-3</sup>

It is assumed that the detector has prior knowledge of  $m, \{c_i\}$  and  $\{S_i\}$ , where

$$c_i = |z_i|, \text{ for } i = 1, \dots, m, \dots\dots(11)$$

so that it knows the  $2^m$  different possible values of  $ZS$ . Each time a channel ceases transmission or transmission commences on a new channel, the corresponding changes

in the values of  $m$ ,  $\{c_i\}$  and  $\{S_i\}$  must be fed to the receiver, preferably via a separate channel. The techniques involved here are beyond the scope of this paper, but are considered briefly elsewhere.<sup>1</sup>

2.2 Unique Detectability

Consider the arrangement just described, using linear multiplexing. If a subset of the  $m$  elements  $\{z_i S_i\}$  adds to zero for some set of values of the corresponding  $\{z_i\}$ , then, from eqn. (4), the subset must also add to zero for the complementary set of values of the  $\{z_i\}$ , and the subset is not uniquely detectable. It follows that a necessary (but not always sufficient) condition for the unique detectability of a set of  $m$  elements, for all permissible values of  $Z$ , is that no subset adds to zero.<sup>1</sup>

2.3 Detection Processes

If the  $m$  elements of a group all belong either to the orthogonal set A of t.d.m. elements or else to the orthogonal set B of c.d.m. elements, then the detection process which minimizes the probability of error per channel is one of matched filter or correlation detection of the individual received elements. The  $i$ th element in the group of  $m$  is here detected by feeding  $R$  (the set of  $n$  sample values of the received signal) to the correlation detector matched to  $S_i$ . The correlation detector multiplies the  $j$ th component of  $R$  by the  $j$ th component of  $S_i$ , for  $j = 1, \dots, n$ , and adds the products, to give, from eqn. (10), the output signal

$$\begin{aligned} RS_i^T &= ZSS_i^T + WS_i^T \\ &= z_i S_i S_i^T + WS_i^T \\ &= z_i + q_i \end{aligned} \dots\dots(12)$$

where  $q_i$  is a sample value of a Gaussian random variable with zero mean and variance  $\sigma^2$ .<sup>3</sup>  $z_i$  is now detected as  $c_i$  or  $-c_i$ , depending upon whether  $RS_i^T$  is positive or negative respectively.

Unfortunately the  $m$  elements of a group are not normally all members of an orthogonal set, and under these conditions the output signal of a correlation detector matched to a received element in one of the two orthogonal sets A and B, will contain interference components from the received elements in the other orthogonal set.

The detection process which here minimizes the probability of error in the detection of the  $m$  elements of a group, generates in turn each of the  $2^m$  different possible vectors  $\{ZS\}$  and determines which of these is at the minimum distance from  $R$ .<sup>3</sup> The corresponding vector  $Z$  gives the detected element values. But, when  $n = 16$ ,  $m$  may have a value up to 32, so that a quite excessive number of sequential operations may be required here.

An alternative detection process is as follows. The best linear estimate of  $Z$  is the  $m$ -component vector  $X$ , whose components may have any real values and are such that  $XS$  is the point in the subspace spanned by the  $\{S_i\}$  at the minimum distance from  $R$ .<sup>3</sup> The  $m$  vectors  $\{S_i\}$  are here assumed to be linearly independent, so that they span an  $m$ -dimensional subspace of the  $n$ -dimensional signal-space. By the projection theorem,<sup>4</sup>  $XS$  is the orthogonal projection of  $R$  onto the subspace.  $Z$  is now

detected from  $X$  by setting  $z_i$  to  $c_i$  or  $-c_i$ , for  $i = 1, \dots, m$ , depending upon whether  $x_i$  is positive or negative respectively.

The condition here for the unique detectability of  $Z$  is that the  $\{S_i\}$  are linearly independent.<sup>1</sup> This is a more restrictive condition than the requirement for the previous detection process, which is that no subset of the  $m$  elements adds to zero for any combination of their binary values.<sup>1</sup>

Since  $XS$  is the orthogonal projection of  $R$  onto the subspace spanned by the  $\{S_i\}$ , it satisfies the equation

$$XSS^T = RS^T \dots\dots(13)$$

so that

$$X = RS^T(SS^T)^{-1} \dots\dots(14)$$

assuming that  $S$  has rank  $m$ . A necessary (but not sufficient) condition for  $S$  to have rank  $m$  is that  $m \leq n$ , so that the detection process clearly cannot be used when  $m > n$ . Even when  $m \leq n$ ,  $S$  does not necessarily have rank  $m$ . Although this limits the usefulness of the arrangement for the applications considered here, the detector can be implemented in a very simple manner, as will now be shown.

When  $SS^T$  is nonsingular,  $R$  can be fed to the  $n$  input terminals of the linear network  $S^T(SS^T)^{-1}$  to give at its  $m$  output terminals the vector  $X$ . However, any change in the  $\{S_i\}$  normally results in changes in the majority of the components of  $S^T(SS^T)^{-1}$  and these changes are not simply related to that in the  $\{S_i\}$ . Considerable equipment complexity would clearly be involved in the practical implementation of such a system. The linear transformation is therefore best carried out by means of an iterative process using the arrangement of Fig. 2. Each line carrying a vector, in Fig. 2, is in fact a number of separate lines, each carrying the corresponding component of that vector.

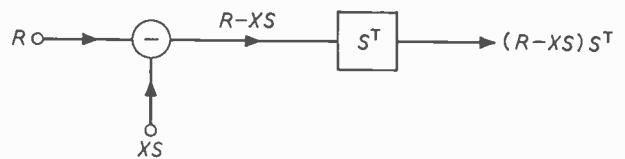


Fig. 2. Iterative process to determine  $X$  from  $R$ .

The received vector  $R$  is here fed to the input and  $X$  is initially set to zero.  $X$  is then adjusted in successive steps until eventually the  $m$ -component output signal-vector  $(R - XS)S^T$  is reduced to zero, when

$$XSS^T = RS^T \dots\dots(15)$$

as in eqn. (13). The  $i$ th column of  $S^T$  is  $S_i^T$  and the  $i$ th component of the output signal-vector is  $(R - XS)S_i^T$ . Clearly,  $S^T$  is a set of  $m$  correlation detectors matched to the  $m \{S_i\}$ . The advantage of the iterative process is that only  $R$  and  $S$  are used and these are both known at the receiver. Furthermore, the only effect on the detector of the addition or removal of a channel with address-vector  $S_i$ , is the addition or removal of the correlation detector matched to  $S_i$ , without changing the remaining correlation detectors.

The following arrangements of the iterative detection process have been tested.

2.4 System 1

The detector is shown in Fig. 2. At the start of the first cycle of the iterative detection process,  $X = 0$ . The detector computes the change in the value of  $x_i$ , for  $i = 1, \dots, m$ , such that if only this component of  $X$  were changed, the output signal from the  $i$ th correlation detector (at the  $i$ th output terminal of  $S^T$ ) would become zero. The  $i$ th correlation detector is of course matched to  $S_i$ . The computed changes in the values of the  $m$  components of  $X$  are then added to  $X$ , and the new value of  $X$  is fed to the detector of Fig. 2. The  $m$  output signals from  $S^T$  will not normally now be zero. The process just described is the first cycle of the iterative detection process. It is repeated for the second cycle, starting with the new value of  $X$ , and so on for as many cycles as required.

This is the point Jacobi iterative process.<sup>5</sup> It has been shown that with the two sets of orthogonal signal-elements the process will converge to give a zero output signal-vector from  $S^T$  and thus to give the required value of  $X$ , so long as the  $m \{S_i\}$  are linearly independent.<sup>1</sup>

2.5 System 2

This is a modification of System 1 and differs from System 1 in the following details. In a cycle of the iterative process the detector adjusts the components of  $X$  separately and sequentially, each time so that the corresponding component in the output signal-vector from  $S^T$  is reduced to zero. Thus the  $i$ th component of  $X$  is adjusted to reduce to zero the output signal from the correlation detector matched to  $S_i$ .  $X$  is here adjusted  $m$  times instead of just once, in one cycle of the iterative process, and the components of  $X$  are adjusted in order, starting with  $x_1$ . As before, the process may be repeated for as many cycles as required.

This is the point Gauss-Seidel iterative process.<sup>5</sup> The process converges for any set of linearly independent vectors  $\{S_i\}$ .<sup>1</sup>

It is assumed that the first  $u$  signal-elements ( $i = 1, \dots, u$ ) in a received group of  $m$  are t.d.m. elements and so are members of the orthogonal set A. The remaining  $v$  signal-elements are members of the orthogonal set B.

2.6 Constraints I, J and K

The operation of Systems 1 and 2 may be modified, and in some cases improved, by introducing constraints on the values of  $X$  during an iterative process.

The most severe constraint on the permissible values of  $X$  is that where, after a change in the value of  $x_i$ , for any  $i$ ,

$$|x_i| = c_i \dots\dots(16)$$

This is the constraint K.  $X$  is initially set to zero, as before, and after the first cycle of the iterative process,  $X$  must have one of the  $2^m$  possible values of  $Z$ . The detector sets  $x_i$  to whichever of the values  $\pm c_i$  gives the smaller magnitude output signal from the  $i$ th correlation detector.

A less severe constraint is that where, for any  $i$ ,

$$|x_i| \leq c_i \dots\dots(17)$$

This is the constraint J. The detector here determines the change in each  $x_i$ , exactly as with no constraint, but if, after making a change, it is found that  $|x_i| > c_i$ ,  $x_i$  is immediately set to the nearest of the values  $\pm c_i$ , so that  $x_i$  is held within the range of values given by eqn. (17).

The absence of any constraint on the values of  $X$  during an iterative process will for convenience be referred to as the constraint I.

The constraint applied in a detection process will be indicated by adding the appropriate letter after the number of the system. Thus System 2J is the System 2 using the constraint J.

The purpose of studying the constraints J and K has been to investigate whether these non-linear techniques provide a useful improvement in the maximum number of signal elements which may be uniquely detected.

3. System 3

The weakness of the arrangements using a linear combination of the orthogonal sets A and B is that where there are many more than  $\sqrt{n}$  elements in each orthogonal set and all elements have the same level, there is an appreciable probability that a subset of the signals will add to zero. When this occurs the signal elements cannot be detected correctly, whatever detection process is used. Furthermore, even when the signal elements are uniquely detectable there may be an unacceptably low tolerance to additive noise.<sup>1</sup> The situation can be improved by using different levels for the signal elements in the two orthogonal sets, but even now a poor performance is likely to be obtained when there are more than  $\frac{1}{2}n$  elements in each orthogonal set, since the  $\{S_i\}$  are always linearly dependent when  $m > n$ .

System 3 is an arrangement aimed at overcoming these weaknesses. For each transmitted group of  $m$  elements in System 3, the coder and multiplexer form the linear sum of the  $u$  signal-elements in the orthogonal set A to give

$$\sum_{i=1}^u \sum_{j=1}^n z_i s_{ij} \delta(t-jT) = \sum_{j=1}^n a_j \delta(t-jT) \dots\dots(18)$$

and the linear sum of the  $v$  signal-elements in the orthogonal set B to give

$$\sum_{i=u+1}^m \sum_{j=1}^n z_i s_{ij} \delta(t-jT) = \sum_{j=1}^n b_j \delta(t-jT) \dots\dots(19)$$

where  $a_j$  and  $b_j$  are the resultant values of the  $j$ th impulses in eqns. (18) and (19) respectively, for  $j = 1, \dots, n$ . The set of  $n$  impulses given by eqn. (19) are now combined non-linearly with the  $n$  impulses given by eqn. (18), as follows. For each  $j$ , if  $b_j$  is positive, its sign is taken to be the same as that of  $a_j$ , whereas if  $b_j$  is negative, its sign is taken to be the opposite to that of  $a_j$ , the magnitude of  $b_j$  being as given by eqn. (19). Whenever  $a_j$  is zero, the corresponding  $b_j$  is as given by eqn. (19).  $b_j$ , with a change in sign where necessary, is then added to  $a_j$ , for  $j = 1, \dots, n$ , to give the resultant set of  $n$  impulses, which are fed to the transmitter filter.

The detection process uses a set of  $m$  correlation detectors matched to the  $m \{S_i\}$ , as before, but these are

now separated into two groups corresponding to the orthogonal sets A and B. The detection process is a modification of System 2K, where the  $\{x_i\}$  are constrained to satisfy eqn. (16) and are the detected values of the  $\{z_i\}$ .

In the first cycle of the iterative process, the detector determines the binary values  $\{x_i\}$  of the  $u$  elements in the orthogonal set A, from the signs of the appropriate  $u$  components of  $R$ . A correlation detector matched to one of these signal-elements simply determines the value of the corresponding  $r_j$ . A received element of set A is for convenience identified with its one non-zero component in its signal-vector  $z_i S_i$ . The signs of all  $\{r_j\}$  which contain received elements of the orthogonal set A are now made positive, so that each of these becomes the corresponding  $|r_j|$ . The value of  $c_i$  for set A ( $i = 1, \dots, u$ ) is then subtracted from each of these  $\{|r_j|\}$ . The remaining  $\{r_j\}$  contain no elements of set A and are left unchanged. The resultant  $n$ -component vector is fed to the  $v$  correlation detectors matched to the address-vectors  $\{S_i\}$  of the received elements of the orthogonal set B, and the elements in this set are detected from the signs of the corresponding correlation-detector output signals, to give the appropriate  $v \{x_i\}$ .

In the second cycle of the iterative process, the detected binary value  $x_i$  of each of the  $v$  elements in set B is used to generate the corresponding vector  $x_i S_i$ , having one of the values  $c_i S_i$  or  $-c_i S_i$ , and these vectors are then added together to give the detected value of the sum of the received elements in set B. Let this be the  $n$ -component vector  $D = (d_j)$ . With correct detection,  $d_j = b_j$  for  $j = 1, \dots, n$ , where  $b_j$  satisfies eqn. (19).

Each of the  $u$  received elements in set A is now detected from the sign of the corresponding component  $r_j$  of the original received vector  $R$ , according to the following rule. Whenever  $d_j$ , the component of  $D$  having the same position as  $r_j$ , is more positive than  $-c_i$  for set A ( $i = 1, \dots, u$ ),  $x_i$  for the element in set A is given the value  $c_i$  or  $-c_i$ , depending upon whether  $r_j$  is positive or negative respectively. Whenever  $d_j$  is more negative than  $-c_i$  for set A,  $x_i$  is given the value  $c_i$  or  $-c_i$ , depending upon whether  $r_j$  is negative or positive respectively.

The sign of each  $r_j$  that contains a received element in set A is now made positive, except for the  $\{r_j\}$  whose corresponding  $\{d_j\}$  are more negative than  $-c_i$  for set A. The signs of these  $\{r_j\}$  are made negative. The remaining  $\{r_j\}$  are left unchanged, as before. The value of  $c_i$  for the set A is then subtracted from each of the resultant components containing an element of set A. The  $n$ -component vector obtained from this operation is fed to the  $v$  correlation detectors matched to the  $\{S_i\}$  of set B, to give another set of detected binary values  $\{x_i\}$  for the  $v$  elements in set B.

The cycle may now be repeated as often as required.

When  $c_i$  has the same value for sets A and B ( $i = 1, \dots, m$ ), the most frequent cause of non-unique detectability of the received elements is that the sum of all the received elements in set B has a component with the same position (value of  $j$ ) as that of a received element in set A and with

the negative of the value of the element in set A. In other words, before the changes in sign of the appropriate  $\{b_j\}$  at the transmitter,  $b_j = -c_i$  and  $a_j = \pm c_i$  for some  $j$ , where  $a_j$  and  $b_j$  are given by eqns. (18) and (19) respectively. The resultant received component value is now zero and unaffected by the binary value of the corresponding received element in set A. Non-unique detectability is not however caused by this effect when it involves only a subset of the received elements in set B.

When  $n = 2^{2k}$ , with  $k$  a positive integer, and when  $c_i$  is the same for both orthogonal sets, the effect just described can be avoided by ensuring that there are always an odd number of received elements in set B.

#### 4. Comparison of Systems 1, 2 and 3

##### 4.1 Tests by Computer Simulation

The performances of Systems 1, 2 and 3 have been compared by computer simulation and the results of these tests are given in Figs. 3–7. In all tests  $n = 16$ . Each test simulates the detection of a number of groups of  $m$  received elements, and for every group a random selection is made of the  $u$  and  $v$  address-vectors from the available addresses in sets A and B respectively. In each detection process the detector is assumed to have prior knowledge of the  $m$  addresses. In every case tested,  $c_i$ , the level of an individual signal-element, has a fixed value for each orthogonal set, but the value for one set is not necessarily the same as that for the other.

After each cycle of an iterative detection process, the signs of the  $m \{x_i\}$  are compared with the signs of the corresponding  $\{z_i\}$  and the number of errors (differences in signs) counted. Suppose that there are  $e$  errors in the  $u$  elements of set A and  $f$  errors in the  $v$  elements of set B. Then for each pair of values of  $u$  and  $v$  tested, the average values of  $e/u$  and  $f/v$  are determined for  $l$  received groups of  $m$  elements, to give  $p_u$  and  $p_v$  respectively.  $l$  remains constant throughout a complete test. For each orthogonal set,  $p$  is the average of the values of the corresponding  $p_u$  or  $p_v$ , taken over all pairs of values of  $u$  and  $v$  tested. Thus  $p$  is an estimate of the long-term element error probability per channel of the appropriate orthogonal set, in an arrangement where at any instant  $u$  and  $v$  are equally likely to have any of the different pairs of values tested.  $p$  is also a weighted estimate of the fraction of the total number of possible signal combinations which will be correctly detected in the appropriate orthogonal set, so that the value of  $p$  after  $k$  cycles of an iterative detection process is a measure of the degree of convergence of the process. The variation of  $p$  with  $k$  gives an indication of the rate of convergence of the process.

##### 4.2 Results of Computer Simulation Tests

Figures 3 and 4 compare the performances of different arrangements of the Systems 1–3, where  $c_i = 1$  for  $i = 1, \dots, m$ , so that the levels of the individual received signal-elements are all equal. The signals are received in the absence of noise. The quoted values of  $l$  refer to the number of trials for each pair of values of  $u$  and  $v$  tested.

For a given constraint I, J or K, Systems 1 and 2 have similar convergence properties, and the best performance

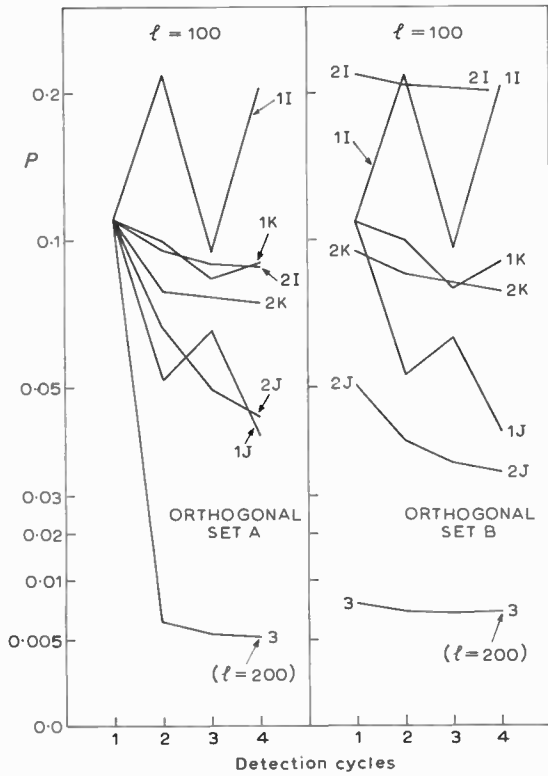


Fig. 3. Orthogonal sets A and B, equal levels, no noise;  $p$  averaged over all combinations of odd numbers in the two sets, between 7 and 15.

of these systems is obtained with the constraint J. System 3 not only converges to much lower values of  $p$  than Systems 1 and 2 but it does so much more rapidly. Systems 1 and 2 fail when  $m \rightarrow n$ , and System 3 fails when  $m \rightarrow 2n$ . Although the constraint J increases both the rate and degree of convergence for the Systems 1 and 2,

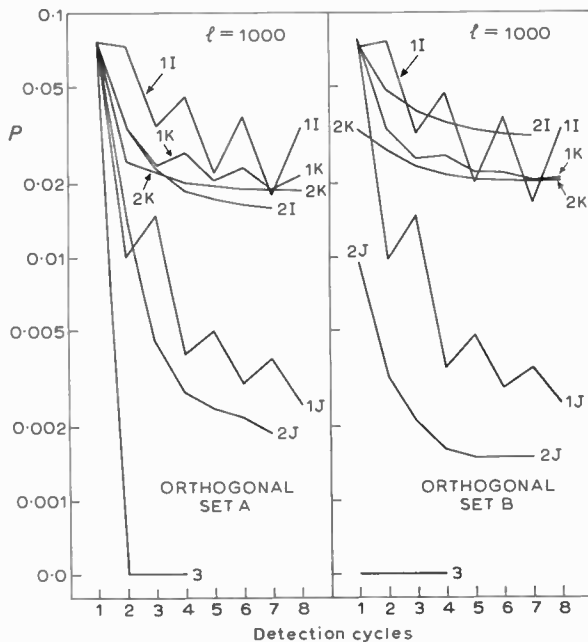


Fig. 4. Orthogonal sets A and B, equal levels, no noise;  $p$  averaged over all combinations of odd numbers in the two sets, between 7 and 9.

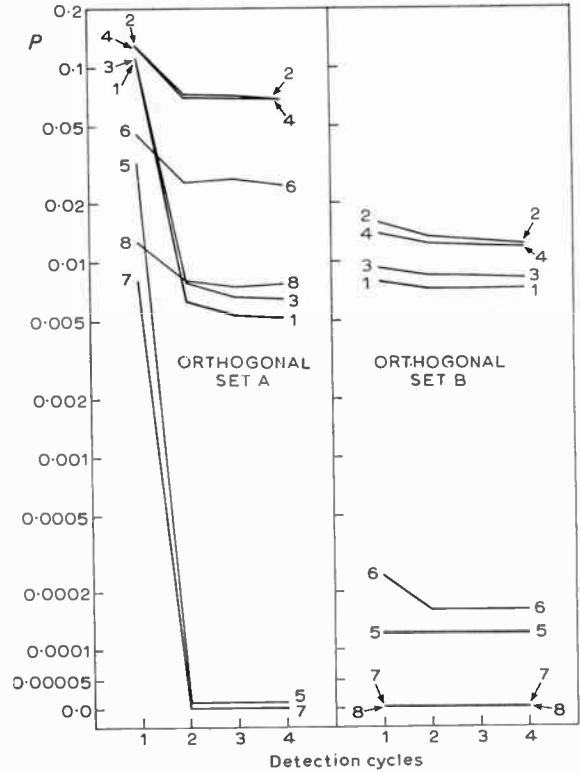


Fig. 5. System 3 with no noise.

the improvement is not sufficient to make these systems really useful. Systems 1 and 2 are not therefore considered further.

Figure 5 shows the performance of System 3 for various values of the received signal levels in sets A and B. The parameters associated with the different graphs in Fig. 5 are given in Table 1. Where  $u$  is marked 'odd' in Table 1,  $p$  is determined from all combinations of  $u$  and  $v$  such that  $u$  has an odd value in the range 7 to 15. Where  $u$  is marked 'even',  $p$  is determined from all combinations of  $u$  and  $v$  such that  $u$  has an even value in the range 8 to 16. These conventions apply similarly for  $v$ .

These tests, together with more detailed tests whose results are not shown here, suggest that, with  $n = 16$

Table 1

Parameters associated with the different graphs in Fig. 5

Graph No.	Set A		Set B		$l$
	$u$	$c_i$	$v$	$c_i$	
1	odd	1.0	odd	1.0	200
2	even	1.0	even	1.0	200
3	even	1.0	odd	1.0	100
4	odd	1.0	even	1.0	100
5	odd	1.0	odd	0.6667	100
6	even	1.0	even	0.6667	100
7	odd	1.0	odd	0.5	100
8	even	1.0	even	0.5	100

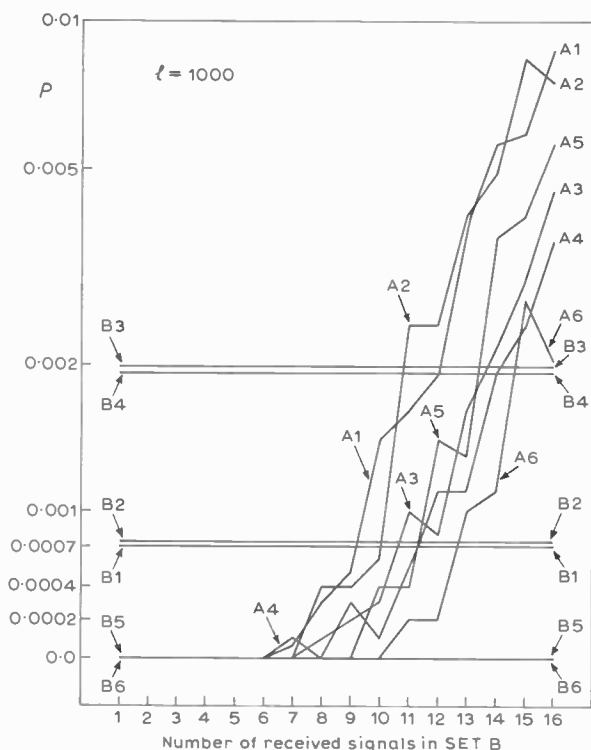


Fig. 6. System 3 with noise, first detection cycle.

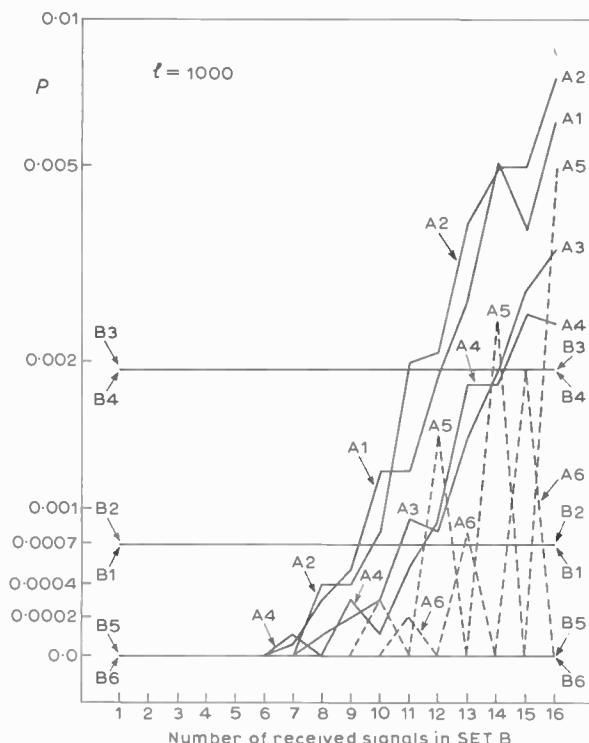


Fig. 7. System 3 with noise, second detection cycle.

and in the absence of noise, there are no errors in detection for System 3, so long as  $v$  is always odd and  $c_i$  for set A is equal to  $k/2$  times  $c_i$  for set B, where  $k$  is any integer not less than 4.

Figures 6 and 7 show the performance of System 3 when the signal is received in the presence of additive white Gaussian noise (Fig. 1). The letter A or B against a graph here indicates the orthogonal set to which the values of  $p$  apply. The parameters associated with the different graphs are given in Table 2, where  $\sigma^2$  is the two-sided power spectral density of the additive white Gaussian noise at the input to the receiver filter.

Table 2

Parameters associated with the different graphs in Figs. 6 and 7

Graph No.	Set A $u$	Set A $c_i$	Set B $c_i$	$\sigma$
A1, B1	16	1.0	0.4	0.125
A2, B2	8	1.0	0.4	0.125
A3, B3	16	1.0	0.3636	0.125
A4, B4	8	1.0	0.3636	0.125
A5, B5	16	1.0	0.4	0.0
A6, B6	16	1.0	0.3636	0.0

Figures 6 and 7 give the values of  $p$  at the end of the first and second cycles respectively of the iterative detection process. No significant reduction in the values of  $p$  is obtained in the subsequent cycles of the iterative process. The values of  $p$  plotted here are the estimates of

the error probability per channel for given values of  $u$  and  $v$ . The values of  $p$  originally determined for each of the graphs B1 to B4 remain approximately the same, regardless of the number of received signals in set B. Thus to simplify Figs. 6 and 7, the graphs plotted for B1 to B4 show in each case a constant value of  $p$ , which is its average value determined over all values of  $v$  from 1 to 16.

It can readily be shown that for the signal/noise ratio which applies to the graphs B1 and B2, the probability of an element error in set B, when no other elements are received, is 0.00069. For B3 and B4 it is 0.00181. It appears therefore that in the arrangement of System 3 tested, the tolerance to noise of the received signal-elements in set B is not significantly different from that of these elements when transmitted and detected with no other signal-elements present.

Figure 7 suggests that when there are normally around 9 received signal-elements in set B, the best overall tolerance to additive Gaussian noise should be obtained with  $c_i = 0.4$  for set B and an odd number of elements in this set. It is assumed that  $c_i = 1.0$  for set A, and that there are usually as many or more elements in set A as there are in set B. When there are normally around 14 signal-elements in set B, the best overall tolerance to additive Gaussian noise should be obtained with  $c_i = 0.3636$  for set B and an even number of elements in this set.

### 4.3 Assessment of System 3

It is clear that System 3 is by far the most effective of the different arrangements studied in this paper.

When it is required to multiplex  $m = n + k$  binary signals, where  $n$  is the maximum number which may be multiplexed orthogonally and  $1 \leq k \leq n$ , it is possible to transmit  $k$  quaternary signals (each carrying two binary signals) together with another  $n - k$  binary signals, the  $n$  different signals being orthogonal. For a given average transmitted element energy and the most efficient signal design, the tolerance of a transmitted quaternary element to additive white Gaussian noise is approximately 7dB below that of a transmitted binary element. Conventional pulse amplitude modulation (p.a.m.) is of course assumed here. Some of the transmitted binary elements in a group of  $m$  now have a considerably lower tolerance to noise than others. In System 3, however, the tolerance to noise of the signal elements in set B is not significantly affected by the number of elements in set A, whereas the tolerance to noise of an element in set A decreases slowly as the number of elements in set B increases, assuming a fixed value for the  $\{c_i\}$  in Set B. With  $n = 16$  and with suitable transmitted signal levels, the overall tolerance to noise of System 3, for  $n$  signal elements in set A and less than  $\frac{1}{2}n$  elements in set B, is better than that of the previous arrangement, where this has the same total number of binary signals. Furthermore, as the number of signal elements in set B decreases, so the tolerance to noise of System 3 steadily increases to its maximum value, obtained where all signal elements are in set A. Clearly, System 3 achieves its greatest advantage over the previous arrangement when there are  $n$  signal-elements in set A and just one or two signal-elements in set B.

## 5. Conclusions

If the t.d.m. and c.d.m. signals (the orthogonal sets A and B) are combined linearly and the number of multiplexed signals approaches the maximum number orthogonally multiplexed, with a similar number of signals in each orthogonal set, then there is either an appreciable probability that the signals are not uniquely detectable or else there is an unacceptably low tolerance to noise for many of the possible combinations of the signal waveforms (address vectors). However, with non-linear multiplexing of the two orthogonal sets and a suitable choice of the transmitted signal levels, as implemented in System 3, unique detectability can readily be ensured for up to twice as many signals as may be multiplexed orthogonally, and this does not result in an excessive reduction in tolerance to additive noise. System 3 is particularly well suited to those applications where the number of signals is typically a little greater than the maximum number orthogonally multiplexed and where most signals are normally t.d.m.

## 6. Acknowledgments

Much of the work reported in this paper was carried out at the Imperial College of Science and Technology, University of London, as part of a course of research for

the Ph.D. degree.<sup>1</sup> The work was sponsored jointly by the Science Research Council and Plessey Telecommunications Research Ltd., under the Industrial Fellowship Scheme, and the author gratefully acknowledges their financial support.

## 7. References and Bibliography

1. Clark, A. P., 'The Transmission of Digitally Coded Speech Signals by means of Random Access Discrete Address Systems', Ph.D. Thesis, Faculty of Engineering, University of London, 1969.
2. Clark, A. P., 'Adaptive detection of distorted digital signals', *The Radio and Electronic Engineer*, 40, No. 3, pp. 107-19, September 1970.
3. Clark, A. P., 'A synchronous serial data-transmission system using orthogonal groups of binary signal elements', *I.E.E.E. Trans. on Communication Technology*, COM-19, No. 6, Pt. 1, pp. 1101-10, December 1971.
4. Franks, L. E., 'Signal Theory', pp. 44-7 (Prentice-Hall, Englewood Cliffs, N.J., 1969).
5. Varga, R. S., 'Matrix Iterative Analysis'. (Prentice-Hall, Englewood Cliffs, N.J., 1962).
6. Glenn, A. B., 'Code division multiplex system', *I.E.E.E. Internat. Conv. Rec.*, 12, Pt. 6, pp. 53-61, 1964.
7. Chang, R. W., 'Synthesis of band-limited orthogonal signals for multichannel data transmission', *Bell Syst. Tech. J.*, 45, No. 10, pp. 1775-96, December 1966.
8. Saltzberg, B. R., 'Performance of an efficient parallel data transmission system', *I.E.E.E. Trans. on Communication Technology*, COM-15, No. 6, pp. 805-11, December 1967.
9. Uglow, K. M., 'Multiplex telemetry modulation and demodulation methods', *I.E.E.E. Trans. on Communication Technology*, COM-16, No. 1, pp. 133-41, February 1968.
10. Smith, J. W., 'A unified view of synchronous data transmission system design', *Bell Syst. Tech. J.*, 47, No. 3, pp. 273-300, March 1968.
11. Chang, R. W. and Gibby, R. A., 'A theoretical study of performance of an orthogonal multiplexing data transmission scheme', *I.E.E.E. Trans. on Communication Technology*, COM-16, No. 4, pp. 529-40, August 1968.
12. Harmuth, H. F., 'Transmission of Information by Orthogonal Functions' (Springer-Verlag, Berlin, 1969).
13. Schmid, P. E., Dudley, H. S. and Skinner, S. E., 'Frequency-domain partial-response signals for parallel data transmission', *I.E.E.E. Trans. on Communication Technology*, COM-17, No. 5, pp. 536-44, October 1969.
14. Kaye, A. R. and George, D. A., 'Transmission of multiplexed PAM signals over multiple channel and diversity systems', *I.E.E.E. Trans. on Communication Technology*, COM-18, No. 5, pp. 520-6, October 1970.
15. Brayer, K., 'Euclidean orthogonal data transmission', *Proc. I.E.E.E.*, 59, No. 1, pp. 79-80, January 1971.
16. Dijon, B. and Hansler, E., 'Optimal multiplexing of sampled signals on noisy channels', *I.E.E.E. Trans. on Information Theory*, IT-17, No. 3, pp. 257-62, May 1971.

Manuscript received by the Institution on 11th May 1972. (Paper No. 1479/Com. 55).

# LETTERS

From: Professor P. B. FELLGETT  
M.A., Ph.D., C.Eng., F.I.E.R.E.  
and Mr. D. E. CHARLTON, B.A.

## Sensitivity of Radiation Detectors

Too much should not be read into diagrams drawn on a compact logarithmic scale, but some comment may nevertheless be helpful on aspects of Fig. 6 of the paper of Baker *et al.* on 'High performance pyroelectric detectors'.<sup>1</sup>

More than two decades ago, I measured<sup>2</sup> a Schwartz radiation thermocouple having a detectivity<sup>3</sup> at low frequencies approximately twice as great as that indicated by the 'thermopile' line on Fig. 6. This means that thermocouples can, at least exceptionally, exceed the sensitivity shown by the 'pyroelectric' line on the diagram.

P. B. FELLGETT

Department of Applied Physical Sciences,  
The University of Reading,  
Whiteknights,  
Reading RG6 2AL.  
5th July 1972.

Professor Fellgett is correct in pointing out that thermocouples can have specific detectivities exceeding those shown by the lines for both 'thermopiles' and 'pyroelectric detectors' in Fig. 6. Our intention was to show the behaviour to be expected from typical commercial detectors.

We have ourselves seen both pyroelectric detectors and thermopiles with specific detectivities of  $2 \times 10^9 \text{ cm Hz}^{-1} \text{ W}^{-1}$ . As a result of our most recent measurements we now believe

that the thermocouple line, which was deduced from literature values,<sup>4</sup> understates the case for the best commercial thermocouples.

A decision to replace thermopile by pyroelectric detectors based on consideration of detectivity alone would be contentious. However, even at low frequencies the pyroelectric detector offers real advantages: increased reliability due to the absence of vacuum or delicate optical train, high responsivity, a uniform spectral response and an exceptionally uniform response over the sensitive area which leads to good phase stability in the electrical output. When the increased flexibility offered to system designers by the wide choice of operating frequency and sensitive area is considered, we believe that the attraction of pyroelectric detectors is very great.

D. E. CHARLTON

Mullard Southampton,  
Millbrook Industrial Estate,  
Southampton,  
Hampshire SO9 7BH.  
18th August 1972.

1. Baker, G., Charlton, D. E. and Lock, P. J., *The Radio and Electronic Engineer*, 42, p. 260, June 1972.
2. Fellgett, P. B., *Proc. Phys. Soc.*, 62B, p. 351, 1949.
3. Jones, R. Clarke, *Nature*, 170, p. 937, 1952.
4. 'Semiconductors and Semimetals: Vol. 5, Infrared detectors,' Ed. R. K. Willardson and A. C. Beer, pp. 307. (Academic Press, New York, 1970.)

## STANDARD FREQUENCY TRANSMISSIONS—September 1972

(Communication from the National Physical Laboratory)

September 1972	Deviation from nominal frequency in parts in $10^{10}$ (24-hour mean centred on 0300 UT)			Relative phase readings in microseconds N.P.L.—Station (Readings at 1500 UT)		September 1972	Deviation from nominal frequency in parts in $10^{10}$ (24-hour mean centred on 0300 UT)			Relative phase readings in microseconds N.P.L.—Station (Readings at 1500 UT)	
	GBR 16 kHz	MSF 60 kHz	Droitwich 200 kHz	GBR 16 kHz	†MSF 60 kHz		GBR 16 kHz	MSF 60 kHz	Droitwich 200 kHz	GBR 16 kHz	†MSF 60 kHz
1	-0.1	-0.1	0	620	607.3	17	0	0	-0.1	629	618.5
2	0	0	0	620	607.2	18	0	0	-0.1	629	618.5
3	0	0	0	620	607.2	19	+0.1	0	-0.1	628	618.1
4	-0.1	0	0	621	607.4	20	0	0	-0.1	628	617.8
5	-0.1	-0.1	0	622	608.1	21	0	0	0	628	617.5
6	-0.1	-0.2	0	623	609.7	22	0	+0.1	-0.1	628	616.7
7	-0.1	-0.1	-0.1	624	610.8	23	0	+0.1	-0.1	628	616.1
8	-0.1	-0.1	-0.1	625	611.7	24	+0.1	+0.1	0	627	615.2
9	-0.2	0	-0.1	627	614.0	25	0	0	0	627	615.0
10	-0.1	-0.2	-0.1	628	615.8	26	0	0	0	627	614.3
11	-0.1	-0.1	-0.1	629	617.0	27	0	0	-0.1	627	614.4
12	0	-0.1	-0.1	629	618.3	28	0	0	-0.1	627	614.2
13	0	0	-0.1	629	618.3	29	+0.1	0	0	626	614.1
14	0	0	-0.1	629	618.4	30	0	0	-0.1	626	614.1
15	0	0	0	629	618.8						
16	0	0	-0.1	629	618.7						

All measurements in terms of H.P. Caesium Standard No. 334, which agrees with the N.P.L. Caesium Standard to 1 part in  $10^{11}$ .

† Relative to AT Scale;  $(AT_{NPL} - \text{Station}) = +468.6$  at 1500 UT 31st December 1968.